Determining the Spring Water Provenance in the Warm Springs Valley Subarea of the Silver Creek Watershed in the Harney Hydrologic Basin, Harney County, Oregon

Halley J. Barnett

A report prepared in partial fulfillment of the requirements for the degree of:

Master of Science
Earth and Space Sciences: Applied Geosciences

University of Washington
March 2018

Project Mentors:
Michael Brown, UW ESS
Gerald Grondin, OWRD
Darrick Boschmann, OWRD
Justin Iverson, OWRD

Internship Coordinator:
Kathy Troost

Reading Committee:
Michael Brown
Kathy Troost

MESSAGe Technical Report Number: 060

Executive Summary

Due to the importance of springs as a water source for marshland habitat, which is vital for Pacific Flyway waterfowl in a portion of the Malheur National Wildlife Refuge in southeast Oregon, this work aims to determine the provenance of the groundwater that discharges from springs in the Warm Springs Valley (WSV) by qualitatively and quantitatively characterizing the area geology, spring discharge, groundwater hydraulic gradients, precipitation, geochemical properties, and spatial distributions of temperature, pH, and specific conductance in well and spring water. Along the southwestern margin of the WSV a number of slightly thermal springs discharge from the base of a faulted upland. Discharge was measured from seven springs during August of 2017. Discharges were estimated from groundwater evapotranspiration and remote sensing climate data for two springs lacking outflow channels necessary for field discharge measurements. Measured spring discharge values were on the low end of historical ranges for each spring, but none were less than the lowest historical values. Each spring shows both variability in measurements made in the same month for different years and a lack of consistent interannual measurements made in the same season, causing difficulty in evaluating seasonal variability. Fluctuations in discharge values could also indicate climatic variability or measurement error due to complex spring geometries.

Potential WSV spring water sources include shallow surface water infiltration from Silver Creek and its tributaries flowing into the subsurface to the WSV from the northwest (Source A), precipitation infiltration and deep circulation from precipitation along the Brothers Fault Zone to the southwest of the WSV (Source B), and deep groundwater flow from the Steens Mountains to the southeast (Source C). Source B was found to be the most probable contributor to spring water by process of elimination. While no evidence was found to support or deny that the WSV springs are receiving water from Source C, groundwater from the Steens is expected to flow toward Malheur Lake and not through the WSV. A groundwater level contour map plotted using static water level measurements in wells taken by Oregon Water Resources Department (OWRD) staff in the fall of 2017 shows groundwater flowing southeast down the valley (Source A) and northeast from the southwest faulted upland (Source B). Horizontal hydraulic gradients calculated using a groundwater level contour map and aquifer transmissivity values based on well pump tests in and around the WSV allow for estimations of expected spring discharge that were zero to two orders of magnitude different from measured and calculated values. There is an apparent vertical gradient that, in combination with the slightly elevated temperature at the WSV warm springs, could support a hypothesis that groundwater is rising at the springs (Source B). Precipitation within the Silver Creek watershed was found to be enough to supply the springs if at least two percent of precipitation supplies spring water. No spatial trends for total dissolved constituents in the entire Harney Basin were found either by well depth or by subwatershed, but plots by relative flow path shows an evolution from calcium-sodium to sodium-calcium type water. Specific conductance values are consistent with groundwater flowpaths as determined by the gradient in hydraulic head.

Table of Contents

List of Figures

List of Tables

Acknowledgements

I would like to express my deepest gratitude to Justin Iverson, Jerry Grondin, and Darrick Boschmann from the Oregon Water Resources Department for your continuous support and guidance. Thank you to Kathy Troost and Mike Brown of the University of Washington for your help and encouragement. I'd also like to thank Jonathan LaMarche for his help in making discharge measurements and to Jordan Beamer for helping with groundwater evapotranspiration estimation. Thank you also to Hank Johnson, Steve Gingerich, and Amanda Garcia from the US Geological Survey Portland office for your advice. Thanks to the Malheur National Wildlife Refuge and various private landowners for providing access to springs. Finally, thank you to Kiri Hargie for visiting the springs with me. This work would not have been possible if not for the support of the Oregon Water Resources Department and its affiliates.

Determining the Spring Water Provenance in the Warm Springs Valley Subarea of the Silver Creek Watershed in the Harney Hydrologic Basin, Harney County, Oregon

Halley Barnett, University of Washington

1.0 Introduction

The Harney Basin is a 5,243 mi^2 closed, semiarid basin within the Malheur Lake Basin in southeast Oregon (***Figure 1***) (Oregon Water Resources Department, 2015). Three major watersheds, the Silvies River, the Donner und Blitzen River, and Silver Creek, drain water from the basin margins toward Harney and Malheur Lakes, in the basin center (***Figure 2***). The Silvies River supplied 55,000 acre-feet of water to Malheur Lake in 1972 and 1,000 acre-feet in 1973 while the Donner und Blitzen supplied 110,000 acre-feet in 1972 and 46,000 acre-feet in 1973 (Hubbard, 1975). Sodhouse Spring, in the Donner und Blitzen watershed south of the lakes supplied 8,000 acre-feet in 1972 and 9,000 acre-feet in 1973, accounting for a significant portion of inflows into Malheur Lake (Hubbard, 1975). Estimated annual evapotranspiration losses from Malheur Lake is 40 inches (Hubbard, 1975).

The area surrounding the Malheur and Harney Lakes provides a vital freshwater marsh habitat for Pacific Flyway waterfowl and includes a portion of the federally-owned Malheur National Wildlife Refuge (***Figure 3***), and covers the lower reaches of Silver Creek and Silvies River and much of the Donner und Blitzen River below Frenchglen. Located to the west of Harney Lake within the lower portion of the Silver Creek watershed is a northwest-southeast trending subarea known as Warm Springs Valley (WSV)[1] (***Figure 4***). The WSV contains a number of warm (50-80°F) springs that discharge along the base of a faulted upland to the southwest and lies partly within the Refuge.

The Refuge (***Figure 3***) was established in 1908 and encompasses 191,000 acres around Malheur and Harney Lakes as critical habitat for migratory birds and waterfowl (Carnahan et al., 1967). Because the Refuge relies heavily on natural water fluxes (Rinella and Schuler, 1992), there is a need to understand the source and reliability of the spring water. Previous reports indicate that deep circulation into young volcanic material could explain geothermal anomalies along the Brothers Fault Zone (BFZ) in general, but there is still no clear consensus with regards to source areas and groundwater circulation mechanisms (Piper et al., 1939; Benoit, 1978; and Brown et al., 1980a and b).

[1] A complete list of abbreviations can be found in Appendix A.

WaterWatch of Oregon (2014) claimed that the Oregon Water Resources Department (OWRD) had been approving too many groundwater permits in Harney County, arguing that groundwater is likely overappropriated. Prior to 2015, OWRD had noticed some declining groundwater levels in the Weaver Springs and Crane-Buchanan areas within a subarea of Harney Basin that has since been classified as the Greater Harney Valley Area. Subsequently, state administrative rules (OAR 690-512-0020) were adopted that significantly limit issuing new groundwater permits until a quantitative study is completed by December 2020 (OWRD, 2015) and OWRD has been organizing and critically examining the quality and distribution of their existing well and spring information (including well locations, lithology, well construction, water chemistry, pump tests and water levels) in preparation for and as a part of the currently ongoing collaborative OWRD-U.S. Geological Survey (USGS) Harney Basin Groundwater Investigation scheduled for completion in 2020. News media, including Oregon Public Broadcasting (OPB), have interpreted the regulatory reform to mean that there will be no new wells in Harney County, which has caused some local concern over the economic future of the county (Peacher, 2015). Subsequent to the rule adoption, OWRD has partnered with the USGS to conduct the science-based investigation to quantitatively understand the hydrogeology of the entire Harney Basin, including a groundwater budget, that will result in a basin hydrogeologic characterization report to be published in 2020 and a numerical groundwater flow model scenario result report to be published by December 2020 (OWRD, 2015 and 2017).

2.0 Objectives and Scope of Work

The main objective of my work is to determine the provenance of the groundwater that discharges from springs in the WSV by qualitatively and quantitatively characterizing the area geology, spring discharge, groundwater hydraulic gradients, precipitation, geochemical properties, and spatial distributions of temperature, pH, and specific conductance in well and spring water. Along the southwestern margin of the WSV a number of slightly thermal springs discharge from the base of a faulted upland to inform a larger collaborative OWRD- USGS Harney Basin Groundwater Investigation. My work assesses the hydrogeologic groundwater-surface water relationships for springs along the base of a faulted upland that bounds the southern edge of the WSV. My work resulted in the creation of a dataset containing spring and well location information, measured water levels, spring discharge, and geochemical data from previously published reports and new information collected for the Harney Basin Groundwater Investigation. The results of my work will inform the groundwater investigation team on study efforts needed to better understand groundwater flow in the WSV.

The scope of work includes gathering available information such as well and spring locations and elevations, water levels in wells, lithology, pump test data at wells, spring discharge measurements, precipitation, major ion concentrations, and water temperature, pH, specific conductance at area wells and springs. These data are from published reports, the USGS National Water Information System (NWIS) database, the OWRD Groundwater Site Information

System (GSIS) database, and additional field work. A complete list of data and their sources can be found in ***Table 1***.

Desk work involved a review of all available literature on geology and water resources in the Harney Basin; compiling and entering all available data (***Table 1***) on wells and springs into the OWRD database including lithology, well construction, water level measurements, approximate locations of wells based on available information, and spring discharge measurements; and estimating spring discharge for low-yield springs using available remote sensing information.

Field work included measuring spring discharge at each spring's outflow channel where present and accessible, determining GPS locations for springs, and measuring temperature, pH, and conductance at spring upwellings. Additional data was provided by Kiri Hargie, a graduate student from Portland State University studying springs in Harney Basin. Field work for this study was limited to two and a half weeks during the summer of 2017 before the fall rains created unfavorable road conditions. The first two weeks were spent locating springs, collecting samples, and taking field measurements. The last half week was spent measuring spring discharge.

3.0 Background

3.1 Previous Studies

The studies discussed in this section include a variety of geographic areas that include portions of Harney Basin and the surrounding areas. Some studies cover the entire Harney Basin where others are largely outside the basin but overlap all or part of the basin.

I.C. Russell first characterized the geologic history of Southeastern Oregon in 1884. He returned to southeastern Oregon and southwestern Idaho in the summer of 1902 to determine where large amounts of land could be irrigated using deep artesian wells (Russell, 1903). He returned to Oregon yet again three years later and identified a favorable supply of water within valley fill in the vicinity of Lawen within the Harney Valley, but found that it was not conducive to irrigation and expressed a need to investigate deeper artesian water sources (Russell, 1905).

More detailed studies on the water resources of the Harney Basin include Waring (1909) and Van Winkle (1914). Waring engaged in reconnaissance from 1906 to 1907, mapping topography and land surface features while talking to local ranchers and settlers to gain information on drainage and water supplies. He reached the conclusion that there was not enough storage in Harney Basin to support a large number of flowing artesian wells as Russell had previously thought (Waring, 1909). Van Winkle analyzed the chemical character of surface waters in the basin and recommended draining and irrigating in the marshlands around Malheur and Harney Lakes (Van Winkle, 1914).

One of the more detailed studies of groundwater resources completed in Harney Basin is Piper et al. (1939), which describes the climate, drainage system, geologic history, geologic structure, aquifers, and water chemistry in the Silvies River and Donner und Blitzen watersheds. The authors asserted that no large artesian flow in the basin existed, but shallow water could be useful in irrigation (Piper et al., 1939). Their report contains numerous well locations, water level measurements, well depths, pump tests, and temperature and specific conductance measurements. Most wells available for analysis in their report were shallow (less than one hundred feet deep).

A Department of Agriculture report detailed several suggestions including construction of reservoirs, improvement of existing channels, and implementation of more efficient uses of water (Carnahan et al., 1967). Leonard (1970) later noticed that water levels had declined by several feet since 1930 in the Crane-Buchanan area.

A series of new wells drilled in the 1960's resulted in the collection well locations, lithology, and water chemistry reported by Leonard (1970). His report expanded on the findings of the Piper et al. (1939) report while being constrained to the northern portion of the Harney Basin and proclaimed a greater potential for groundwater development in the basin while noting that water quality was unpredictable and identified several problematic areas, including the Crane-Buchanan area. The author concluded that there was still considerable development potential of groundwater sources in Sage Hen Valley and the northern part of the Silvies fan and poor prospects in the southern part of the Silvies fan and in the central Harney Valley area. He noted that there is a lot of unpredictability related to the depth and character of aquifers as well as the yield and quality of water from irrigation and domestic wells (Leonard, 1970). Additional well locations, water levels, and chemical analyses for the Drewsey resource area in the eastern portion of Harney Basin and the Riley and Andrews resource areas in the northwest and southeast portions of Harney Basin can be found in Gonthier et al. (1977) and Townley et al. (1980).

G.W. Walker (1979) presented revisions to the Cenozoic stratigraphy and proposed new stratigraphic nomenclature that currently remains in use. Gonthier (1985) provided descriptions of aquifer units in eastern Oregon by lumping hydrogeologic units with similar properties. Several studies of major Tertiary volcanic deposits such as the Rattlesnake Ash-flow Tuff and associated tuffs are reported in Johnson (1994), Sheppard (1994), and Streck and Grunder (2008). Several more recent studies on tectonics and volcanism include graduate theses by Scarberry (2008), Trench (2008), and Milliard (2010).

One technical report by Aquaveo, LLC (Yinger, 2012) characterized the groundwater system in Harney Basin through the compilation and organization of existing lithologic and depth information. Due to a lack of funding and adequate data, Aquaveo recommended that geologists be involved in new borehole logging and in pump tests. Construction of a 3D groundwater model was also recommended.

Currently, the most exhaustive hydrogeologic characterizations in the Harney Basin come from Piper et al. (1939) and Leonard (1970), and systematically-collected groundwater data can be found Gonthier et al. (1977), and Townley et al. (1980). It has long been clear that surface water in the basin is insufficient for irrigation (Russell, 1905), and subsequent investigations that have attempted to identify potential groundwater sources that could be used for irrigation have found high variability and unpredictability in the depth and water-bearing properties of geologic materials and the chemical character of groundwater (Piper, 1939 and Leonard, 1970). Additionally, Significant groundwater development in Harney Basin has been occurring since 1970, with irrigation being the largest permitted groundwater use (OWRD, 2015). The Weaver Springs and Crane-Buchanan areas have shown groundwater level declines and OWRD has since identified declining groundwater levels within the majority of the "Greater Harney Valley Area" (OWRD, 2015). The WSV lies directly to the southwest of the Weaver Springs area.

3.2 Hydrologic and Climatic Setting

The Harney Basin is a semiarid basin with an average of 11 inches of annual precipitation near Burns, shown in ***Figure 1*** (Leonard, 1970). Mild summers receive ten percent of annual rainfall as a result of sporadic thunderstorms and a cold wet season extends from November to February. Rain and snowfall is higher in the surrounding mountains than in the valley (Waring, 1909). Mean annual precipitation in the WSV is about 10 inches (Gonthier, 1985). Temperatures measured near Burns range from 14°F in December to 86°F in July (Western Regional Climate Center, 2016). Falling mostly from November through March, precipitation along the basin margins provides the majority of recharge into the basin for the entire water year. This precipitation then reaches the valley through upland springs and streams that then recharge valley aquifers as water seeps into the ground at alluvial fans and stream mouths along the valley margins (Leonard, 1970). The lowest annual precipitation within the basin occurs around the center of the valley at lower elevations and the highest precipitation occurs in the uplands, especially on the Steens Mountains, which can be seen in ***Figure 5***. Annual precipitation in the Silver Creek watershed (***Figure 5***) ranges from 9.09 to 29.13 inches with an average of 11.51 inches (OWRD, 2015).

Harney and Malheur Lakes lie in the center of the Malheur Lake Basin, and eventually all water that is not diverted or lost through evapotranspiration makes its way into these lakes (Piper et al., 1939). When the stage of Malheur Lake reaches an elevation of 4,091 ft, water spills over into Mud Lake and flows into Harney Lake via the Narrows (OSWRB, 1967).

Silver Creek runs from Big Mowich Mountain in the Blue Mountain Range from an elevation of about 6,000 ft down through the Silver Creek Valley and into the Lower Silver Creek Watershed (LSCW), which encompasses the WSV, where it ultimately discharges into Harney Lake (OSWRB, 1967). At its flood stage, Silver Creek splits into three branches as it reaches the WSV, directing a considerable amount of water into Silver Lake (OSWRB, 1967). Smaller tributaries of Silver Creek flow seasonally and are prone to flooding (OSWRB, 1967).

There are five main dams along Silver Creek, including Chickahominy Reservoir, Faye Canyon Reservoir, Moon Reservoir, Zoglman, and Delintment used for irrigation and recreation (Harney County Watershed Council, 2000).

Portions of the LSCW receive minor flood damage each year, including range and cropland (Carnahan et al., 1967). A small portion of the area surrounding Silver Creek (estimated to be about 1,200 acres in 1967) has the potential for drainage using open ditches, but such control structures may require regradation of the land surface to control the flow (Carnahan et al., 1967). The Refuge has almost no water supply controls and is strongly dependent on natural water fluxes (Rinella and Schuler, 1992). Flooding in the early 1980's caused increased water levels that were unable to support growing wetland vegetation and caused a loss of habitat (Rinella and Schuler, 1992).

4.0 Geologic and Tectonic Setting

4.1 Harney Basin

The Harney Basin is covered in alluvial plains, cinder cones, lava fields, and eroded fault-block terrain. It is a structurally-controlled closed basin with Miocene and early Pliocene beds sloping toward the center of the Harney Basin. The northernmost boundary is a section of the Blue Mountains. Southern boundaries include elevated fault blocks to the south and a tilted fault block which includes the Steens Mountains to the southeast. The westernmost boundary is a series of uplands dominated by rhyolitic domes and younger basaltic vent complexes and flows (Walker, 1979). A generalized stratigraphic section of units from Walker (1979) for Harney Basin can be found in ***Figure 6***.

Pre-Tertiary units consist mainly of accreted oceanic terrain (Camp et al., 2002 and Parker, 1974). Within the northwest Basin and Range province, which is roughly associated with the southern portion of the basin, three main periods of structural development have been identified (Camp et al., 2002 and Scarberry, 2008). The first is concurrent with Oligocene magmatism, which accounts for the formation of numerous volcanic formations such as dikes and domes. The next is Late Cenozoic faulting, which ranges from about 16 to 7 Ma and offsets the Steens Basalt but not the Rattlesnake Ash-Flow Tuff. The third is Late Cenozoic faulting after 7 Ma which cuts the Rattlesnake Tuff (Scarberry, 2008).

Flood basalt deposition began in the Early Miocene at about 16.6 ± 0.02 Ma and extended to about 13.5 ± 0.1 Ma, during which the Steens Basalt was deposited (Camp et al., 2002). There was then a transition in the Mid-Miocene from mainly flood basalt volcanism to Basin and Range extension volcanism that led to the deposition of several lava flows and tuff deposits, and is associated with northward propagation of regional uplift, basalt regression, and vent migration (Camp et al., 2002).

The Late Miocene saw the deposition of three main tuffaceous units: Devine Canyon Ash-Flow Tuff (~9.7 Ma), Prater Creek Ash-Flow Tuff (~8.4 Ma), and Rattlesnake Creek Ash-Flow Tuff (~7.1 Ma) (Trench, 2008; Streck and Grunder, 2008). The extents of these ash-flow tuffs can be seen in ***Figure 7***. Many of the tuff deposits in the basin are likely associated with caldera collapse, and several caldera locations have been proposed by several sources (Greene, 1973; Walker, 1979; Streck and Grunder, 1997; Meigs et al., 2009; and Khatiwada and Keller, 2015). Walker (1979) and Khatiwada and Keller (2015) show the Rattlesnake caldera in the approximate location of the WSV. Harney Basin is thought to have originally formed as a result of both extensional faulting and caldera collapse as loss of material through eruptions caused down warping (Walker, 1979 and Brown et al., 1980b).

The Brothers Fault Zone (BFZ) is a 300 km N60°W trending zone extending from the Steens fault to the Vale fault zone consisting of a series of discontinuous en echelon fractures that mainly trend N40°W (***Figure 8***). Most of these fractures are 10-20 km long normal faults separated by horsts and grabens. Recent deformation north of the BFZ involves east-west and northwest trending folding and faulting (Lawrence, 1976).

The exact age of the BF is not known (Streck, 1999), but Trench (2008) found that faults within the BFZ cut through the Prater Creek Ash-Flow Tuff (8.41 Ma), which was the oldest unit in his study area, with a maximum relief of 107 m. Trench suggests that the BFZ may have been a set of horsetail fractures at the propagating tips of the northwest Basin-Range faults, but cross-section reconstructions show an independent slip history since 5.68 Ma, which has consisted of primarily dip-slip movement. Within the NW-trending fault fabric, basaltic vents and fissures have erupted (Trench, 2008). The BFZ is currently seismically inactive (Benoit, 1978).

Harney Basin's landscape is defined by broad ridges and horst and graben terrain due to Cenozoic extension and erosion (Lawrence, 1976). An ancient lake formed during the Pleistocene with its outlet at Malheur Gap to the east, through which the lake was drained by the Malheur River (Waring, 1909 and Van Winkle, 1914). Around 1.93 Ma, a basalt flow near Voltage blocked the Malheur Gap, causing deposition within this paleolake (Piper et al., 1939 and Camp et al., 2003). Several more outlets subsequently drained the lake, but the water was rerouted as more basalt flows dammed these outlets (Deubbert, 1969). The paleolake then naturally drained to form the present Malheur and Harney Lakes in the center of the basin and the surrounding marshland (Deubbert, 1969).

4.2 Warm Springs Valley

According to Piper et al. (1939), stratigraphic units within the WSV include the upper and lower Danforth Formation separated by a tuff-breccia member which is separated from the underlying Steens Basalt by an unconformity (***Figure 6***). Since 1939, the stratigraphy in the WSV has been revised and re-classified. The faulted upland to the southwest of the WSV and the fault separating the two (***Figure 9***) do not currently have common names and will be referred to

here as Warm Springs Plateau (WSP) and the Warm Springs Fault (WSF) respectively. Walker and Swanson (1968) characterize the WSP deposits as olivine basalt, welded ash-flow tuff, stratified tuffs, tuffaceous sedimentary rocks, and minor ash-flow tuffs. Surficial deposits within the WSV include sedimentary deposits, playa deposits, and alluvium (Walker and Swanson, 1968). The majority of the alluvial deposits are poorly consolidated clastic sediments eroded from the adjacent bluffs and highlands and from volcanic ash (Walker and Swanson, 1968). Sedimentary deposits in the WSV include lake sediments (fine sand, silt, and clay with occasional spits, bars, and beaches from old shorelines), caliche zones, and clastic debris mixed with organic material to form slightly peaty to peaty soils (Walker and Swanson, 1968).

Structurally, the WSP is characterized by numerous northwest-southeast trending normal faults with the downthrown side typically on the northeast side, creating a horst and graben landscape with fault scarps ranging from a few tens of feet of displacement to several hundred feet high (Walker and Swanson, 1968; Greene et al., 1972; and Benoit, 1978). All of these faults are associated with the BFZ (***Figure 8***) and have high exposure at the surface to the west of Harney Lake (Benoit, 1978).

5.0 Hydrogeologic Setting as Presented in Previous Studies

5.1 Harney Basin

The relative permeabilities of geologic units mapped by Greene et al. (1972) and Milliard (2010) were described in Yinger (2012) and were based on pump tests and lithologic descriptions found in well logs for wells in Harney Basin (***Table 2***). Units with the highest permeabilities include Diamond and Voltage Basalts, mafic vent complexes, Drinkwater Basalt, basin fill, intra-basin basalts and cinders, basalt lavas and cinders, and rhyolite-rhyodacite. Moderately permeable units include basin fill, sedimentary rocks, Harney Formation, Steens Basalt, and tuffaceous and volcaniclastic sediments. The least permeable units include the Rattlesnake, Prater Creek, and Devine Canyon Ash-Flow Tuffs and volcaniclastic sedimentary rocks. Underlying the majority of the basin, tuffaceous and volcaniclastic sediments lose porosity as they are hydrothermically altered into clay and claystone by circulating hydrothermal water and compaction (Yinger, 2012). According with the Oregon Department of Environmental Quality (2001), Tertiary volcanic layers could be hydraulically connected to basin fill aquifers at basin margins.

Yinger (2012) defined several hydrogeologic units for Harney Basin, which are similar to geologic units, but are grouped based on their hydraulic properties based on porosity and permeability rather than age and rock type and therefore are not necessarily equivalent to geologic units (Table 3). A similar exercise is currently underway for the Harney Basin Groundwater Investigation, but definitions, properties, and extents of hydrogeologic units were not yet available at the time of this study. Most water wells in the Harney Basin are located in the central lowland area and draw water from valley fill deposits, given the name “Basin Fill” in

Table 3 (Leonard, 1970; CH2MHill, 2001; and Yinger, 2012). These units are mostly shallow, unconsolidated sand and gravel separated by clay interbeds and range in thickness from less than 50 feet to about 270 feet, with a maximum thickness of 500 feet to the south of Malheur and Harney Lakes (Leonard, 1970; CH2MHill, 2001; and Yinger, 2012).

A significant portion of wells are constructed with large uncased intervals in the lower water-bearing units to capture water between clay interbeds, resulting in intermingling between units (Leonard, 1970). Although the presence of these large uncased intervals increases the interconnectedness between units, further investigation is needed to determine whether these units were formerly independent or already connected (Gerald Grondin, personal communication).

Surficial deposits show fining from sand and gravel at the alluvial fans where streams enter the valley to clay at the center of the basin (Leonard, 1970). Other features within the central lowland area include aeolian sand dunes, playa lakes, and tongues of gravel and sand deposited by streams that might show some degree of interconnectedness (Leonard, 1970). The water table generally reflects the surface topography and the slope closely resembles that of the potentiometric surface of deeper water-bearing basin fill units (Oregon Department of Environmental Quality, 2001).

5.2 Warm Springs Valley

The WSV springs are generally supplied by small orifices located along the bottoms of sizeable pools where intermittent diversions cause variability in pool stage (Piper et al., 1939). Table 4 summarizes source geologic units proposed by Piper et al. (1939) which includes valley fill and jointed rhyolite and tuff of the Danforth Formation. The geologic units have since been updated (***Figure 6***) and the following paragraphs discuss other potential source geologic units based on geologic maps from Greene et al. (1972), Parker (1974), and Brown et al. (1980a and b). The names of the springs in Table 4 reflect the currently recognized names of the springs based on more recent USGS publications and the USGS and OWRD databases.

The uppermost layer and first main unit of the WSP was mapped as a welded ash-flow tuff variously named the Rattlesnake Ignimbrite Tongue (Parker, 1974) and Rattlesnake Ash-Flow Tuff (Walker, 1979). On the northern end of WSP, the second main unit is an exposed layer of rhyolite and rhyodacite that reaches six different springs in the WSV and is a part of the Danforth Formation as described in Piper et al., 1939 (***Figure 10***, ***Figure 11***, and Figure 12). This layer has also been called the Rhyolite of Double O Ranch by Parker (1974) and Brown et al. (1980a and b). The third main unit is present further south and toward the edge of the WSP and is composed of tuffaceous sedimentary rocks and comes into contact with four springs as mapped by Greene et al. (1979) and two springs as mapped by Parker, 1974 (***Figure 10***, ***Figure 11***, and Figure 12). Parker mapped another unit, the Prater Creek Ash-Flow Tuff, coming into

contact with Upper and Lower Sizemore springs (***Figure 11***). The springs previously mentioned are located along lateral contacts between WSP units and alluvium (Table 5).

According to Piper et al. (1939), both the Danforth Formation and the Steens Basalt yield thermal water along fault conduits and that the unconformity controls local circulation of thermal groundwater. Alluvial material in the WSV receives water from surface water and precipitation and loses water mainly through transpiration within the marshland. Spring water discharging along the WSF into the WSV is slightly thermal in nature, which could indicate deep circulation into young volcanic material, but there is no clear consensus in the literature with regards to the exact source of heat (Piper et al., 1939; Benoit, 1978; and Brown et al., 1980a and b). Piper et al. (1939) suggest that the Double O (OO) Cold Spring on the northern end of the valley are fed by cold valley fill water percolating southeastward and mixing with some slightly thermal water traveling northward from springs to the south that are fed by fault conduits. Brown et al. (1980a and b) speculate that the thermal water south of Harney Lake is controlled by the intersection between the Rattlesnake collapsed caldera and the BFZ based on high concentrations of dissolved solids, and recommend isotope analysis.

One potential source of heat could be circulation within the Steens Basalt, which receives recharge from rain and melting snow infiltrating on the westward-dipping Steens Mountain block (Piper et al., 1939). The authors propose that groundwater circulation in the Steens Basalt occurs between 300 to 800 feet below the land surface based on the actual depth-temperature measurements and is controlled by faults and joints (Piper et al., 1939). The authors additionally state that the source aquifers are within the Steens Basalt and are confined by the Danforth Formation that unconformably overlies the Steens Basalt and presumably could restrict lateral movement from the aquifer units across the fault, causing net upward movement of water (Piper et al., 1939).

Another potential source of the spring water is meteoric water that falls on the WSP and percolates downward through faults exposed at or near the surface along the BFZ (Benoit, 1978). Piper et al. also indicate that the area to the south of the WSV provides a large catchment area (Piper et al., 1939). ***Figure 13*** summarizes potential sources and flow paths for groundwater in the WSV as conjectured by previous investigations. Gonthier (1984) developed a conceptual geologic model (Figure 14) of aquifers in Harney Basin (modified by Smitherman, 2015). Underlying the Harney Valley are unconsolidated deposits over volcanic and sedimentary rock aquifers overlaying Miocene basaltic rock aquifers. I propose that groundwater is circulating within the volcanic and sedimentary rock aquifers, obtaining heat from the Miocene basaltic rock aquifers, and rising in the center of the Harney Basin around Harney and Malheur Lakes, including the warm springs in the WSV. The flowpaths proposed in Figure 14 show groundwater flowing from the uplands to the northwest of the WSV to the southeast. Although the cross section in this conceptual model does not go directly through the WSV, a similar flow regime could be expected along the NW-SE trending BFZ (Figure 8).

6.0 Data Sources for This Study

6.1 Publications

For my study, available published data were first compiled for wells and springs in and around the WSV and entered into a database. Available information includes well and spring locations and elevations, water levels in wells, lithology, pump tests, spring discharge measurements, precipitation, major ion concentrations, and water temperature, pH, specific conductance at area wells and springs. These data were then supplemented by more recent information as it became available during the data collection process for the Harney Basin Groundwater Investigation. Additional wells and springs were added to the database by correlating wells and springs to additional data sources, including OWRD water right files, published reports, water level measurement field sheets, well inspections, and well logs. In cases where several locations were found for a single site, the location was reviewed and the most accurate location was retained. Springs locations in the WSV were found in published reports and refined in the field using GPS. The resulting dataset includes sites for 345 wells and 33 springs and contains the most accurate available information up until this work was completed.

Published values for spring discharge measurements in the WSV from 1907 to 1932 were found in Piper et al. (1939) and Waring (1909). The springs referenced in these publications include OO Cold Spring, Barnyard Spring, Basque Spring, Johnson Spring, Hughet Spring, and Upper and Lower Sizemore Springs. Measurements for Hibbard and Ross Springs are grouped together in these publications, but they were assumed to belong to Hibbard Spring for this work due to the larger relative size of Hibbard Spring. Soldier Spring had only one measurement estimated from 1931 (Piper et al., 1939).

6.2 Well Logs

Well locations are from the OWRD GSIS database and were digitized in ESRI's ArcMap using GPS locations, legal locations found in water right files, and satellite imagery where GPS locations were unavailable. Springs in the WSV were field-located in July 2017 with help from OWRD and USGS staff as well as USGS topographic maps and Google Earth imagery. GPS locations were documented using Avenza Maps® for iPhone and represent either the location of groundwater discharge to the spring or the center of the spring's pond.

Well information and lithology from well drillers water well reports ("well logs") were converted into an easily queried digital format called "lithcodes." Additionally, well construction reported on well logs was converted into a format that could be easily queried with the lithcodes to determine a well's "open intervals," exposed to receive groundwater from the adjacent materials. These "open intervals" include intervals of screen, perforated casing, open hole, or open annular space between the casing and the borehole.

6.3 Groundwater Level and Other Measurements

Groundwater levels within wells were measured by OWRD and USGS staff using steel tapes and electrical tapes (E-Tapes), recorded on field sheets, and entered into the OWRD groundwater database. For the Harney Basin Groundwater Investigation, about 230 wells within the entire Harney Basin were measured semi-annually (in the spring immediately before the beginning of groundwater use for irrigation and immediately after groundwater use for irrigation ends in the fall). About 140 of those wells were measured quarterly, of which about 20 wells were measured every two hours with digital measurement and recorder equipment. Other wells have a few irregular to no water level measurements recorded. Only static water levels were used in creating a groundwater level contour map, which was then used to estimate a horizontal hydraulic gradient at WSV springs. Groundwater level drawdown, pumping rate, well diameter, and testing time at pumping and/or observation wells were taken from well logs and were used for aquifer properties calculations. Other groundwater level data came from published reports and professional measurements submitted to OWRD in compliance with groundwater permit conditions requiring such measurements. Water chemistry data came from published reports and the USGS database.

7.0 Distribution of Study Data

The distribution of data points is similar for each data type. The majority of the 2,296 lithcoded wells and springs (Figure 15) are located just north of Malheur and Harney Lakes in the central lowland region within the Silvies River drainage. Less data exists in the upland areas, particularly to the southwest of the WSV. Of the 1,462 wells with pump or bailer test data used to calculate specific capacity and transmissivity (Figure 16), the majority are associated with areas with a greater density of lithcoded wells. The distribution of synoptic wells (Figure 17) shows a greater density in the central lowland area but are more evenly distributed than other data types plotted in this area. Of the 209 spring and well water samples with published chemical analyses (Figure 18), there are no published chemical analyses for the area to the southwest of the WSV, but there are several from upstream along Silver Creek and up in the Steens. A summary of the data available for use in this study can be found in Table 6.

8.0 Overview of Methods for Study Observations and Analyses

My project analyzed available information to determine WSV spring water provenance using the basic hydrogeologic methods outlined below and assessed the adequacy of these methods and the need for more sophisticated analytical methods to determine spring water provenance. Observations and analyses conducted for this study include making field observations, comparing historical and recent spring discharge measurements, developing a water level contour map, assessing the hydraulic gradients and aquifer properties around WSV warm springs, conducting a quantitative assessment of precipitation on the Warm Springs

Plateau (WSP), characterizing the chemical character of well and spring water in Harney Basin, and mapping and assessing the spatial distribution of temperature, pH, and specific conductance. An overview of the basic methods are described in the following paragraphs. More detailed descriptions can be found later within each separate section.

Spring Discharge: Spring discharge measurements were taken at seven springs on August 2017 by OWRD staff using a SonTek FlowTracker Handheld ADV and following USGS protocols for wading discharge measurements (Nolan and Shields, 2000). Spring discharge was successfully measured at Hibbard, Barnyard, Basque, Johnson, Hughet, and Upper and Lower Sizemore Springs in outflow channels (Table 7 and Figure 19). Spring discharge measurements were made under challenging conditions that included channels with flows at the lower end of the flowmeter's effective flow measurement range. OO Cold Spring was inaccessible due to flooding and Ross and Soldier Springs did not have outflow channels that could be measured in the field. Ross and Soldier are two springs for which no outflow channel was present during the summer of 2017 and could not be measured in the field. Because these springs have no surface water flow losses, ascribing groundwater evapotranspiration to spring discharge using Landsat coverage and the methodology outlined in Huntington et al. (2014) assumed that all spring discharge was lost through evapotranspiration and that the entire area of discharge was captured in calculations (Table 8 and Figure 20).

Hydraulic Gradients and Properties: Water level contour maps were created using static water level measurements from the OWRD Fall 2017 groundwater level synoptic, during which OWRD staff successfully visited and measured 218 wells in late October/early November 2017. Static water levels were interpolated using the Kriging tool in ESRI's ArcMap after converting depth to water to elevation using the NGVD1929 datum (Figure 21). The water level contour map was then used to estimate a horizontal hydraulic gradient (Figure 22). Horizontal gradient and transmissivity calculated for wells in an around the WSV (Figure 23) using pump test information found in drillers' well logs (Table 9) were used to calculate expected spring discharge (Table 10). Measured WSV spring discharge was then used to calculate expected transmissivity (Table 11) and compared with transmissivities calculated at area wells. Vertical hydraulic gradient was determined at two WSV wells (HARN0001085 and HARN0052022) whose logs report static water levels that vary with depth (Table 12). The approximate width of the faulted zone (measured orthogonal to the WSF) was calculated using the average vertical gradient from hydraulic conductivity from nine wells (Table 13 and Figure 24).

Precipitation and Catchment Area Analysis in the Silver Creek Watershed: Average annual precipitation and instantaneous spring discharge were used to estimate percent of precipitation needed to supply water to the springs for each subwatershed (HUC-12 delineations) and several groupings of subwatersheds in the Silver Creek watershed, assuming that 100 percent of spring water comes from precipitation in the Silver Creek watershed (Table 14, Figure 25, Figure 26, and Figure 27).

Groundwater Chemistry: Data plotted included samples from well and springs within Harney Basin for which concentrations of Ca^{2+}, Mg^{2+}, Na^{+}, K^{+}, CO_3^{2-}, HCO_3^{-}, Cl^{-}, and SO_4^{2-} were reported (Piper et al., 1939; Leonard, 1970; Hubbard, 1975; Gonthier et al., 1977; Townley et al., 1980; Brown et al., 1980b; USGS, 2017; and Kiri Hargie, 2017). Samples were grouped by depth (Figure 28); subwatershed and flowpath for the Silvies River watershed (Figure 29 and Figure 30), the Donner und Blitzen watershed (Figure 31 and Figure 32), and the Silver Creek watershed (Figure 33 and Figure 34); and by WSV spring (Figure 35).

Field Measurements: Field measurements of temperature (Figure 36), pH (Figure 37), and specific conductance (Figure 38) were compiled and plotted for wells and springs in Harney Basin to analyze spatial trends.

9.0 Description of WSV Spring Sites

The following paragraphs provide a description of the spring geometry, substrate at the bottom of the pool and/or channel, and riparian vegetation at each of then WSV spring sites. These descriptions are directly related to the quality of discharge measurements, however; the determination of measurement uncertainty is made qualitatively by the lead hydrologist and statistically by the flowmeter. The pools at each spring are about two to four hundred feet across.

Ross and Soldier Springs (Figure 39A and J) are pools with no visible surface outflow. The pools are characterized by the presence of dark green phreatophyte[2] vegetation with a distinct lateral extent and abrupt transition to sagebrush. The water is dark and organic-rich with no visible flow. At Ross Spring, collapsed reeds floated on the surface of a deep pool with no evidencce of movement. Soldier Spring was shallow and muddy.

OO Cold, Barnyard, Basque, and Hibbard Springs (Figure 39C, D, E, and B) are characterized by a firm substrate covered in a layer of algal blooms, which increased in thickness downstream along outflow channels. Along the bottom of each pool are numerous spring discharge vents through which groundwater wells up and displaces sediment and algae. At Barnyard Spring, there are two patches of stinging nettles growing out of a pile of cobbles along the southwest edge of the pool, under which water was seen flowing into the pool. OO Cold and Basque Springs each have one outflow channel, where Barnyard has two and a leaky head gate, behind which is a channel filled with phreatophytes but no visible surface water.

Hibbard Spring (Figure 39B) has the largest pool and flows out into two channels. One channel appears to be stagnant and therefore was not measured, and the other channel flows under the road through a four-foot culvert located several hundred feet downstream of the pool.

[2] A phreatophyte is a plant that relies on groundwater that its roots can reach (Robinson, 1958). Some Harney Basin examples of anthropogenic and native phreatophytes include, but are not limited to, alfalfa, greasewood, oak, reed, saltgrass, spruce, and waterwillow.

Riparian vegetation along this outflow channel could account for significant evapotranspiration losses.

Johnson and Hughet Springs (Figure 39F and G) each have groundwater visibly discharging from the ground through multicolored gravel into a pool. Along the bottom of these pools are vents through which groundwater wells up. Floating on the top of the pools are mats of algae. Johnson spring supplies a large flooded marshland after flowing by the house and under the road through a culvert. Hughet Spring flows from its pool into a channel with a substrate of silty sand and occasional cobbles.

Upper and Lower Sizemore Springs (Figure 39H and I) discharge at the base of a steep slope from beneath large porous cobbles covered in evaporite deposits into large pools. Upper Sizemore flows through a small channel to Lower Sizemore and through a culvert running through a mound of loose material subject to sloughing. The Lower Sizemore pool flows out through a culvert into another large pool that flows out through a channel.

10.0 Spring Discharge

10.1 Major Assumptions and Limitations

Spring discharge measurements were made under challenging conditions that included channels with flows at the lower end of the flowmeter's effective flow measurement range and soft algae layers on the channel beds, which further decreased flow and created an artificial stream bed. Additionally, dark green riparian vegetation around the springs upstream of the measurement points could possibly indicate an unmeasured loss of water through evapotranspiration, creating a source of error for determining a given spring's discharge. Spring outflow channels were accessible for measurements at Hibbard, Barnyard, Basque, Johnson, Hughet, and Upper and Lower Sizemore. OO Cold Spring was inaccessible due to flooding and Ross and Soldier Springs did not have outflow channels and could not be measured in the field.

The historical measurements for Hibbard Spring can be found in Piper et al. (1939) and represent both Ross and Hibbard Springs, however; there is no way of separating the two springs. For this study, the measurements were assumed to represent Hibbard Spring alone.

Attributing discharge measured at the outflow channels to spring discharge assumes steady state conditions within the spring pools. For the springs with no outflow channel, ascribing groundwater evapotranspiration to spring discharge assumed that all spring discharge was lost through evapotranspiration and that the entire area of discharge was captured in calculations.

10.2 Methods for Measuring Spring Discharge

On August 2017, Jonathan LaMarche (OWRD) took spring discharge measurements at seven springs using a SonTek FlowTracker Handheld ADV, following USGS protocols for

wading discharge measurements (Nolan and Shields, 2000). One additional measurement was a weir measurement made July 20th, 2017 on Lower Sizemore Spring. Statistical outputs from the FlowTracker rated uncertainties as below a fifteen percent error, but a qualitative assessment of measurement uncertainty was made based on the field experience of the lead hydrologist making the measurements and is higher than the statistical output for each measurement. Spring vents contributed to large pools which were subsequently routed into outflow channels at which discharge was measured. Ascribing discharge at the outflow channel to spring discharge assumed steady state conditions in the pool. Where large areas of open water and/or phreatophyte vegetation were present, evaporative and phreatophyte losses were considered less than minimal and a note was made on the summary and measurement forms, which are on file at the OWRD office in Salem. Pipe or culvert measurements are included where these flow control structures were present. Measurements at each spring took one to three hours to complete.

10.3 Methods for Calculating Spring Discharge Using Remote Sensing

Field measurements could not be taken at Ross and Soldier Springs due to the lack of outflow channels during the summer of 2017. Because these springs have no apparent surface water flow losses, groundwater evapotranspiration (ET_g) was used to calculate spring discharge as an evapotranspirative flux using Landsat coverage and the methodology outlined in Huntington et al. (2014). This method uses the enhanced vegetation index (EVI), precipitation (PPT), and standardized grass reference evapotranspiration (ET_0). Using Climate Engine, a polygon (Figure 20) was drawn around the distinct phreatophytic green area for each spring (Google Earth Engine, 2017). A list of the vertex locations for each polygon can be found in Appendix B. EVI values were first generated using the Landsat 4/5/7/8 Surface Reflectance dataset for the annual midsummer average of the years 1984 through 2016, which includes the entire available period of record. These values were used to compute a normalized ET value, ET* using Equation 1,

$$ET^* = \beta_0 + \beta_1 EVI + \beta_2 EVI^2, \qquad \textit{Equation 1}$$

where β values are regression model coefficients found in Table 15. Yearly totals of ET_0 and PPT were then generated using the UI Metadata/gridMET dataset for northern water years 1984 through 2016 and used to estimate ET in Equation 2.

$$ET = (ET_0 - PPT) * (ET^* + PPT) \qquad \textit{Equation 2}$$

Groundwater evapotranspiration, ET_g, was then estimated using Equation 3.

$$ET_g = (ET_0 - PPT) * ET^* \qquad \textit{Equation 3}$$

The resultant value for groundwater ET is the approximate value for annual spring discharge.

10.4 Results and Discussion

Figure 19 shows measured spring discharge plotted with historical measurements ranging from 1907 to 1932. Discharge values are summarized in Table 7. The measured discharge values were on the low end of the range of historical values for each spring (which range from 1907 to 1932), but none were less than the minimum of historical values. It is unclear whether this represents a long-term decrease in discharge or a seasonal low, which could be determined with additional data such as continuous measurements over several years to capture seasonal and other changes. Historical measurements show seasonal variations, but no consistent seasonal trends between springs was found from the existing data. Each spring shows annual variability for measurements made in the same month for different years, and not enough data is available to assess the possible influences on this variability.

Discharge calculated as groundwater evapotranspiration for Ross and Soldier Springs for water years 1983 through 2016 is summarized in Table 8 and plotted in Figure 19. One historical estimation for Soldier Spring in 1931 is 0.06 cfs. For years 1984 through 1987, estimated discharge for Soldier Spring was negative, which could indicate that the vegetation within the spring polygon was mostly covered by water during those years because this method relies on EVI values associated with dry vegetated land (Beamer et al., 2013). This is supported by the localized increase in spring discharge at Ross Spring and the relatively high annual precipitation near Burns for years 1981-1984 (Western Regional Climate Center, 2017).

The spring discharge values calculated as groundwater evapotranspiration (ET) for Soldier Spring have a high degree of uncertainty. Estimated values based on ET are one to two orders of magnitude smaller than 0.06 cfs (cubic feet per second), the estimated discharge reported for 1931. This reported 1931 discharge is closer in value to the Ross Spring estimates based on calculated ET. When visited, Ross Spring had a much larger pool than Soldier Spring. Previously, the Soldier Spring pool may have been as large as the current Ross Spring pool and at some point decreased in size, which could explain the drop in calculated Soldier Spring discharge from the reported 1931 discharge, otherwise calculating groundwater evapotranspiration is an insufficient method for estimating spring discharge in this case. Nevertheless, Soldier Spring discharge is much smaller than the other WSV springs and thus its significance to this study's efforts in determining WSV spring water provenance may be relatively low.

11.0 Hydraulic Gradients and Aquifer Properties

11.1 Major Assumptions and Limitations

Water level analyses were conducted on a number of assumptions. For estimating aquifer transmissivity from pump tests, aquifers were assumed to be fully saturated, homogeneous, and isotropic and flow was assumed to be laminar, continuous, and steady (Fetter, 1994). These

assumptions allow for mathematic simplification in a complex system characterized by non-homogeneous geologic units and geologic structure.

The interpolated groundwater elevation (potentiometric surface) is limited to the distribution of static groundwater level measurements and is limited to the accuracy of elevation values. Spring elevations were not surveyed and not all well and spring elevations in the OWRD GSIS database were associated with the same datum, so elevations were extracted from a digital elevation model (DEM). Because LiDAR coverage does not currently cover the entire Harney Basin, a DEM interpolated from USGS 1:24,000 scale (7.5-minute) topographic maps with a ±10-ft interpolation error (equivalent to about half the contour interval) was used. The resultant elevation values are relative to the NGVD1929 datum and are limited by the horizontal errors. An elevation survey at the springs may prove necessary for future analyses.

All groundwater elevations were treated equally due to the complexity of the system and a current lack of information to justify treating any individual water level measurements differently. Consequently, this approach and the resultant dataset will likely skew the groundwater level contours plotted by creating localized high and low points that could represent aquifer systems that have a limited connection to the flow system as a whole. A more detailed analysis may involve plotting only water levels that draw from a particular hydrostratigraphic unit, however; assigning hydrostratigraphic units to individual wells is outside the scope of this work.

11.2 Water Level Contour Map Methods and Results

A groundwater level contour map was created using static groundwater level measurements from the OWRD Fall 2017 Synoptic, during which OWRD staff visited and measured 223 static groundwater levels in 218 wells in late October/early November. Water levels were plotted on a map as elevations using the Kriging tool in ESRI's ArcMap. Depth to water values were converted to elevation above mean sea level using the land surface elevation at each well. Inputs for this tool were well and spring locations as points with static water elevations as Z values.

Elevations for ten warm springs in the WSV were extracted from a DEM based on the USGS 7.5-minute topographic map due current elevation uncertainties. Due to the elevation uncertainties and because the hydraulic gradient is expected to be similar between these springs, the elevations of all ten springs were averaged to a value of 4120 ft above land surface. This averaging simplifies calculations by placing springs between the same two contour lines. Initial contouring using individual spring elevations placed The groundwater level contour map in Figure 21 was created using the Kriging tool in ArcMap and water level measurements in Appendix E and spring elevations in Appendix F. Springs were grouped into Group A and Group B based on location between contour lines to simplify hydraulic gradient calculations (Figure 22).

The contours show a steep gradient cone of depression in the Weaver Springs area to the northeast of the WSV and a steep gradient from the faulted upland plateau (WSP) to the southwest of the WSV where well coverage is sparse. On the WSP, a single well with a much higher groundwater elevation is largely responsible for the steep gradient which may represent the actual gradient given the presence of numerous faults between that well and the next set of wells downgradient, but also may be an artificial gradient generated by the Kriging tool.

Overall, the contouring suggests groundwater flow toward the springs is coming from two directions: from the southwest plateau and down the Silver Creek watershed drainage to the northwest. Groundwater then flows southeast toward Harney Lake and then curves northeast toward the Weaver Springs area. There is an apparent local sink around Double O School with a water level elevation of about 4,110 feet (MALH0002322). These contours are based on static water levels for all synoptic wells and do not account for well depth or water-bearing unit, which could partially account for the steep gradients to the northeast and the southwest of the WSV and may also account for the local sink around Double O School, however; the steep gradients are more likely to be artificial gradients from interpolations based on sparse data. Additionally, the water level at the springs along the main fault is estimated at about 4,120 feet.

11.3 Analyses for Estimating Aquifer Properties Methods and Results

11.3.1 Estimating Spring Discharge Using Transmissivity Values from Nearby Wells and Horizontal Hydraulic Gradient

Expected spring discharge using Darcy's Law was calculated based on aquifer properties determined at nearby wells using Equation 4 (modified from Fetter, 1994). In lieu of local aquifer tests, specific capacity values from pump tests reported on well driller well logs for nine wells in and around the WSV (Figure 23) were used to calculate the transmissivity (T) at each well (Table 9) using the methods laid out in Theis (1952). To simplify calculations, hydraulic gradient (dh/dL) was found by drawing a box around each group of springs to create a simple two-dimensional box oriented approximately parallel to contour lines (Figure 22). The change in head (dh) from contour to contour was divided by the distance between the two contour lines (dL) at each group of springs (represented by the length of each box). Width (w) was determined by measuring the distance between grouped springs along a line parallel to contour lines for each group (represented by the width of each box). Discharge was then calculated for each spring group using transmissivity values and Equation 4 (Table 10).

$$Q = \mathrm{KA}\frac{dh}{dL} = Tw\frac{dh}{dL} \qquad \textit{Equation 4}$$

Where: Q = volumetric flow (ft^3/second)
K = hydraulic conductivity of the geologic units (ft/day)
A = cross-sectional area of groundwater flow = w x h (ft^2)
w = width of groundwater flow cross-section (ft)

h = height of groundwater flow cross-section (ft)
T = transmissivity of geologic units = K x h (ft^2/day)
dh = change in head (ft)
dL = measured horizontal distance (ft)
$\frac{dh}{dL}$ = hydraulic gradient (no units given the units cancel)

Spring discharge expected to occur at WSV springs based on local aquifer properties and gradients was then calculated using Equation 4. To estimate hydraulic gradient (dh/dL), a box was drawn around each group of springs roughly parallel to contour lines (Figure 22). Group A includes springs between the 4,130 and 4,120 contour lines (Ross, Hibbard, OO Cold, and Barnyard Springs) and Group B includes springs between the 4,120 and 4,110 contour lines (Basque, Johnson, Hughet, Upper Sizemore, Lower Sizemore, and Soldier Springs). Box A represented a 10 ft drop in head (dh) across a distance of about 18,500 ft (dL) and Box B a 10 ft drop in head across a distance of 13,750 ft. The width for each Group A spring was the width of Box A (5,500 ft) divided by four, and the width used for each Group B spring was the width of Box B (28,500 ft) divided by six.

The average discharge calculated for Group A springs using Equation 4 is 0.072 cfs, which is within an order of magnitude of the ET discharge estimate for Ross Spring in 2016 and two orders of magnitude smaller than values measured for the most recent measurements at Hibbard and OO Cold Spring. Average discharge expected for Group B springs is 0.499 cfs, which is an order of magnitude greater than the 1931 measurement of 0.06 cfs for Soldier Spring but two orders of magnitude greater than estimated values based on evapotranspiration. This 0.499 cfs is two orders of magnitude smaller than measurements for most of the remaining springs except for Hughet Spring.

11.3.2 Estimating Transmissivity Using Observed Spring Discharge and Horizontal Hydraulic Gradient

To assess the well transmissivity values based on specific capacity, measured spring discharge was then used to back-calculate the transmissivity at each spring and spring group. Hydraulic gradient (dh/dL) was kept the same and group width (w) was divided by the number of springs in each group to calculate transmissivities at individual springs. Spring discharge was taken from measured, estimated, and reported values (Table 11).

Observed spring discharge for WSV springs were used to back-calculate the transmissivity using the hydraulic gradient (dh/dL) and width (w) determined in section 11.3.1 using Equation 4. Calculations are summarized in Table 11. Transmissivity values range from 1,500 ft^2/day at Soldier Spring to 1,100,000 ft^2/day at Hibbard Spring with an average transmissivity of 410,000 ft^2/day for Group A springs and 82,000 ft^2/day for Group B springs. These back-calculated transmissivities are two to three orders of magnitude greater than those calculated from pump tests in nearby wells that range from 278 ft^2/day to 6,440 ft^2/day. This difference in values may

indicate a difference between lithologies and/or a lack of consideration for vertical groundwater flow at the springs. The largest transmissivity values at area wells are associated with clay, sand, and gravel lithologies. The smallest transmissivity values are associated with shale, gravel, claystone, obsidian, and hard broken rock (Table 9).

11.3.3 Estimating a Possible Local Vertical Gradient Using Nearby Well Data

A possible local vertical hydraulic gradient was assessed using two nearby wells located within the WSV whose logs report static water levels that vary with depth (HARN0001085 and HARN0052022). The difference in head was divided by the vertical distance between the top of each water-bearing unit. The calculations to determine vertical gradient are summarized in Table 12. First, hydraulic conductivity was estimated for nine wells using the transmissivities (T) estimated in section 11.3.1 (Table 9) and Equation 5. Saturated thickness (b) was estimated for each well using thickness of water-bearing units as described by the driller and the open interval(s) within each well (Table 13).

$$K = T/b \qquad \textit{Equation 5}$$

Where: K = hydraulic conductivity of the geologic units (ft/day)
T = transmissivity of geologic units = K x h (ft^2/day)
h = height of groundwater flow cross-section (ft)
b = saturated thickness (ft)

Vertical gradient was estimated to be 0.0957 for HARN0001085 and 0.0405 for HARN0052022. These values are one order of magnitude greater than the horizontal hydraulic gradient determined in Section 11.3.1 for Group A springs and two orders of magnitude greater than that determined for Group B.

Hydraulic conductivity was then used to estimate the horizontal length of the groundwater flow cross-section (L_1), which is a value orthogonal to the WSF and to the horizontal width of the groundwater flow cross-section (w) shown in Figure 24, using Equation 6. L1 could be interpreted as an approximation of the thickness of the faulted zone. The discharge (Q) used in these calculations was 24.3 cfs, which is equivalent to the total Q used in previous calculations (Table 11) minus the discharge for Ross and Hibbard Spring because the cross-sectional width only crosses through the other eight springs. Vertical hydraulic gradient (dh/dL) was averaged from the gradients calculated for HARN0001085 and HARN0052022 (Table 12).

$$L_1 = \frac{Q}{Kw\,{}^{\mathrm{dh}}/_{dL}} \qquad \textit{Equation 6}$$

Where: K = hydraulic conductivity of the geologic units (ft/day)
Q = volumetric flow (ft^3/second)
w = horizontal width of groundwater flow cross-section (ft)
L_1 = horizontal length of groundwater flow cross-section (ft)

h = height of groundwater flow cross-section (ft)
dh = change in head (ft)
dL = measured vertical distance between tops of water-bearing units (ft)
$\frac{dh}{dL}$ = vertical hydraulic gradient (no units given the units cancel)

The calculated length of the groundwater flow cross-section, or width of the faulted zone (L_1) ranged from 5.8 to 260 ft with an average of 19 ft (Table 13).

11.4 Aquifer Properties Discussion

Estimates of aquifer properties using horizontal hydraulic gradients resulted in large differences between estimated and measured spring discharge and transmissivities. For eight of the ten WSV springs, the estimated discharge was significantly lower than observed values. The remaining two, Ross and Soldier Springs, are low yield springs and are the furthest northwest and southeast springs respectively. Expected transmissivity calculated using measured spring discharge were two to three orders of magnitude greater than transmissivities determined from pump tests at nearby wells.

The calculated width of the faulted zone (L_1) ranges from 5.8 to 260 ft with an average of 19 ft. The larger estimates of 250 and 260 ft (HARN0050251 and HARN0001841) are more reasonable approximations when compared to the width of the WSV warm springs ponds. The presence of an apparent vertical gradient could support a hypothesis that the water is circulating deeply before rising and discharging at the springs (Source B). Due to the presence of the faulted zone, vertical flow is likely more significant when compared to horizontal flow than in a typical homogeneous isotropic medium.

12.0 Estimation of Catchment Area in the Silver Creek Watershed Using Annual Precipitation and Spring Discharge Measurements

One of the potential sources of warm spring water is infiltration from precipitation on the WSP (Figure 13). This section evaluates whether precipitation alone could provide enough water to supply observed spring discharge.

12.1 Major Assumptions and Limitations

Average annual precipitation and instantaneous spring discharge were used to estimate catchment area needed to supply water to ten warm springs in the WSV, assuming that 100 percent of spring water comes from precipitation in the Silver Creek watershed. The following calculations do not account for aquifer storage or residence time, but provides a simple estimation of catchment area based on the percentage of precipitation that may contribute to spring discharge. This analysis also does not account for several other elements of the water budget, including evapotranspiration, soil properties and infiltration rates, aquifer storage, and infiltration from streams that receive water from snowfall in the mountains on the edges of the

basin. The watershed is assumed to be closed for ease of calculations, meaning that any flow between the Silver Creek watershed and any surrounding basin or watershed is assumed to be zero.

The Silver Creek watershed was broken up into subwatersheds, which are based on HUC-12 delineations (Seaber et al., 1987). Annual precipitation was downloaded for subwatershed centroids as point locations from PRISM dataset downloaded from the Northwest Alliance for Computational Science and Engineering (National Center for Atmospheric Research Staff, 2017), for years 1895 through 2015 and then averaged for each subwatershed. The combined instantaneous spring discharge values for ten springs is 33.5 cfs, calculated using 2017 discharge measurements supplemented with estimated and published values (see Table 11). Due to a lack of discharge measurements, a time series analysis was not feasible, and therefore discharge was assumed to be steady-state and precipitation was averaged for the entire period of record.

12.2 Methods and Results

The total area of the Silver Creek watershed is 2,100 sq. miles, which can be further sub-divided into fifty-eight subwatersheds (Figure 25). Average annual precipitation in the Silver Creek watershed ranges from 9 to 22 inches with an overall average of 11 inches (Figure 26). Subwatersheds were then grouped into potential catchment areas (Figure 27) based on topographic boundaries including the WSF and the Silver Creek river valley and the assumption that all groundwater is flowing toward Harney Lake. Groups are labelled "NW" and "All SW WSP." These groupings are highly subjective and should not be interpreted as the only possible catchment areas. Average annual precipitation for 1895 through 2015 was used to calculate what percent of precipitation would be needed from each subwatershed to supply 33.5 cfs (Table 11) of spring discharge to the WSV springs (Table 14). Precipitation that does not contribute to spring discharge is likely lost to surface runoff, evapotranspiration, or groundwater flow that does not flow past the springs.

If all of the Silver Creek watershed contributes, only 2.0 percent of annual precipitation would be needed. If the area to the northwest of the WSV in the upper Silver Creek valley contributes, 5.3 percent of annual precipitation is needed. If the catchment area is the entire WSP to the southwest of the WSV, about 4.3 percent of annual precipitation would be needed.

12.3 Discussion

For precipitation coming from the Silver Creek watershed, the largest possible catchment area (2,103 mi^2) requires 2.0 percent of the total precipitation. This suggests that if less than 2.0 percent of precipitation within the watershed makes it to the springs, then there must be some additional source outside the watershed. If smaller subsets of the Silver Creek watershed contribute to spring discharge rather than the entire watershed, then more than 2.0 percent of precipitation is needed. The groupings used in this paper were assigned in a somewhat subjective

manner but range from 4.3 to 5.3 percent of precipitation needed to supply spring discharge. Calculations assume that 100 percent of spring discharge originated from precipitation within the specified catchment area.

These analyses do not account for diversions for water use, which is significant along Silver Creek to the northwest of the WSV, but insignificant to the southwest on the WSP. Both catchment area and percentage of precipitation contributing to spring discharge are major unknowns, and these analyses find that it is possible for precipitation to supply sufficient water to the warm springs in most cases. The delineation of subwatersheds into potential catchment areas in Figure 27 is highly subjective and should not be interpreted as the only possible catchment areas. These analyses also did not account for precipitation falling within the WSV.

13.0 Water Chemistry

13.1 Major Assumptions and Limitations

No funding was available for water sampling and chemical analysis for this project. All water chemistry data used in this study were compiled from previous reports. This work was limited by the specific analyses done by each source and not every sample had been analyzed for the same constituents. Relative flow directions were used to plot general evolution at the watershed scale. Relative flow paths are assumed to be toward the center of the Harney Basin and do not reflect actual groundwater flow paths.

13.2 Methods and Results

Water chemistry data were compiled for wells and springs within Harney Basin from published reports and the USGS NWIS database and plotted on Piper Diagrams using the USGS program Gw_Chart Version 1.29.0.0 (Winston, 2000). Data plotted included samples from wells (Appendix G) and springs (Appendix H) within Harney Basin for which concentrations of Ca^{2+}, Mg^{2+}, Na^{+}, K^{+}, CO_3^{2-}, HCO_3^{-}, Cl^{-}, and SO_4^{2-} were reported. Samples were grouped by watershed, subwatershed, and depth.

13.2.1 Major Ion Chemistry by Well Depth

All chemical analyses show a similar linear trend on the cation plot, with increasing Ca^{2+} and decreasing $Na^{+} + K^{+}$ showing a transition from sodium-potassium to sodium-calcium to calcium-sodium type water. Anions show a mostly bicarbonate-chloride-sulphate water type. Piper tri-linear diagrams of major ions show only slight variations between groups of wells of different depths (Figure 28). Deeper wells are more bicarbonate and appear to have slightly less Mg^{2+} and a more precise trend than shallower wells, but this could be deceptive due to the smaller number of deep wells plotted. On the anion plot, the majority of wells appear to be highly carbonate, with only the shallowest wells differing from the majority.

13.2.2 Major Ion Chemistry by Watershed and Subwatershed

The Piper tri-linear diagrams for the Silvies River watershed with chemical analyses organized by subwatershed (Figure 29) shows no clear variation or evolution of water as it travels toward Malheur Lake.There is a linear trend of all data points that appear on the cation plot with a near constant percentage of Mg^{2+} as Ca^{2+} increases and Na^{+} + K^{+} decreases. Samples from the Malheur Lake subwatershed show slightly elevated levels of Mg^{2+} and sulfate when compared to all other samples. Most samples were taken within the Silvies River watershed. A select set of well and spring samples were then plotted (Figure 30) to represent groundwater flow toward the center of Harney Basin (the southwest part of the Silvies River watershed). The Piper tri-linear diagram shows mainly bicarbonate and bicarbonate-chloride-sulfate type (anions) water evolving from calcium-sodium to sodium-calcium type (cations) water downgradient (to the southwest).

The Piper tri-linear diagrams for the Donner und Blitzen watershed (Figure 31) also shows very little variation between samples taken from different subwatersheds. The same linear trend on the cation plot and the grouping of samples on the carbonate corner of the anion plot that was evident in the previous two plots can be seen here, but these trends do not seem to correspond to geography. The greatest variation in samples taken from the same subwatershed is associated with the Lower Donner und Blitzen River subwatershed. A select set of well and spring samples were then plotted (Figure 32) to represent groundwater flow toward the center of Harney Basin (the northwest part of the Donner und Blitzen River watershed). The Piper tri-linear diagram shows mainly bicarbonate type (anions) water evolving from calcium-sodium to sodium-calcium type (cations) water downgradient (to the north). The two samples furthest downgradient (HARN0001562 and HARN0001548) appear to reverse this evolution from sodium-calcium to calcium-sodium type water although both samples have higher relative sodium concentrations than the sample from furthest upgradient (HARN0001666).

The Piper tri-linear diagrams for the Silver Creek watershed (Figure 33) shows the same linear trend on the cation plot and grouping toward the carbonate end of the anion plot as the previous three plots, but with more variation on the anion plot from samples taken east and northeast of Harney Lake and the greatest outlier being Unnamed Hot Spring 361 to the southeast of Harney Lake. The linear portion on the anion plot does not appear to be controlled by geography. Outliers on the anion plot have higher levels Cl^{-} and sulfate. A select set of well and spring samples were then plotted (Figure 34) to represent groundwater flow toward the center of Harney Basin (the southeast part of the Silver Creek watershed). The Piper tri-linear diagram shows mainly bicarbonate type (anions) water evolving from calcium-sodium to sodium-calcium type (cations) water downgradient (to the southwest). The two most upgradient samples (HARN0000238 and HARN0000753) show this evolution in the opposite direction.

13.2.3 Comparison of the Chemical Character of Water from WSV Warm Springs to Harney Basin Well and Spring Water Samples

There are four samples for two of the warm springs (OO Cold and Basque) in the WSV in published reports and the USGS NWIS database that have been analyzed for major ion concentrations. These samples plot in a small cluster on a Piper diagram (Figure 35), showing a similarity between spring water that is sodium-calcium (cations) and bicarbonate-chloride-sulfate (anions). Basque Spring is downgradient of OO Cold Spring and shows slightly higher Mg2+ and lower carbonate/bicarbonate, but these variations could be within measurement error. More samples are needed to determine if there is any downgradient evolution of spring water. The data points for the warm springs plot somewhat in the middle when compared to all other samples in Harney Basin. The sodium-calcium nature of the warm spring waters is consistent with the apparent evolution of groundwater as it moves downgradient within the Silver Creek watershed as shown in Figure 34 and in the Silvies River (Figure 30) and Donner und Blitzen River watersheds (Figure 32).

13.3 Discussion

Most Piper tri-linear diagrams show a linear trend on the cation plot with almost constant Mg^{2+} concentrations and a grouping on the carbonate end on the anion plot. These trends do not seem to be related to depth or subwatershed apart from the noncarbonate waters directly to the east of Harney Lake with elevated chloride levels (Figure 33). The linear trend on the cation plot appears on all plots and shows an evolution from calcium-sodium to sodium-calcium type water that becomes mroe pronounced when samples are plotted by location along a relative flowpath toward the center of Harney Basin. Most chemical analyses pertain to the Silvies River watershed. Additional samples need to be analyzed for major ions at the warm springs before any trends can be determined, but the samples currently available for WSV warm springs plot in the middle of the range of values plotted for all Harney Basin samples and represent sodium-calcium and bicarbonate-chloride-sulfate type waters. Future analyses could show results from samples taken from various hydrostratigraphic units, which vary by both depth and geography, but grouping wells by hydrostratigraphy is outside the scope of this work.

14.0 Spatial Variations in Temperature, pH, and Specific Conductance

14.1 Methods and Sources of Data

At each spring, field measurements of temperature, pH, and specific conductance were taken as near as possible to the discharge point where the groundwater reaches the surface. These locations were often seen as upwellings in the bottom of large pools. Measurements were compiled from site visits by Kiri Hargie from Portland State University and the USGS, who

posted their field measurements in the USGS NWIS database. Measurements were also compiled from published reports (Piper et al., 1939; Leonard, 1970; Hubbard, 1975; Gonthier et al., 1977; Townley et al., 1980; and Brown et al., 1980b). Sampling techniques were based on the USGS National Field Manual (USGS, n.d.).

14.2 Results

Temperature, pH, and specific conductance values can be found in Appendix I. The majority of the warm springs are 10 to 20 degrees (Fahrenheit) warmer than the wells in the WSV and up the Silver Creek valley (Figure 36). There is a hot spring to the southeast of Harney Lake and there are several hot wells and springs to the north of Malheur Lake. The hot wells are also the deepest wells, being 1000, 1345, and 2812 feet deep. The majority of wells range from 50 to 60 degrees, whereas springs throughout the basin range from 37.76 to 176 degrees with most less than 81 degrees.

Spatial distribution of pH measurements are shown in Figure 37. The majority of warm springs in the WSV range in pH from 8.4 to 9.6, which is similar to the deep hot (105-175°F) water wells north of Malheur Lake. Samples taken from wells to the northwest and within the WSV have lower pH values, as do Ross and Thorn Springs on the northwestern end of the WSF. The majority of warm springs are similar in pH, however; there is a decrease in pH at Upper and Lower Sizemore Springs by about 0.5 from the surrounding springs.

Spatial variation in specific conductance, which is also referred to as electrical conductivity, is summarized in Figure 38. Fewer wells and springs were measured for specific conductance than for temperature and pH and there is a large range of values across the basin. Measurements taken at springs to the northwest of the WSV show very low specific conductance values between 32 and 113 μS/cm, which is similar to the specific conductance measured at springs on the Steens Mountains at the southeast edge of the basin. Warm springs show relatively consistent values, but with a slight increase down the valley toward Harney Lake. Specific conductance, which can be used as an approximation for total dissolved solids, appears to increase toward Malheur and Harney Lakes.

14.3 Discussion

Groundwater flowpaths shown by the water level contour map (Figure 21) generally agree with the distribution of specific conductance and pH values. Water level contours indicate that water is flowing southeast down the WSV (Figure 21), which is consistent with the slight increase in specific conductance that shows an increase in dissolved constituents downgradient to the southeast toward Harney Lake. pH is higher at the WSV warm springs than the majority of samples throughout Harney Basin, apart from three deep flowing wells that have no lithologic information that have high pH values.

pH is higher at the WSV warm springs than in samples taken from a majority of the basin. The slight difference in pH occurs at Hughet and Upper and Lower Sizemore Springs. One feature that sets these three springs apart from the others is their proximity to the Prater Creek Ash-Flow Tuff, which has been mapped adjacent to these springs by Brown et al., 1980a and b (Table 4). The specific differences between springs is not necessarily limited to proximity to exposed geologic units and any correlation between the presence of the tuff and the lower pH may be coincidental.

The higher temperature and pH values of WSV warm spring water when compared to the surrounding wells appear to support a hypothesis that there is some deep circulation of groundwater occurring before the groundwater emerges along the southwest edge of the WSV.

15.0 Discussion and Summary of Findings

Three potential WSV spring water sources were previously described. The first (Source A) involves shallow surface water infiltration from Silver Creek running into the WSV from the northwest. This potential source is supported by the increase in specific conductance of water down the WSV, which indicates an evaporative trend, as well as gradients showing flow to the southeast toward Harney Lake. The second (Source B) involves infiltration and deep circulation from precipitation along the Brothers Fault Zone to the southwest of the WSV. There is an apparent vertical gradient that, in combination with the slightly elevated temperature at the WSV warm springs, could support a hypothesis that groundwater is rising at the springs. Sufficient water from the WSP is possible as evidenced by precipitation calculations. High pH at the springs could also support a deep groundwater source because the highest pH values in Harney Basin are associated with the deepest wells. The third (Source C) involes deep groundwater flow from infiltration up on the Steens Mountains on the southeast edge of Harney Basin. While no evidence was found to support or deny that the WSV springs are receiving water from Source C, groundwater in the Donner und Blitzen River watershed is expected to flow toward Malhuer Lake (Piper et al., 1939). While a groundwater level contour map (Figure 21) does not show any flow from the southeast, groundwater level data south of the WSV is sparse and reflects a local gradient and not any deep large-scale groundwater flow.

Spring Discharge: Spring discharge measurements were made under challenging conditions that included channels with flows at the lower end of the flowmeter's effective flow measurement range and soft algae layers on the channel beds, which further decreased flow and created an artificial stream bed. Additionally, dark green riparian vegetation around the springs upstream of the measurement points could possibly indicate an unmeasured loss of water through evapotranspiration, creating a source of error for determining a given spring's discharge. Spring outflow channels were accessible for measurements at Hibbard, Barnyard, Basque, Johnson, Hughet, and Upper and Lower Sizemore. OO Cold Spring was inaccessible due to flooding and Ross and Soldier Springs did not have outflow channels and could not be measured in the field.

Figure 19 shows measured spring discharge plotted with historical measurements ranging from 1907 to 1932. Discharge values are summarized in Table 7. The measured discharge values were on the low end of the range of historical values for each spring (which range from 1907 to 1932), but none were less than the minimum of historical values. It is unclear whether this represents a long-term decrease in discharge or a seasonal low, which could be determined with additional data such as continuous measurements over several years to capture seasonal and other changes. Historical measurements show seasonal variations, but no consistent seasonal trends between springs was found from the existing data. Each spring shows annual variability for measurements made in the same month for different years, and not enough data is available to assess the possible influences on this variability.

Discharge calculated as groundwater evapotranspiration for Ross and Soldier Springs for water years 1983 through 2016 is summarized in Table 8 and plotted in Figure 19. One historical estimation for Soldier Spring in 1931 is 0.06 cfs. For years 1984 through 1987, estimated discharge for Soldier Spring was negative, which could indicate that the area within the spring polygon was mostly covered by water during those years rather than vegetation (Beamer et al., 2013). This is supported by the localized increase in spring discharge at Ross Spring and the relatively high annual precipitation near Burns for years 1981-1984 (Western Regional Climate Center, 2017).

The spring discharge calculated as groundwater evapotranspiration (ET) for Soldier Spring have a high degree of uncertainty. Estimated values based on ET are one to two orders of magnitude smaller than 0.06 cfs (cubic feet per second), the estimated discharge reported for 1931. This reported 1931 discharge is closer in value to the Ross Spring estimates based on calculated ET. When visited, Ross Spring had a much larger pool than Soldier Spring. Previously, the Soldier Spring pool may have been as large as the current Ross Spring pool and at some point decreased in size, which could explain the drop in calculated Soldier Spring discharge from the reported 1931 discharge, otherwise calculating groundwater evapotranspiration is an insufficient method for estimating spring discharge in this case. Nevertheless, Soldier Spring discharge is much smaller than the other WSV springs and thus its significance to this study's efforts in determining WSV spring water provenance may be relatively low.

Hydraulic Gradients and Properties: A water level contour map shows that water is flowing southeast down the valley and northeast from the southwest faulted upland. Estimates of aquifer properties using horizontal hydraulic gradients resulted in large differences between estimated and measured spring discharge and transmissivities. For eight of the ten WSV springs, the calculated discharge when calculated using horizontal gradient was significantly lower than observed values. These eight springs are the only ones with measurable outflow channels. The remaining two, Ross and Soldier Springs, are low yield springs and are the furthest northwest and southeast springs respectively. Expected transmissivity calculated using measured spring

discharge were two to three orders of magnitude greater than transmissivities determined from pump tests at nearby wells.

The calculated width of the faulted zone (L_1) ranges from 5.8 to 260 ft with an average of 19 ft. The larger estimates of 250 and 260 ft (HARN0050251 and HARN0001841) are more reasonable approximations when compared to the width of the WSV warm springs ponds. The presence of an apparent vertical gradient could support a hypothesis that the water is circulating deeply before rising and discharging at the springs. Due to the presence of the faulted zone, vertical flow is likely more significant when compared to horizontal flow than in a typical homogeneous isotropic medium.

Precipitation and Catchment Area Analysis in the Silver Creek Watershed: For precipitation coming from the Silver Creek watershed, the largest possible catchment area (2,103 mi^2) requires 2.0 percent of the total precipitation. This suggests that if less than 2.0 percent of precipitation within the watershed makes it to the springs, then there must be some additional source outside the watershed. If smaller subsets of the Silver Creek watershed contribute to spring discharge rather than the entire watershed, then more than 2.0 percent of precipitation is needed. The groupings used in this paper were assigned in a somewhat subjective manner but range from 4.3 to 5.3 percent of precipitation needed to supply spring discharge. Calculations assume that 100 percent of spring discharge originated from precipitation within the specified catchment area.

These analyses do not account for diversions for water use, which is significant along Silver Creek to the northwest of the WSV, but insignificant to the southwest on the WSP. Both catchment area and percentage of precipitation contributing to spring discharge are major unknowns, and these analyses find that it is possible for precipitation to supply water to the warm springs in most cases. The delineation of subwatersheds into potential catchment areas in Figure 27 is highly subjective and should not be interpreted as the only possible catchment areas. These analyses also did not account for precipitation falling within the WSV.

Groundwater Chemistry: Most Piper tri-linear diagrams show a linear trend on the cation plot with almost constant Mg^{2+} concentrations and a grouping on the carbonate end on the anion plot. These trends do not seem to be related to depth or subwatershed apart from the noncarbonate waters directly to the east of Harney Lake with elevated chloride levels (Figure 33). The linear trend on the cation plot appears on all plots and shows an evolution from calcium-sodium to sodium-calcium type water that becomes mroe pronounced when samples are plotted by location along a relative flowpath toward the center of Harney Basin. Most chemical analyses pertain to the Silvies River watershed. Additional samples need to be analyzed for major ions at the warm springs before any trends can be determined, but the samples currently available for WSV warm springs plot in the middle of the range of values plotted for all Harney Basin samples and represent sodium-calcium and bicarbonate-chloride-sulfate type waters. Future analyses could show results from samples taken from various hydrostratigraphic units,

which vary by both depth and geography, but grouping wells by hydrostratigraphy is outside the scope of this work.

Field Measurements: Groundwater flowpaths shown by the water level contour map (Figure 21) generally agree with the distribution of specific conductance and pH values. Water level contours indicate that water is flowing southeast down the WSV (Figure 21), which is consistent with the slight increase in specific conductance that shows an increase in dissolved constituents downgradient to the southeast toward Harney Lake. pH is higher at the WSV warm springs than the majority of samples throughout Harney Basin, apart from three deep flowing wells that have no lithologic information that have high pH values.

pH is higher at the WSV warm springs than in samples taken from a majority of the basin. The slight difference in pH occurs at Hughet and Upper and Lower Sizemore Springs. One feature that sets these three springs apart from the others is their proximity to the Prater Creek Ash-Flow Tuff, which has been mapped adjacent to these springs by Brown et al., 1980a and b (Table 4). The specific differences between springs is not necessarily limited to proximity to exposed geologic units and any correlation between the presence of the tuff and the lower pH may be coincidental.

The higher temperature and pH values of WSV warm spring water when compared to the surrounding wells appear to support a hypothesis that there is some deep circulation of groundwater occurring before the groundwater emerges along the southwest edge of the WSV.

Conceptual Model: A conceptual model of flow to the WSV warm springs may look something like Figure 40, which is a conceptual block diagram with generalized geology and groundwater flow paths and is not to scale. Groundwater flows southeastward along and down through faults in the Brothers Fault Zone until it reaches the contact between less permeable volcanic ash-flow tuff material and more permeable material (which includes, but is not limited to, broken rock, pumice, and sedimentary volcanic material), where it begins to flow to the north and undergoes some hydrothermal circulation due to underlying heat. It then rises when it reaches the Warm Springs Fault, where it comes in contact with less permeable volcanic tuff, and emerges from small orifices at the bottom of each spring pond. Surface water and shallow groundwater then flows east toward Harney Lake and may come in contact with water from Silver Creek as it is re-routed to the northeast toward the Weaver Springs area (Figure 21). Silver Creek was interpreted to be a losing stream, but future streamflow measurements may challenge this assumption. This model represents a simplification of a complex system and should not be taken as an exact or complete representation of the geology, structure, or hydrology of the WSV.

16.0 Recommendations

At best, this study can suggest a more probable source for the WSV warm spring water provenance. Additional investigation(s) using more advanced hydrogeologic methods is needed to better understand the source of WSV warm spring water. This may include, but is not limited to: isotope analysis, which compare isotopic signatures from around the basin and provide estimates for the age of the water; and noble gas geochemistry, which could be used to test the deep circulation hypothesis. More subsurface and hydraulic gradient information is needed for the Harney Basin, especially in areas with sparse well coverage such as the WSP. Drilling wells and/or conducting additional pump tests using wells in that area would add valuable data points for further analyses. Field measurements and isotope analysis of precipitation falling on the WSP might also be useful in testing the precipitation hypothesis. Careful logging of water-bearing units and static water levels associated with these units would provide more vertical gradient information in addition to the two wells used in vertical gradient calculations in this study. Regular discharge measurements should be implemented for warm springs to determine seasonal variability. Major ion geochemical analyses could be conducted on samples from warm springs and could be used in geochemical modeling to determine downgradient evolution of spring water. Isotope analysis would be useful in testing Source C (groundwater from the Steens Mountains) as a potential WSV warm spring water source.

References

Beamer, J.P., Huntington, J.L., Morton, C.G., and Pohll, G.M., 2013, Estimating Annual Groundwater Evapotranspiration from Phreatophytes in the Great Basin Using LANDSAT and Flux Tower Measurements: Journal of the American Water Resources Association, v.. 49, no. 3, pp. 518-533. DOI: 10.1111/jawr.12058.

Benoit, W.R., 1978, Report on the Brothers Fault Zone: Crook, Deschutes, Lake, and Harney Counties Oregon: 60 p.

Berggren, W. A., and Van Couvering, J. A., 1974, The Late Neogene: Developments in Paleontology and Stratigraphy: Volume 2: Amsterdam, Elsevier, 216 p.

Brown, D.E., McLean, G.D., and Black, G.L. under the direction of Riccio, J.F., 1980,

a. Preliminary Geology and Geothermal Resource Potential of the Northern Harney Basin, Oregon: State of Oregon Department of Geology and Mineral Industries Open-File Report 0-80-6, 55 p.

b. Preliminary Geology and Geothermal Resource Potential of the Southern Harney Basin, Oregon: State of Oregon Department of Geology and Mineral Industries Open-File Report 0-80-7, 94 p.

Camp, V.E., Ross, M.E., Hanson, and W.E., 2002, Genesis of Flood Basalts and Basin and Range Volcanic Rocks from Steens Mountain to the Malheur River Gorge, Oregon: GSA Bulletin, v. 114, no. 12, 24 p.

Camp, V.E., Ross, M.E., and Hanson, W.E., 2003, Genesis of Flood Basalts and Basin and Range Volcanic Rocks from Steens Mountain to the Malheur River Gorge, Oregon: GSA Bulletin, v. 115, no. 1, p. 105-128.

Carnahan, H.E., Vesterby, M.C., Bercheid, G.H., Price, D.G., and Shook, B.B., 1967, USDA Report on Water and Related Land Resources: Malheur Lake Drainage Basin: Oregon: United States Department of Agriculture, 181 p. (preliminary, subject to revision).

CH2MHill, 2001, Remedial Investigation and Site Characterization Texaco (Bennett) Bulk Plant: Burns, Oregon: 132 p.

Duebbert, H.F., 1969, The Ecology and Malheur Lake and Management Implications: U.S. prism Service, 28 p.

Dugas, D.P., 1998, Late Quaternary Variations in the Level of Paleo-Lake Malheur, Eastern Oregon: Quaternary Research 50, QR982005, p. 276-282.

Fetter, C.W., 1994, Applied Hydrogeology, Third Edition: Prentice-Hall.

Gomm, F.B., 1979, Climate and Agriculture of Malheur-Harney Basin, Oregon: Agricultural Experiment Station: Oregon State University, Corvallis, Special Report 530, 24 p.

Gonthier, J.B., Collins, C.A., and Anderson, D.B., 1977, Ground-Water Data for the Drewsey Resource Area, Harney and Malheur Counties, Oregon: Portland: U.S. Geological Survey Open-File Report 77-741, 31 p.

Gonthier, J.B., 1985, A Description of Aquifer Units in Eastern Oregon: Portland: U.S. Geological Survey Water-Resources Investigations Report 84-4095, 45 p.

Google Earth Engine, 2017, Climate Engine. Accessed 5 September, 2017 at http://app.climateengine.org/.

Greene, R.C., Walker, G.W., and Corcoran, ,R.E., 1972, Geologic Map of the Burns Quadrangle, Oregon: United States Geological Survey, Miscellaneous Geologic Investigations Map I-680, scale 1:250,000, 1 sheet.

Greene, R.C., 1973, Petrology of the Welded Tuff of Devine Canyon, Southeastern Oregon: Washington [D.C.]: U.S. Geological Survey Professional Paper 797, 36 p.

Harney County Watershed Council, 2000, Silver Subbasin Assessment: Pamela Street, ed., 26 p.

Hubbard, L.L. 1975, Hydrology of Malheur Lake Harney County, Southeastern Oregon: U.S. Geological Survey Water Resources Investigation 21-75, 48 p.

Huntington, J.L., Morton, C.G., Bromley, M., Liebert, R., and Paudel, K., 2014, Landsat Evapotranspiration from Phreatophyte and Irrigated Areas, Boulder Flat, Humboldt River Basin, Nevada: Prepared by Division of Hydrologic Sciences and Division of Earth and Ecosystem Sciences, Desert Research Institute, Reno, NV, 50 p.

Johnson, J.A., 1994, Geologic Map of the Krumbo Reservoir Quadrangle, Harney County, Southeastern Oregon: U.S. Geological Survey, Miscellaneous Field Studies Map MF-2267, scale 1:24,000, 1 sheet, 11 p. text.

Khatiwada, M. and Keller, G.R., 2015, An integrated geophysical imaging of the upper-crustal features in the Harney Basin, southeast Oregon: Geological Society of America, Geosphere, v. 11, no. 1, p. 1-17.

Lawrence, R.D., 1976, Strike-Slip Faulting Terminates the Basin and Range Province in Oregon: Geological Society of America Bulletin, v. 87, p. 846-850.

Leonard, A.R., 1970, Ground-Water Resources in Harney Valley, Harney County, Oregon: U.S. Geological Survey Ground Water Report 16, 95 p.

Meigs, A., Scarberry, K., Grunder, A., Carlson, R., Ford, M.T., Fouch, M., Grove, T., Hart, W.K., Iademarco, M., Jordan, B., Milliard, J., Streck, M.J., Trench, D., and Weldon, R., 2009, Geological and Geophysical Perspectives on the Magmatic and Tectonic Development, High Lava Plains and Northwest Basin and Range: in: O'Connor, J.E., Dorsey, R.J., Madin, I.P., eds., Volcanoes to Vineyards: Geologic Field Trips through the Dynamic Landscape of the Pacific Northwest: Geological Society of America Field Guide 15, pp. 435-470, DOI: 10.1130/2009.fl d015(21).

Milliard, J.B., 2010, Two-Stage Opening of the Northwestern Basin and Range in Easter Oregon (M.S. thesis): Eugene, Oregon State University, 97 p.

National Center for Atmospheric Research Staff (Eds), Last modified 24 Oct 2017, The Climate Data Guide: PRISM High-Resolution Spatial Climate Data for the United States: Precipitation: Accessed 3 January, 2018 at: https://climatedataguide.ucar.edu/climate-data/prism-high-resolution-spatial-climate-data-united-states-maxmin-temp-dewpoint.

Nolan, K.M. and Shields, R.R., 2000, Measurement of Stream Discharge by Wading: U.S. Geological Survey Water-Resources Investigations Report 2000-4036.

Northwest Alliance for Computational Science and Engineering (NACSE), 2018, PRISM Climate Data: PRISM Climate Group, Oregon State University. Accessed 4 January 2018 at : http://prism.oregonstate.edu/.

Oregon Department of Environmental Quality, 2001, Statewide Groundwater Monitoring Program, Burns-Hines Area Final Report: Oregon Department of Environmental Quality, Water Quality Monitoring Section, Laboratory Division.

Oregon State Water Resources Board, 1967, Malheur Lake Basin: State Water Resources Board, 137 p.

Oregon Water Resources Department, 2015, A Work Plan to Investigate the Harney Basin Groundwater Resources with Emphasis in the Greater Harney Valley Area (draft): Oregon Water Resources Department, Groundwater Hydrology Section, Draft 3: November 2015. Accessed 22 February 2018 at: http://filepickup.wrd.state.or.us/files/studies/harney_gw_study/Harney_gw_workplan_draft_2015_November.pdf.

Oregon Water Resources Department, 2017,

a. Groundwater Site Information System (GSIS): Accessed 17 January 2018 at: http://apps.wrd.state.or.us/apps/gw/gw_info/gw_info_report/Default.aspx.

b. Oregon's 2017 Integrated Water Resources Strategy: Public Review Draft: Oregon Water Resources Department, April 19, 2017. Accessed 3 May 2017 at: http://www.oregon.gov/owrd/LAW/docs/IWRS/2017_04_19_2017_IWRS_Public_Review_Draft.pdf.

Parker, D.J., 1974, Petrology of Selected Volcanic Rocks of the Harney Basin, Oregon (Ph.D. thesis): Eugene, Oregon State University, 131 p.

Peacher, A., 2015, Harney County Groundwater: No New Ag Wells: OPB, July 13, 2015. Accessed 3 May, 2017 at: http://www.opb.org/news/article/harney-county-water-woes-no-new-groundwater-wells-/.

Piper, A.M., Robinson, T.W., and Park, C.F. Jr., 1939, Geology and Ground-Water Resources of the Harney Basin, Oregon: Washington [D.C.]: United States Geological Survey Water Supply Paper 841, 223 p.

Rinella, F.A. and Schuler, C.A., 1992, Reconnaissance Investigation of Water Quality, Bottom Sediment, and Biota Associated with Irrigation Drainage in the Malheur National Wildlife Refuge, Harney County, Oregon, 1988-89: U.S. Geological Survey Water-Resources Investigations Report 91-4085, 113 p.

Robinson, T.W., 1958, Phreatophytes: Washington [D.C.]: U.S. Geological Survey Water-Supply Paper 1423, 92 p.

Russell, I. C., 1884, A Geological Reconnaissance in Southern Oregon: Extract from The fourth annual report of the director [of the U.S. Geological Survey]: 1882-1883, Washington [D.C.]: G.P.O., p. 431-464.

Russell, I.C., 1903, Preliminary Report on Artesian Basins in Southwestern Idaho and Southeastern Oregon: Washington [D.C.]: U.S. Geological Survey Water-Supply Paper 78, 62 p.

Russell, I.C., 1905, Preliminary Report on the Geology and Water Resources of Central Oregon: Washington [D.C.]: U.S. Geological Survey Bulletin 252: Series B, Descriptive Geology, 57, Series O, Underground Waters, 33, 162 p.

Scarberry, K.C., 2008, Extension and Volcanism: Tectonic Development of the Northwestern Margin of the Basin and Range Province in Southern Oregon (Ph.D. thesis): Eugene, Oregon State University, 184 p.

Seaber, P.R., Kapinos, F.P., and Knapp, G.L., 1987, Hydrologic Unit Maps: U.S. Geological Survey Water Supply Paper 2294, 63 p.

Sheppard, R.A., 1994, Zeolitic Diagenesis of Tuffs in Miocene Lacustrine Rocks near Harney Lake, Harney County, Oregon: Washington [D.C.]: U.S. Geological Survey Bulletin 2108, 36 p.

Smitherman, L.L., 2015, Forensic Hydrogeography: Assessing Groundwater Arsenic Concentrations and Testing Methods within the Harney Basin, Oregon (M.S. thesis): Eugene, Oregon State University, 109 p.

Streck, M.J. and Grunder, A.L., 1997, Compositional Gradients and Gaps in High-silica Rhyolites of the Rattlesnake Tuff, Oregon: Oxford University Press, Journal of Petrology, v. 38, n. 1, 133-163 p.

Streck, J.J. and Grunder, A.L., 2008, Phenocryst-poor rhyolites of bimodal, tholeiitic provinces: The Rattlesnake Tuff and implications for mush extraction models: 49 p.

Theis, C.V., 1952, The Relation Between the Lowering of the Piezometric Surface and the Rate and Duration of Discharge of a Well Using Ground Water Storage: Washington D.C.: U.S. Geological Survey Ground Water Notes Hydraulics No. 5, 9 p.

Townley, P.J., Soja, C.M., and Sidle, W.C., 1980, Ground-Water Data for the Riley and Andrews Resource Areas, Southeastern Oregon: U.S. Geological Survey Open-File Report 80-419, 38 p.

Trench, D., 2008, The Termination of the Basin and Range Province into a Clockwise Rotating Region of Transtension and Volcanism, Central Oregon (M.S. thesis): Eugene, Oregon State University, 75 p.

U.S. Geological Survey, variously dated, National Field Manual for the Collection of Water-Quality Data: U.S. Geological Survey Techniques of Water-Resources Investigations, book 9, chs. A1-A10, available online at http://pubs.water.usgs.gov/twri9A.

U.S. Geological Survey, 2017, Water Quality Data for the Nation: USGS 431649119190800 DOUBLE O COLD SPRINGS NR DOUBLE O STATION, OR: National Water Information System (NWIS): Accessed 16 Jan 2018 at: https://nwis.waterdata.usgs.gov/nwis/qwdata?search_station_nm=double%20o%20cold%20spring&search_station_nm_match_type=beginning&group_key=NONE&sitefile_output_format=html_table&column_name=agency_cd&column_name=site_no&column_name=station_nm&inventory_output=0&rdb_inventory_output=file&TZoutput=0&pm_cd_compare=Greater%20than&radio_parm_cds=all_parm_cds&format=html_table&qw_attributes=0&qw_sample_wide=wide&rdb_qw_attributes=0&date_format=YYYY-MM-DD&rdb_compression=file&list_of_search_criteria=search_station_nm.

Van Winkle, W., 1914, Quality of the Surface Waters of Oregon: Washington [D.C.]: U.S. Geological Survey Water-Supply Paper 363, 158 p.

Walker, G.W. and Swanson, D.A., 1968, Summary Report on the Geology and Mineral Resources of the Harney Lake Areas of the Malheur National Wildlife Refuge North-Central Harney County, Oregon and Poker Jim Ridge and Fort Warner Areas of the Hart Mountain National Antelope Refuge, Lake County, Oregon: Washington [D.C.]: U.S. Geological Survey Bulletin 1260-L, M, 52 p.

Walker, G.W., 1979, Revisions to the Cenozoic Stratigraphy of Harney Basin, Southeastern Oregon: Washington [D.C.]: U.S. Geological Survey Bulletin 1475, 41 p.

Waring, G.A., 1909, Geology and Water Resources of the Harney Basin Region, Oregon: Washington [D.C.]: U.S. Geological Survey Water-Supply Paper 231, 103 p.

WaterWatch of Oregon, 2014, Groundwater Crisis Looms for Malheur Lake Basin: *in* Instream: Summer '14 Newsletter, p. 4. Accessed 3 May, 2017 at: http://waterwatch.org/wp-content/uploads/2014/08/WWO_Summer14newsletter_Web.pdf.

Western Regional Climate Center (2017). "Burns Muni AP, OR: Total of Precipitation (Inches)." WRC.DRI.edu. Accessed 30 November, 2017. < https://wrcc.dri.edu/cgi-bin/cliMAIN.pl?or1175>.

Winston, R.B., 2000, Graphical User Interface for MODFLOW, Version 4: U.S. Geological Survey Open-File Report 00-315, 27 p. Accessed 9 December 2017 at https://water.usgs.gov/nrp/gwsoftware/GW_Chart/GW_Chart.html.

Yinger, M., 2012, Harney Basin Groundwater Study: Harney County Final Report, December 27, 2012: Aquaveo, LLC, Mark Yinger Associates, and WPN, Submitted to Harney County Watershed Council, 110 p.

Figures

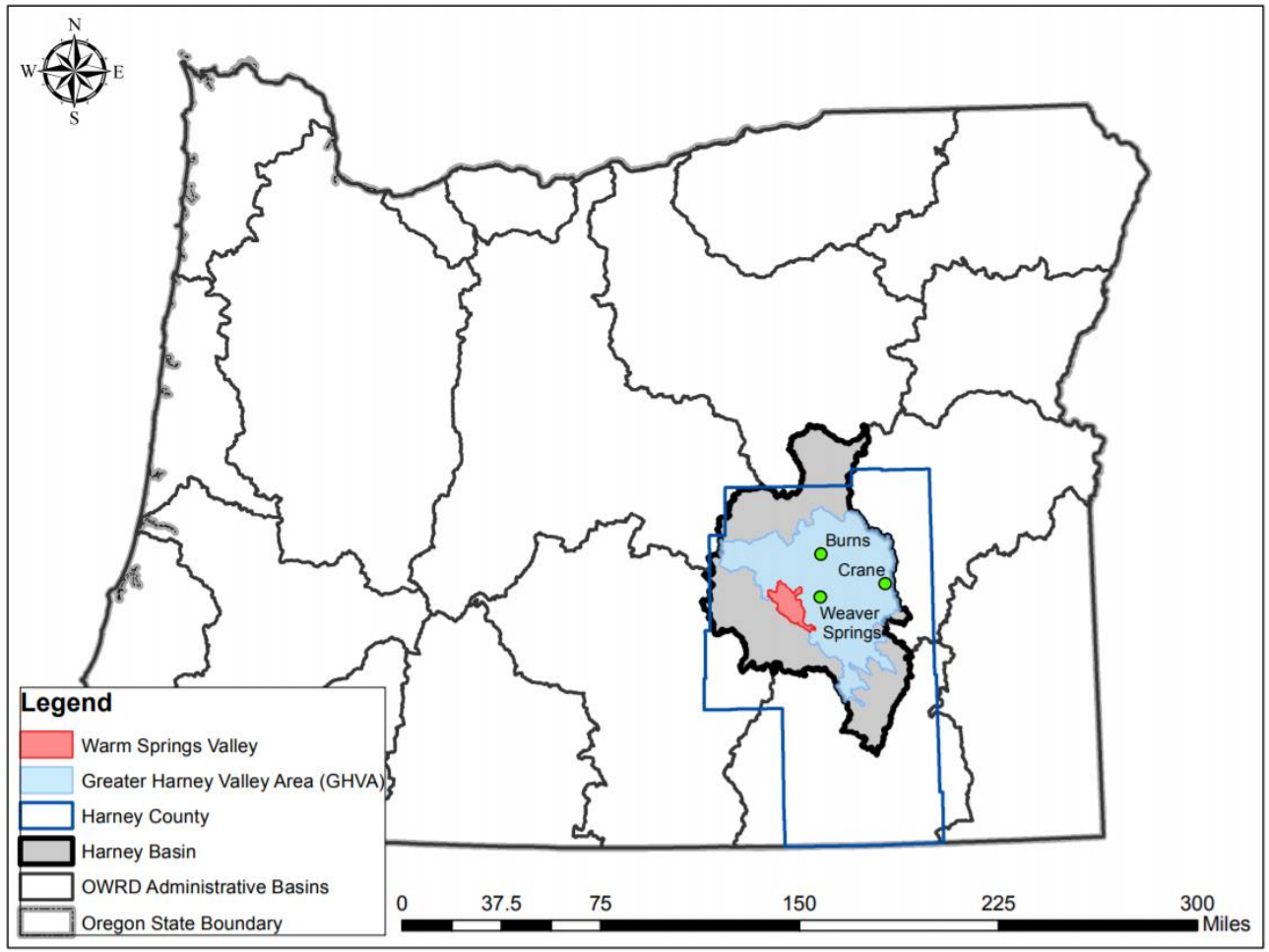

Figure 1: *Harney Basin and Warm Springs Valley.* Location of WSV (red) in relation to Harney County, Malheur Lake Administrative Basin, and Harney Basin. The outline of the WSV is a combination of two HUC-12 outlines modified from Seaber et al. (1987). All other outlines can be found in OWRD (2015).

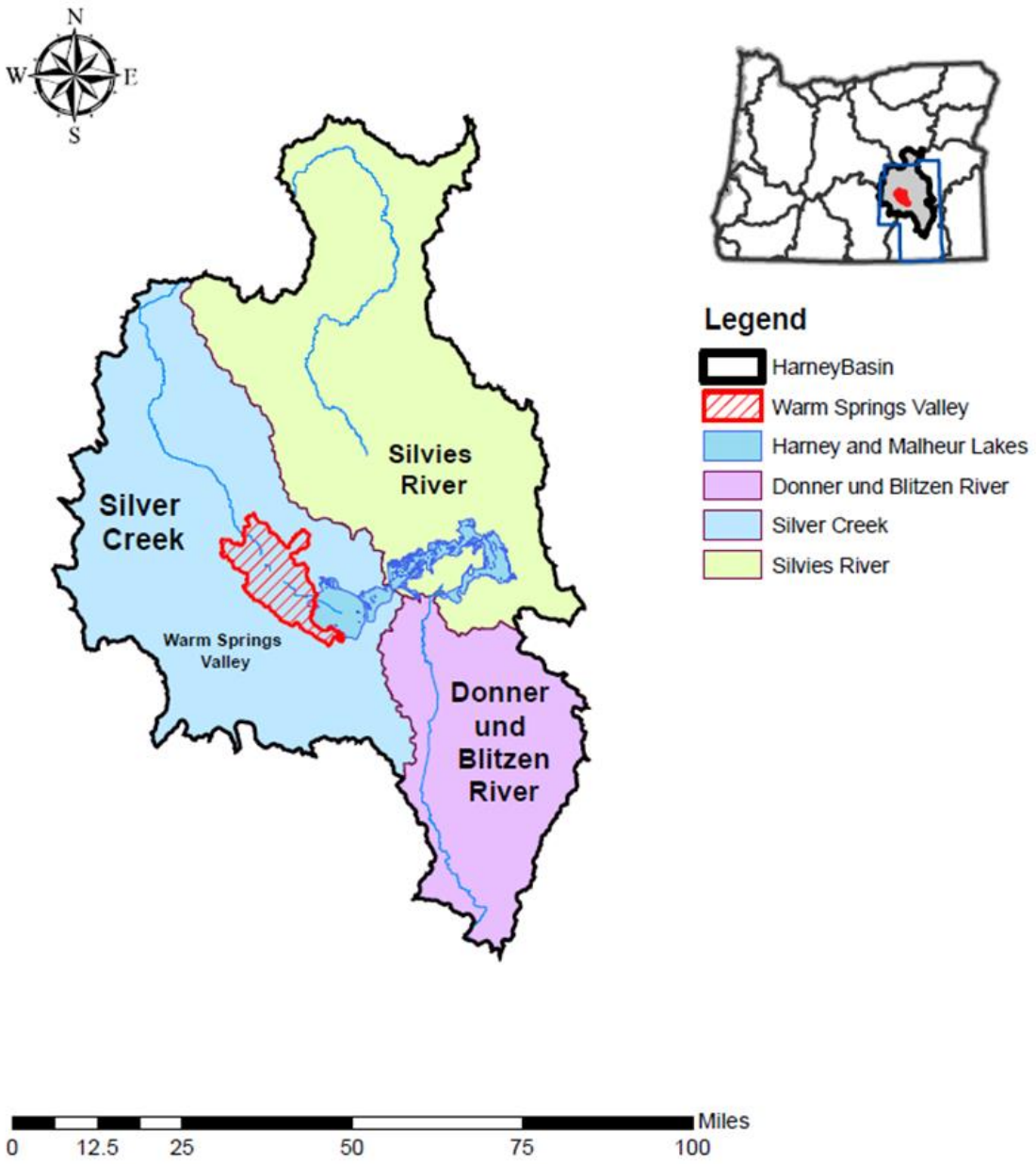

Figure 2: *Harney Basin Major River Drainages.* Harney Basin contains three major watersheds: the Donner und Blitzen River, the Silvies River, and Silver Creek. The WSV is located within the Silver Creek watershed. All three watersheds drain to Harney and Malheur Lakes in the center of the basin.

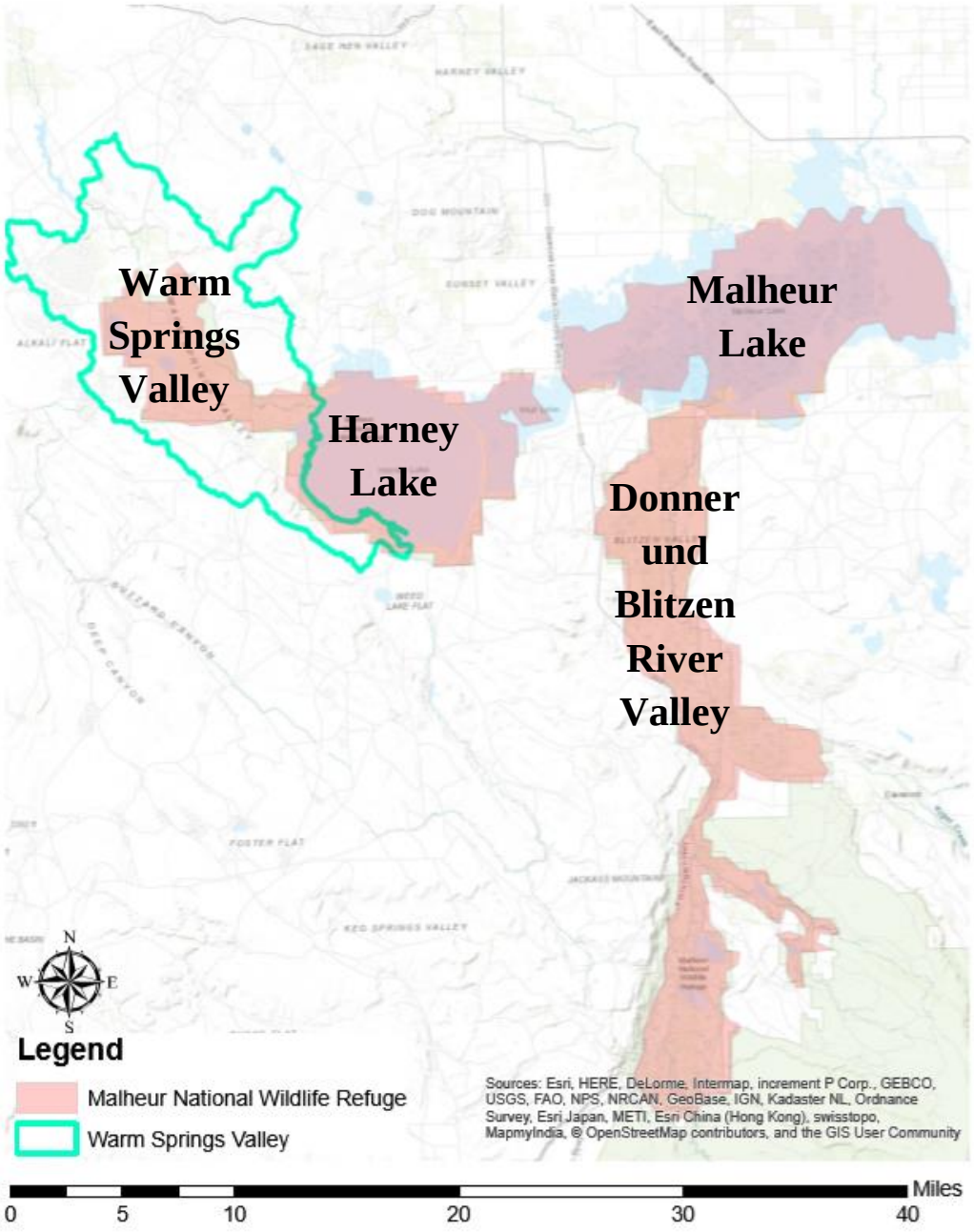

Figure 3: *Malheur National Wildlife Refuge.* Administrative units of the Malheur National Wildlife Refuge (red). The "Double 'O' Unit" is located within the Warm Springs Valley (Modified from: Rinella and Schuler, 1992).

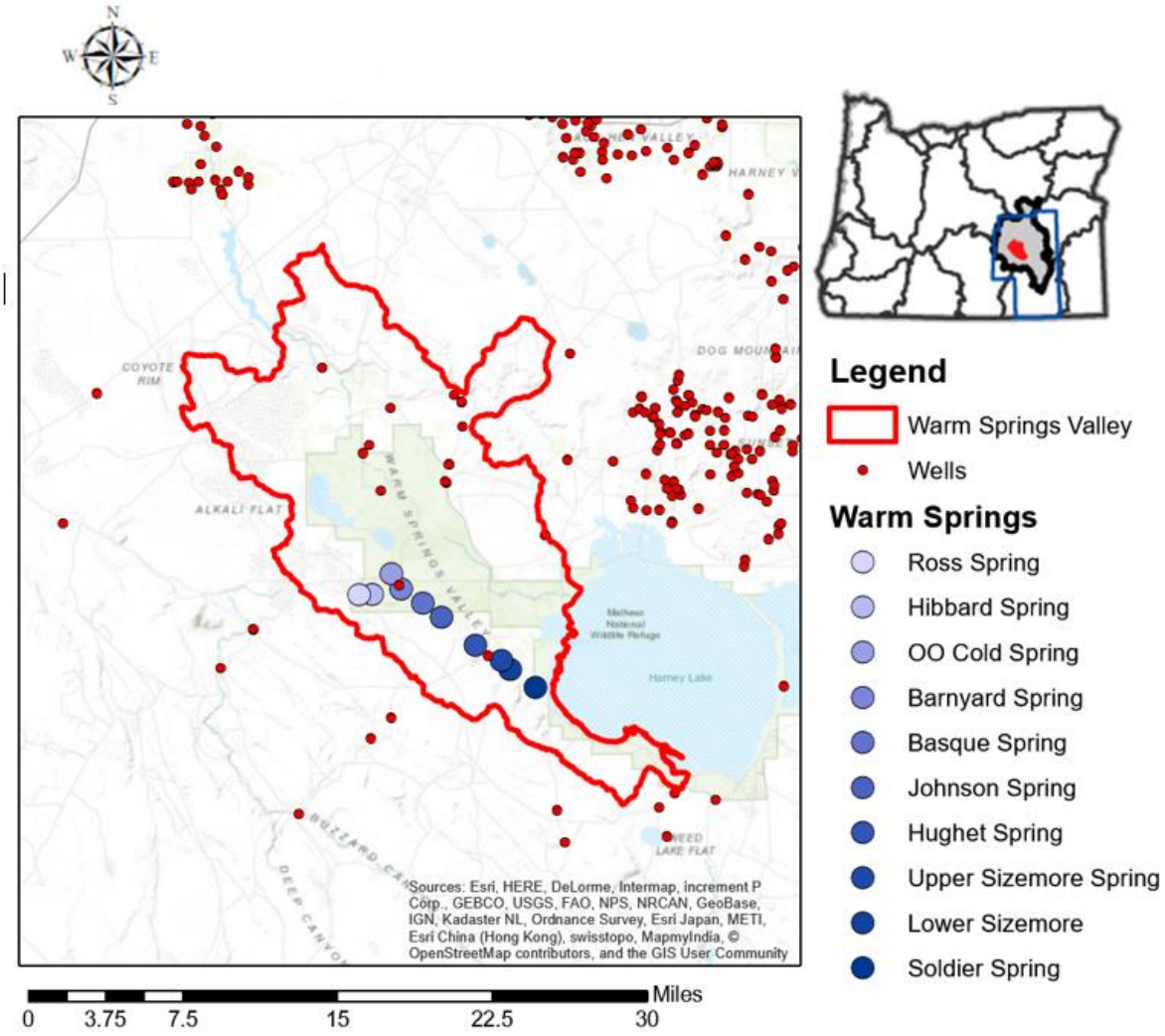

Figure 4: *Warm Springs Valley.* The Warm Springs Valley (WSV) lies directly to the west of Harney Lake. There are a number of springs (blue) near the southern boundary of the valley. Wells (red) are sparse to the southwest of the WSV and slightly clustered in the northern portion of the WSV. Wells to the northwest are clustered within the Silver Creek valley and to the east just north of Harney Lake in the Weaver Springs area. The outline of the WSV is a combination of two HUC-12 outlines modified from Seaber et al. (1987).

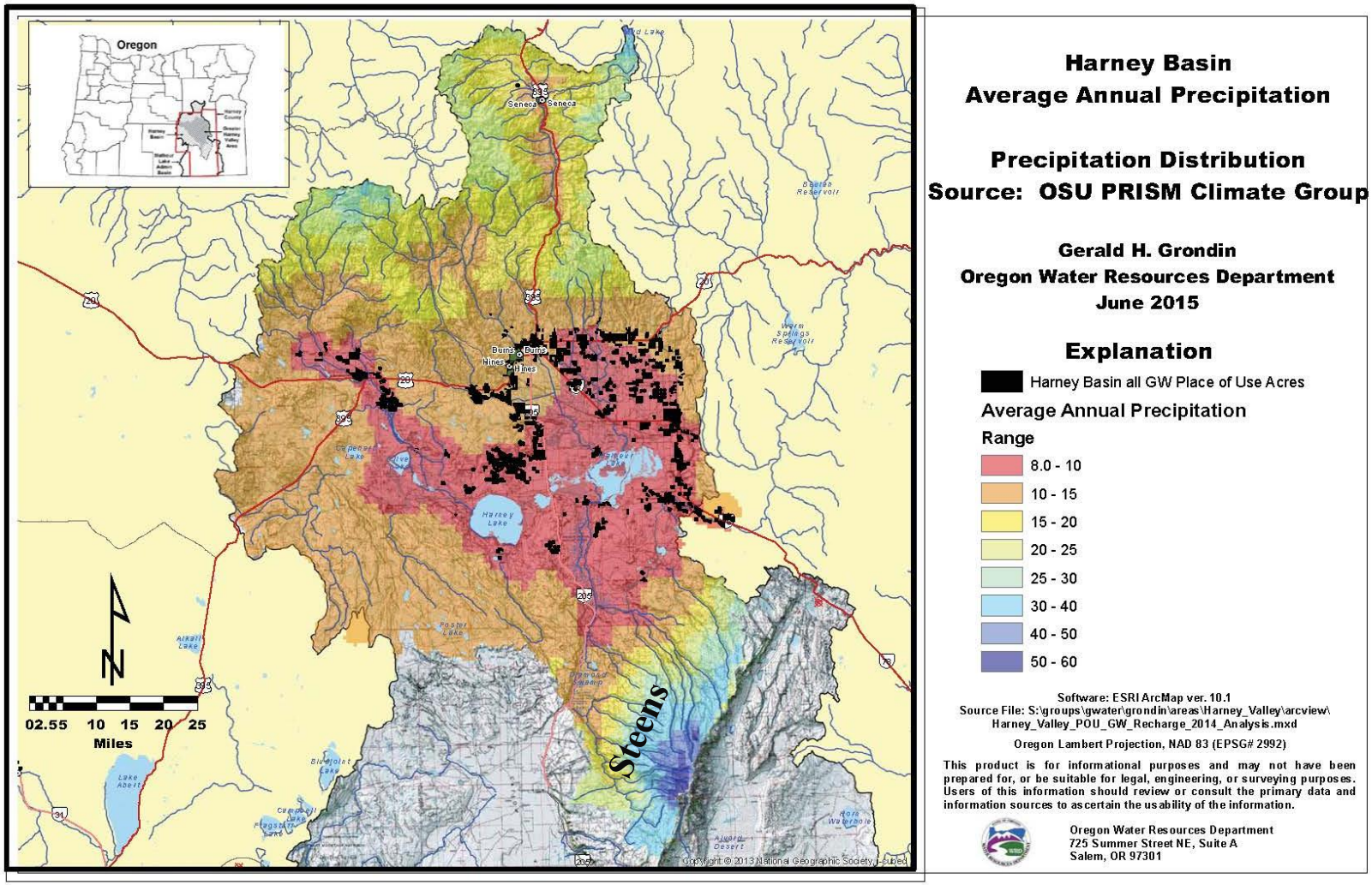

Figure 5: *Harney Basin Annual Precipitation.* Map of PRISM precipitation data (inches) from OWRD (2015). The highest average annual precipitation is found on the Steens Mountains to the southeast.

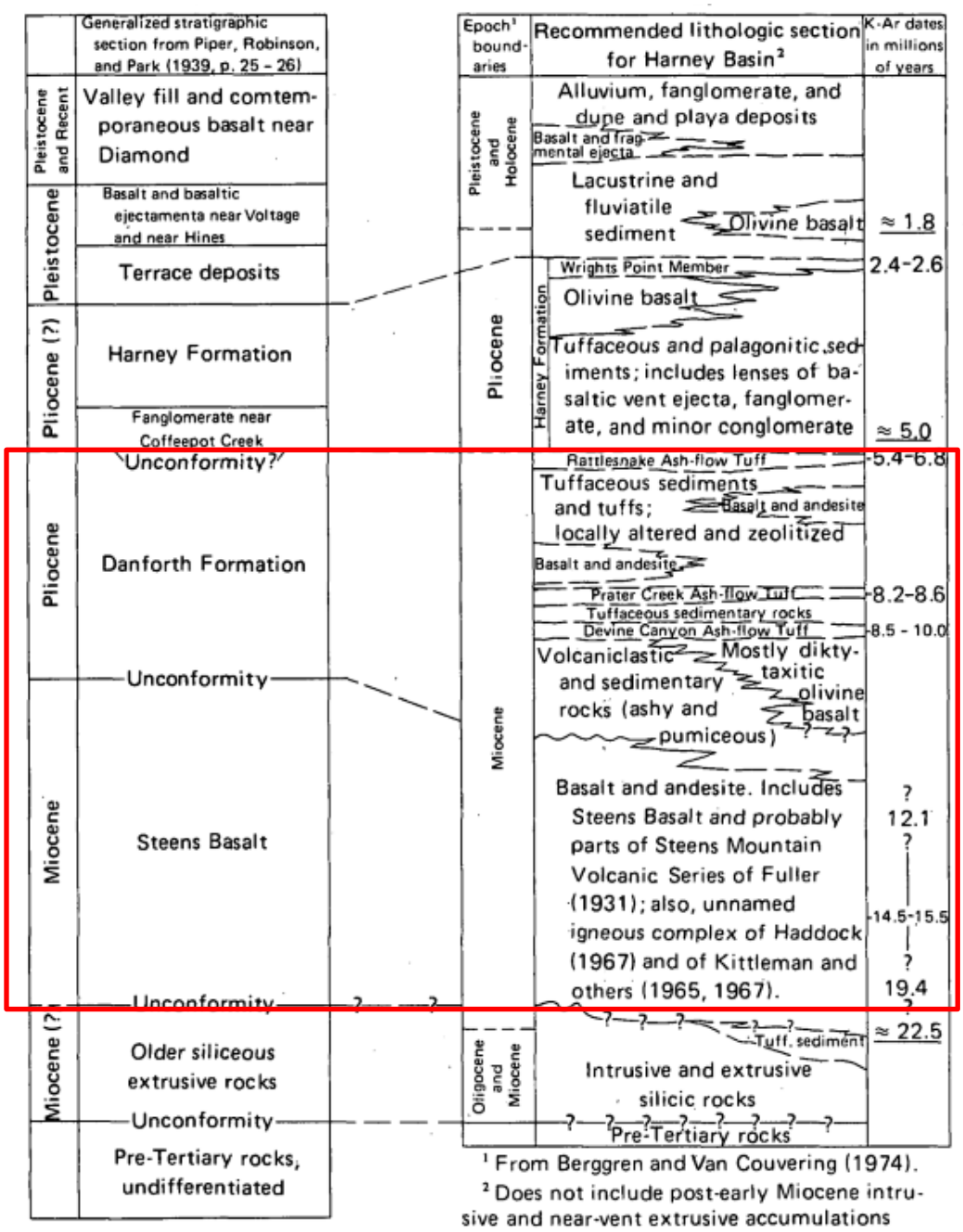

Figure 6: *Generalized Stratigraphic Column.* Generalized stratigraphic column of the Harney Basin from Walker, 1979 (right) compared to Piper et al., 1939 (left). The red box indicates the units noted in Piper et al., 1939 to appear within the Warm Springs Valley and their associated units in the revised stratigraphic section (Modified from Walker, 1979).

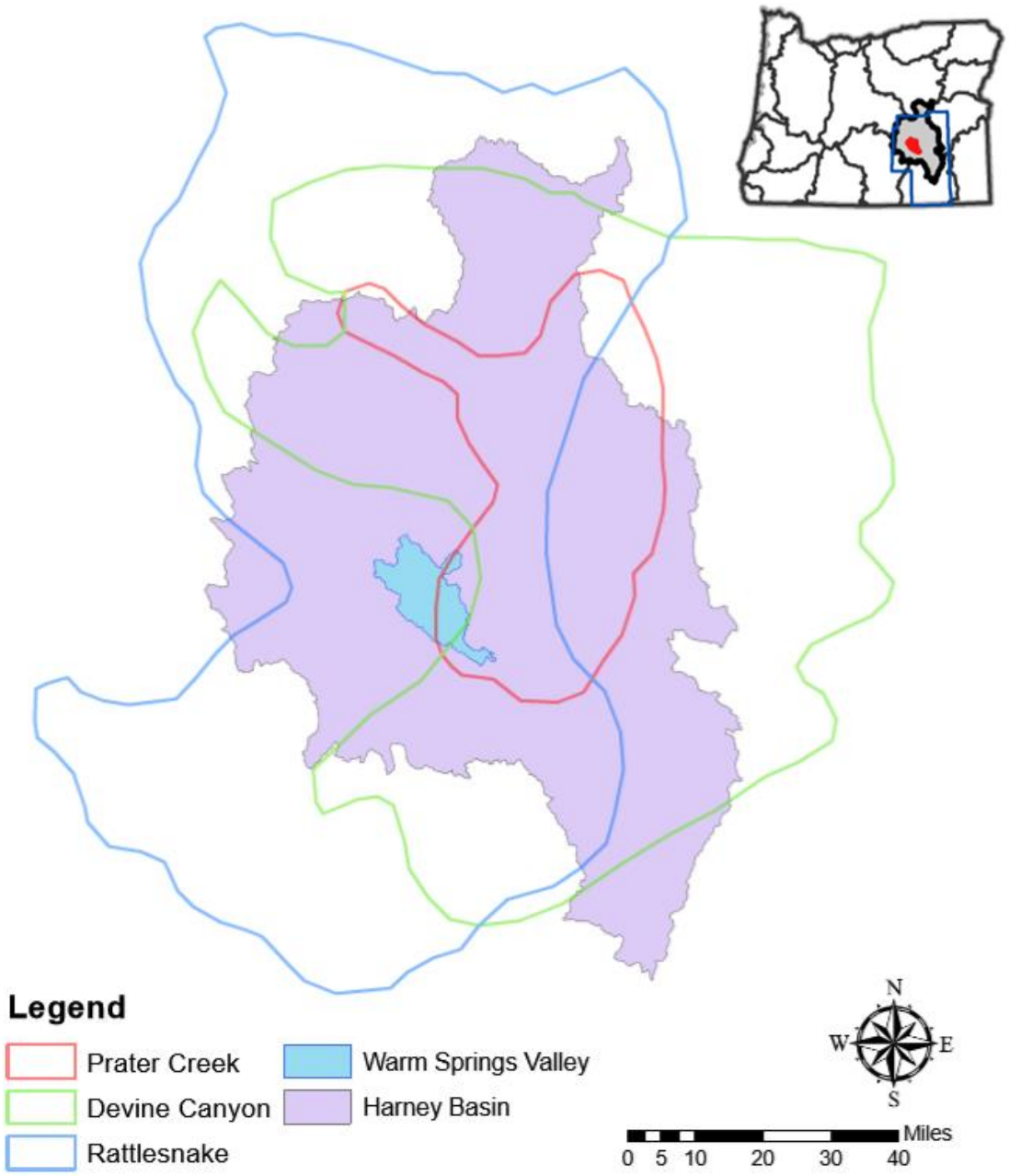

Figure 7: *Extents of Major Ash-Flow Tuffs.* Extents of Devine Canyon (green), Prater Creek (red), and Rattlesnake (blue) ash-flow tuffs underlying the Malheur Lake Basin (Modified from: Walker, 1979).

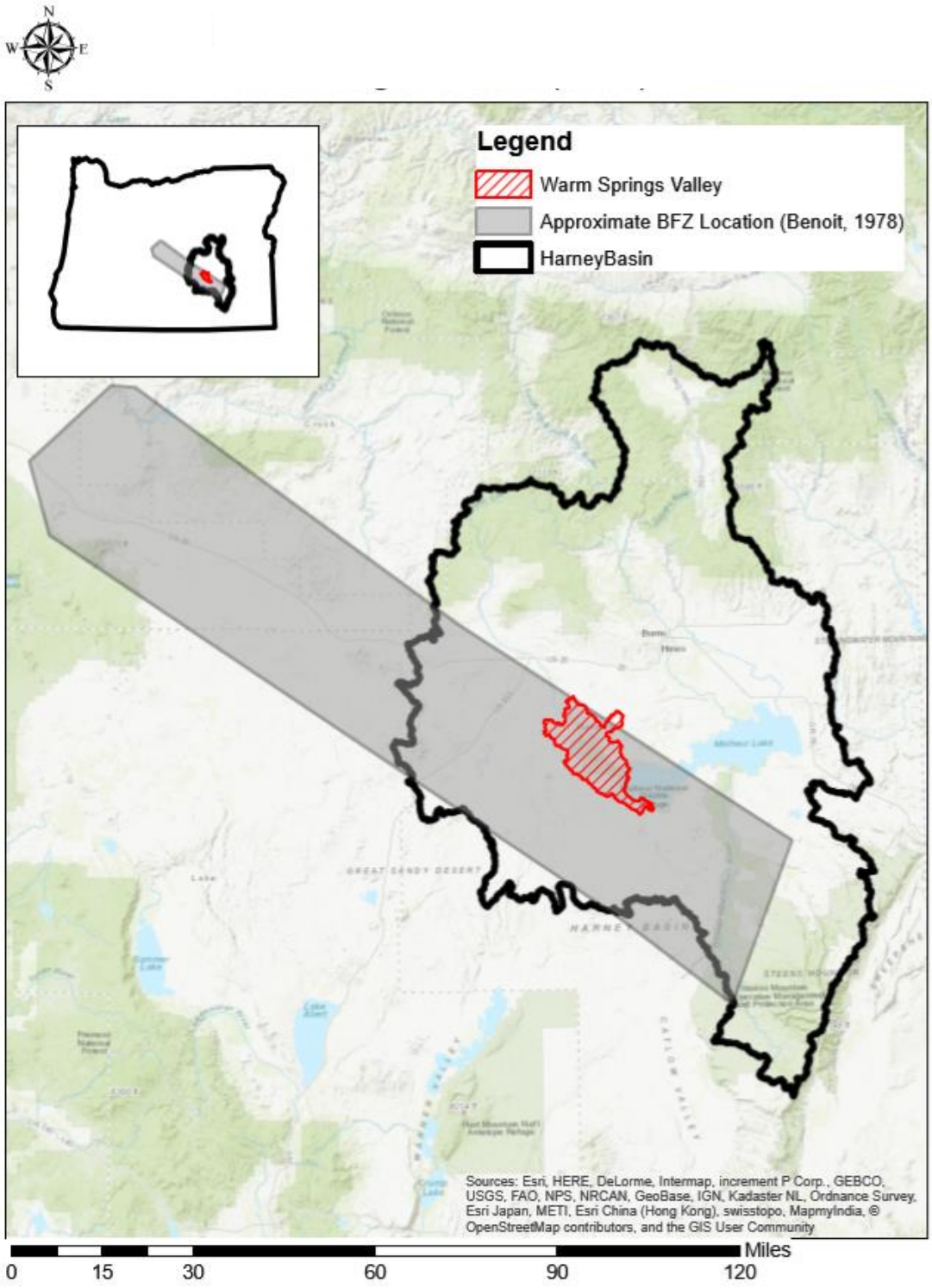

Figure 8: *Approximate Location of BFZ.* Approximate location of the Brothers Fault Zone (BFZ) in relation to Harney Basin modified from Benoit (1978).

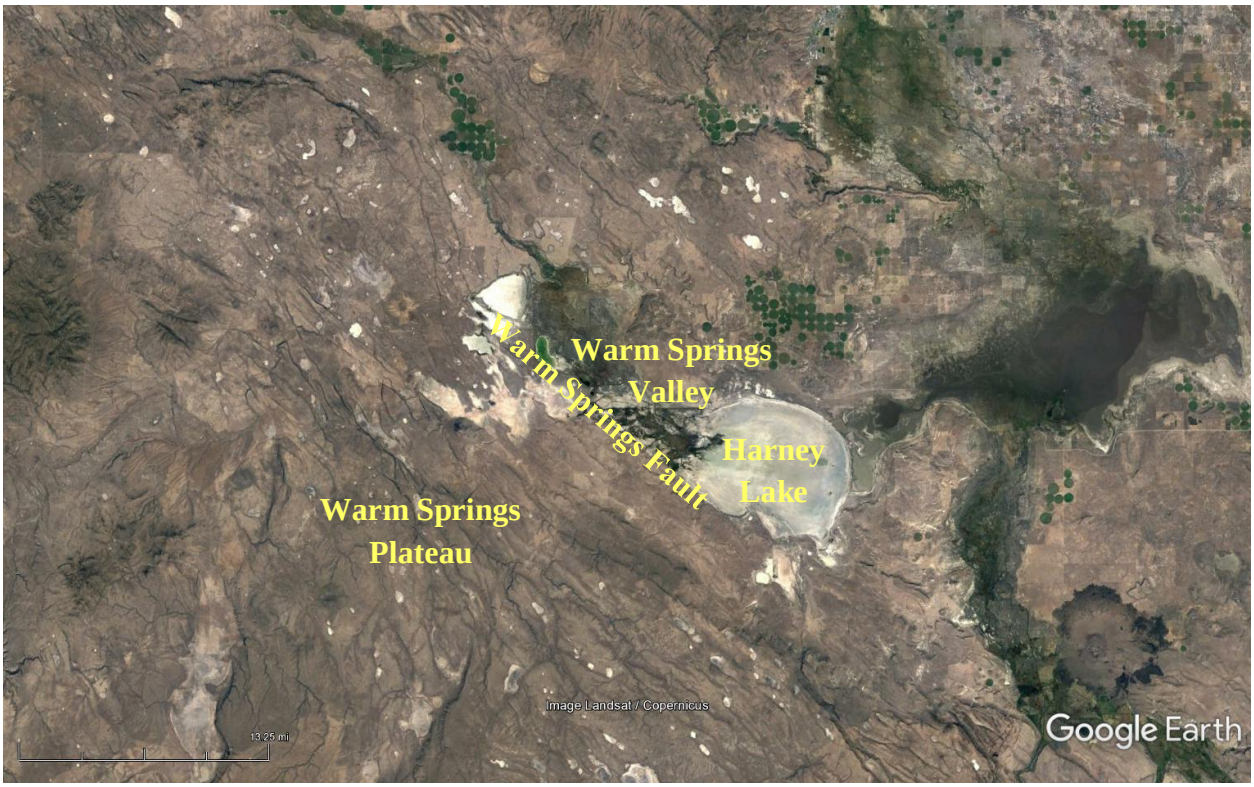

Figure 9: *Terminology used in this Paper.* Locations mentioned in this report. The Warm Springs Valley is located to the northwest of Harney Lake, which lies in the center of the Harney Basin. The area to the southwest of the Warm Springs Valley and the fault on the southwest margin of the Warm Springs Valley do not currently have common names and are refered to in this report as the "Warm Springs Plateau" and "Warm Springs Fault."

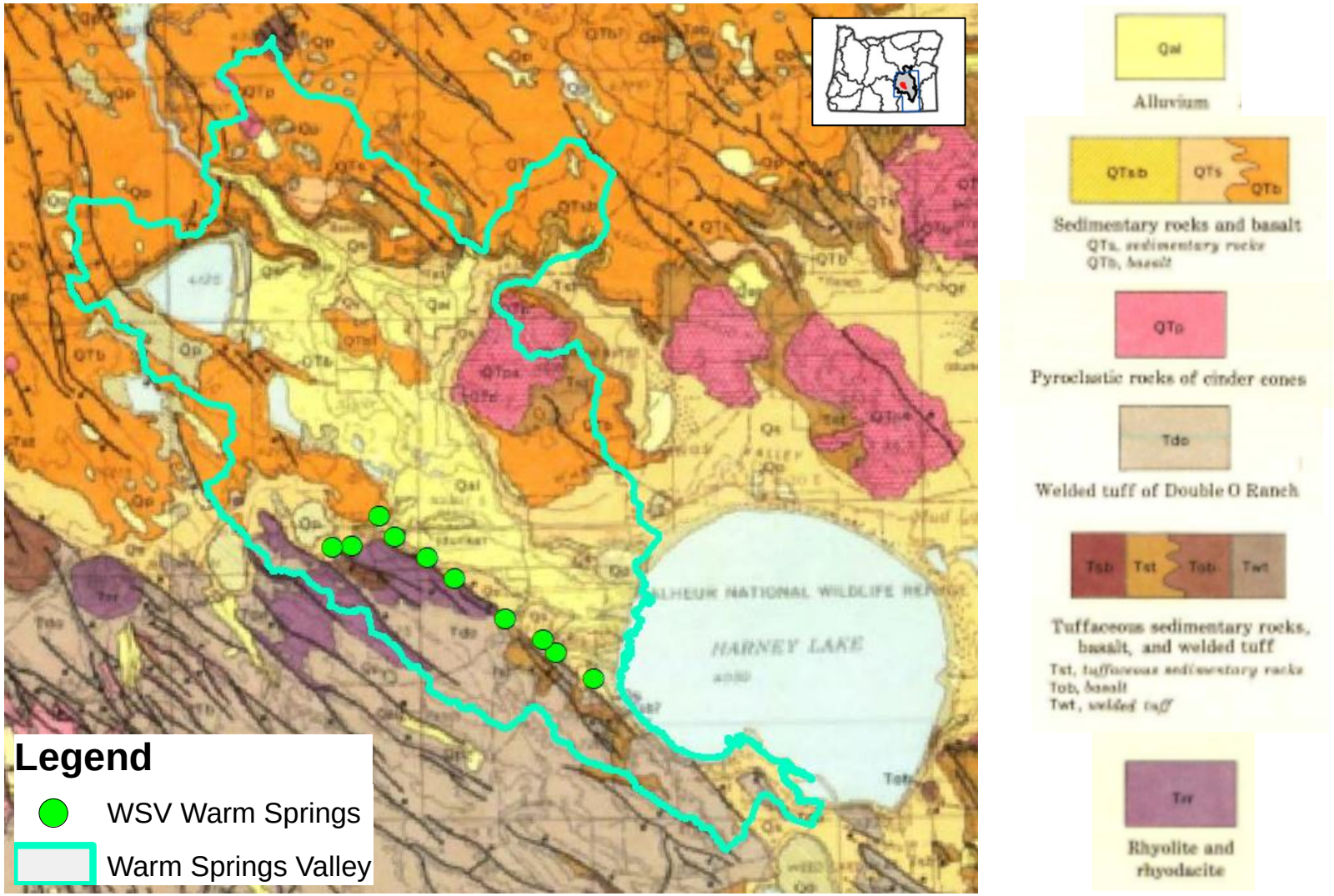

Figure 10: *1972 Geologic Map.* Geologic map of Warm Springs Valley (Modified from: Greene et al., 1972).

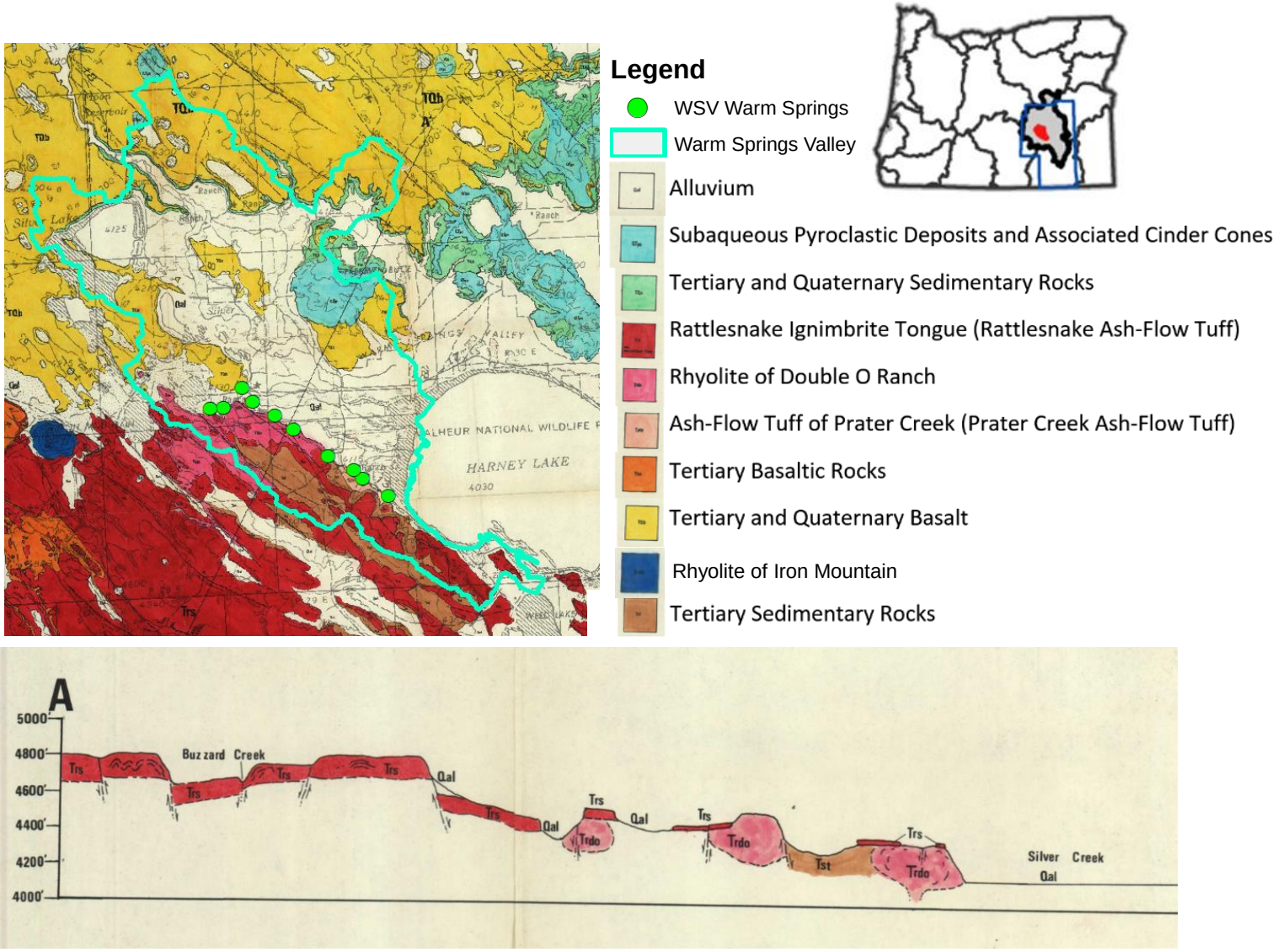

Figure 11: *1974 Geologic Map and Cross Section.* Geologic map and cross section along the Warm Springs Valley (Modified from Parker, 1974).

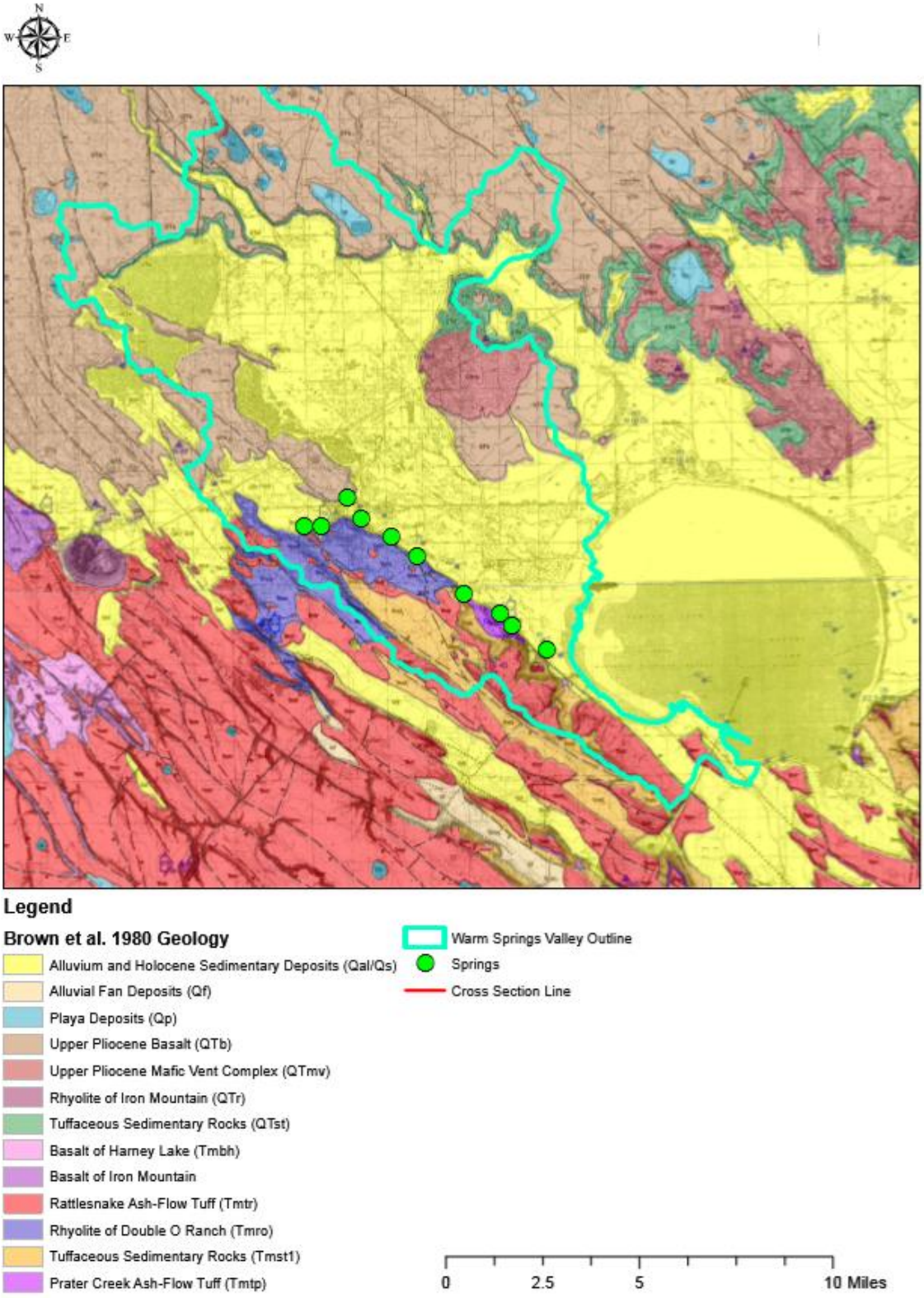

Figure 12: *1980 Geologic Map.* Geologic map modified from Brown et al. (1980a and b). Colors were assigned randomly.

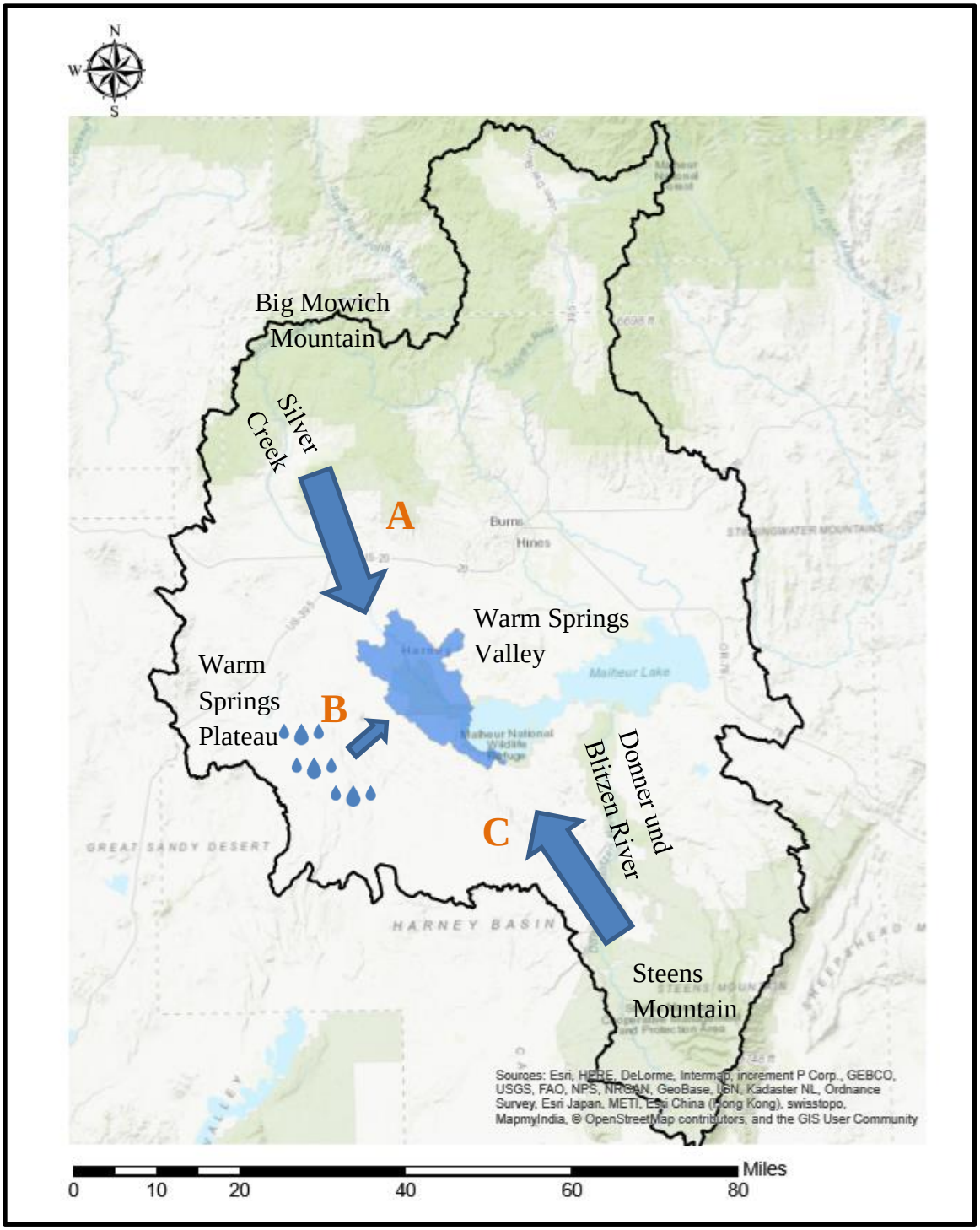

Figure 13: *Possible Source Locations for Warm Springs Water.* Potential spring water sources include shallow surface water infiltration from Silver Creek and its tributaries flowing into the subsurface to the WSV from the northwest (Source A), precipitation infiltration and deep circulation from precipitation along the Brothers Fault Zone to the southwest of the WSV (Source B), and deep groundwater flow from the Steens Mountains (Source C).

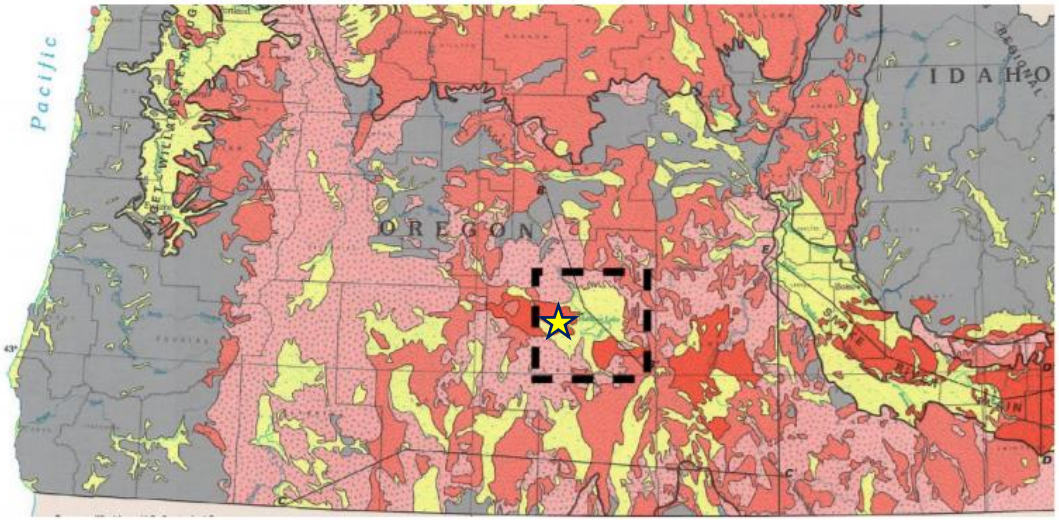

Aquifers of the Harney Basin (Modified from Gonthier, 1984) indicate a central unconsolidated deposit aquifer surrounded by a broad volcanic and sedimentary aquifer with zones of Pliocene and younger basaltic rocks.

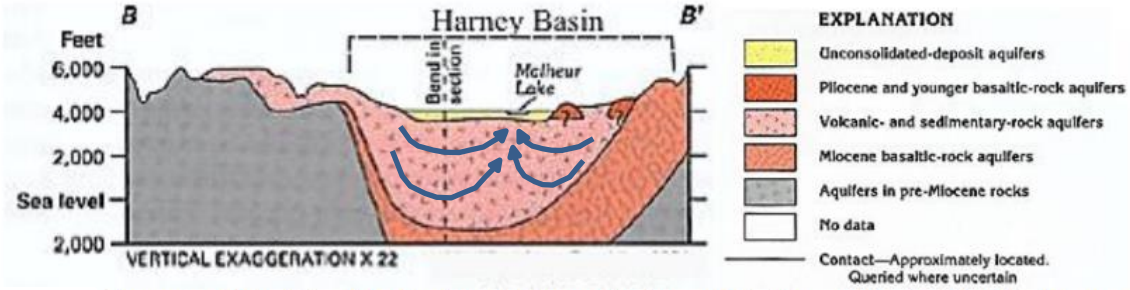

Conceptual Models of the Basin and Range Geology of the Harney Basin (Modified from Gonthier, 1984)

Figure 14: *Harney Basin Conceptual Groundwater Model.* Conceptual geologic model modified from Gonthier (1984) and Smitherman (2015). A star shows the general location of the WSV. Proposed groundwater flow paths (blue arrows) were added in the "volcanic and sedimentary rock aquifers" unit traveling toward Malheur Lake from higher elevations to the northwest and the southeast.

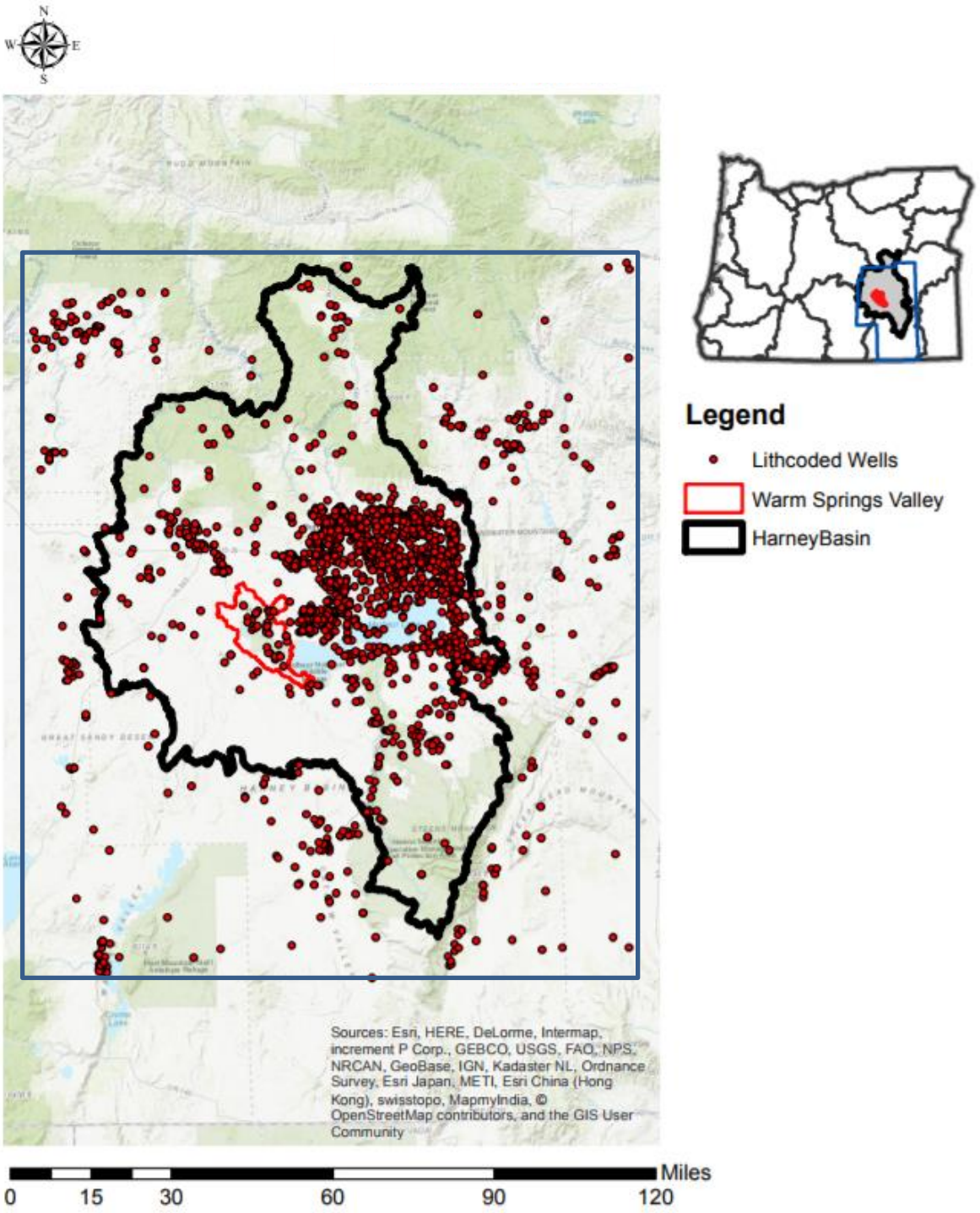

Figure 15*: Lithcoded Wells.* Wells in and around Harney Basin that have been lithcoded, meaning that a well log exists for the well and the lithology reported on the log has been entered into the OWRD database. There are 2,296 wells shown here. Some wells that are measured regularly as part of the Harney Basin Groundwater Investigation are located outside the basin. A box was drawn around the basin to include these wells. Additional wells located within the boxed area are included in this figure.

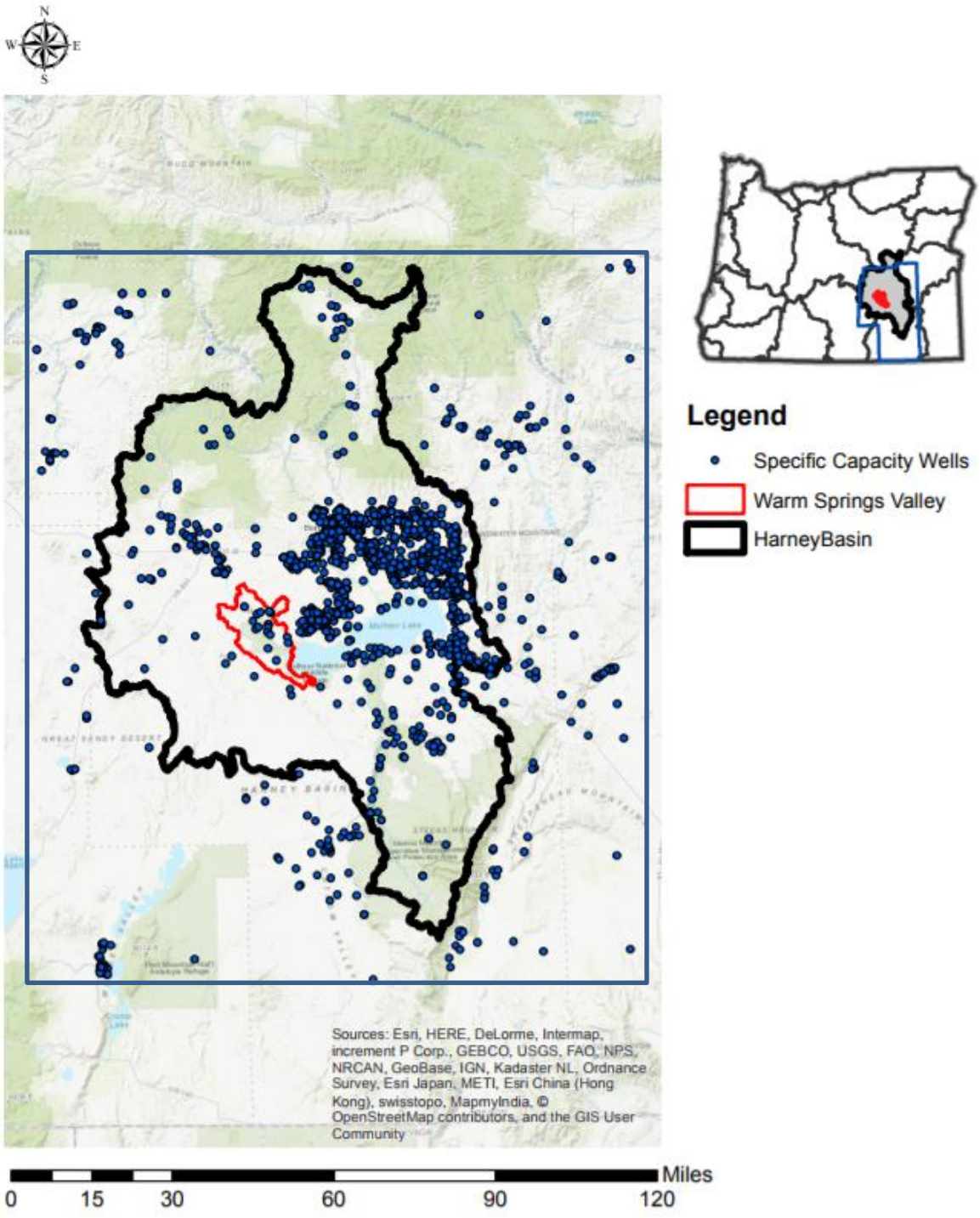

Figure 16: *Wells with Pump Tests for Estimating Specific Capacity and Transmissivity.* Wells in and around Harney Basin that have pump or bailer test data that can be used to calculate specific capacity and transmissivity. There are 1,462 wells shown here. Some wells that are measured regularly as part of the Harney Basin Groundwater Investigation are located outside the basin. A box was drawn around the basin to include these wells. Additional wells located within the boxed area are included in this figure.

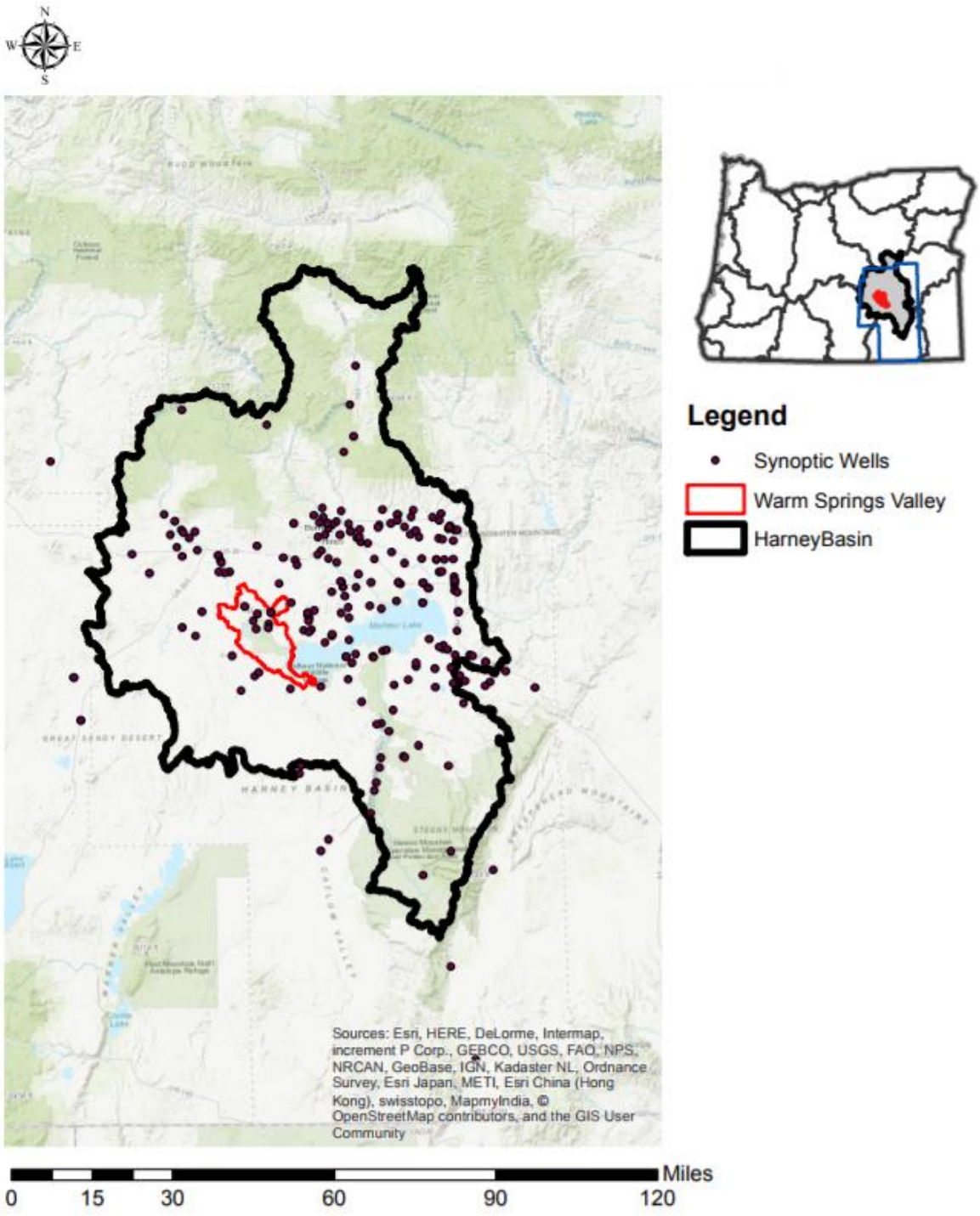

Figure 17: *2017 Fall Synoptic Wells with Static Water Level Measurements.* Wells measured for static water levels in late October and early November. OWRD staff made 223 static groundwater level measurements in 218 wells in and around Harney Basin as a part of the 2017 Fall Synoptic.

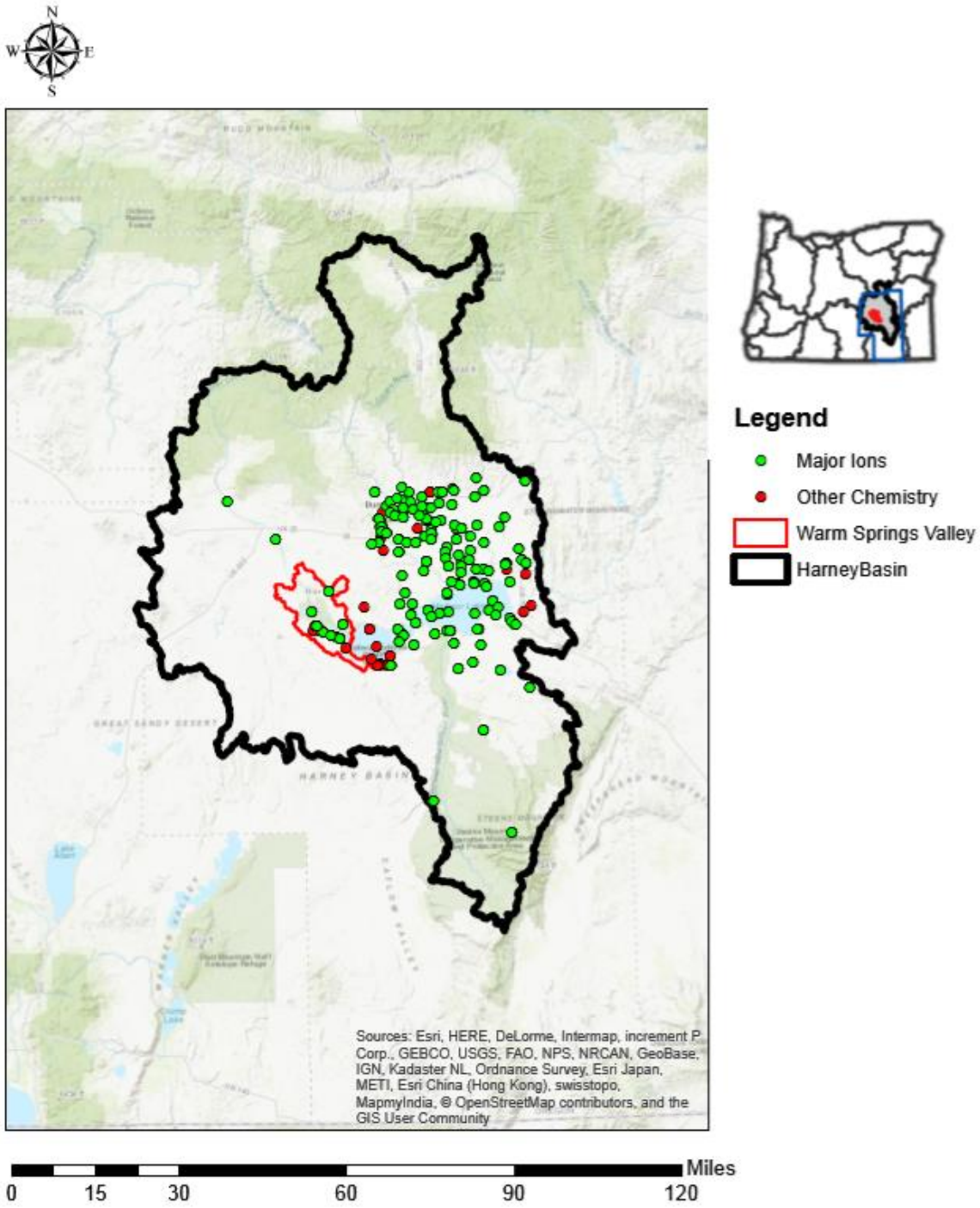

Figure 18: *Published Chemical Analyses in Harney Basin.* Within Harney Basin, 209 spring and well samples have published chemical analysis data. Of these 209 samples, 159 include major ion concentrations needed to plot Piper diagrams.

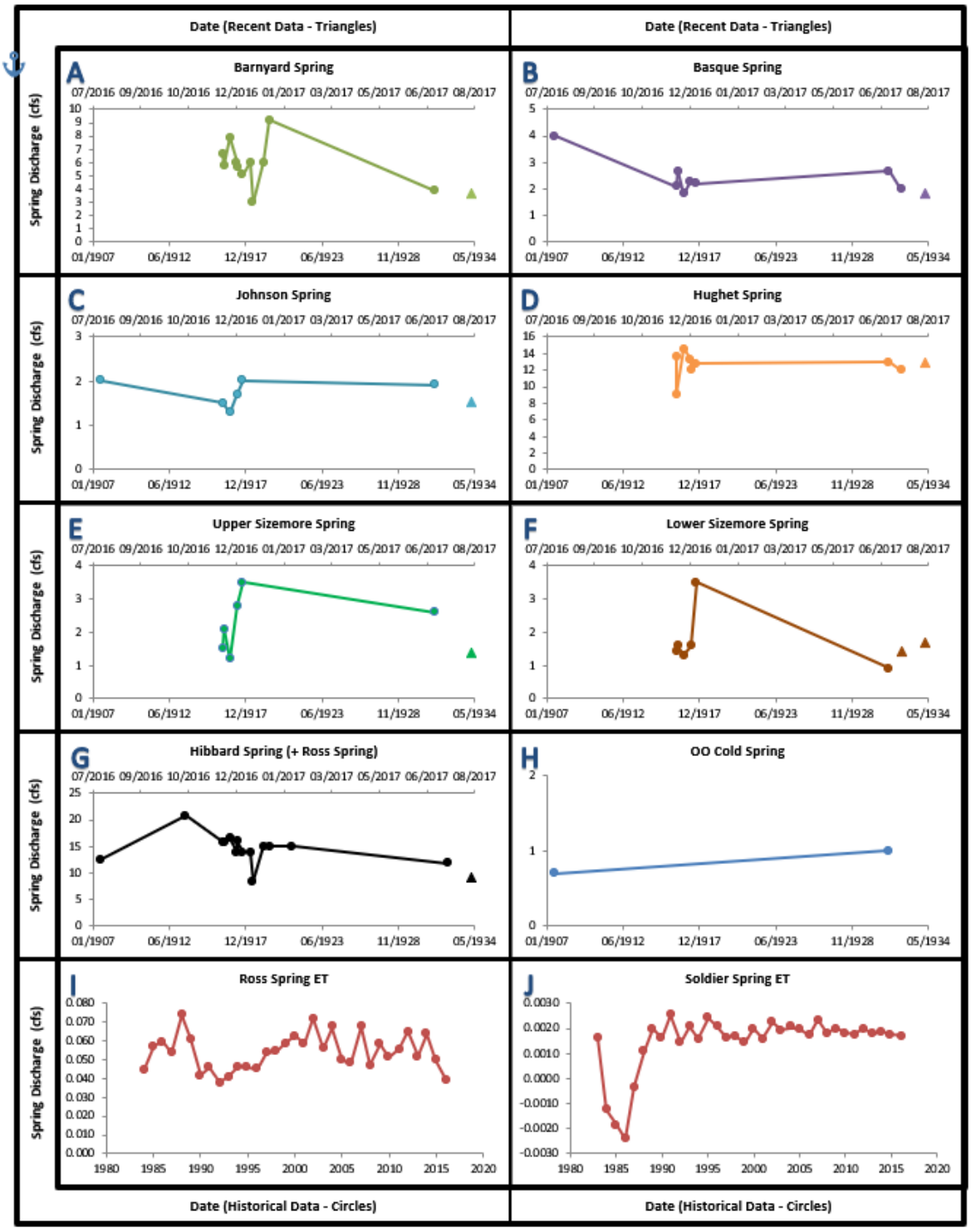

Figure 19: *Historical and Recently Measured Spring Discharge.* Spring discharge measurements for WSV springs. Circles indicate historical discharge either reported or estimated as ET. Triangles are plotted next to historical measurements and indicate measurements taken during the summer of 2017.

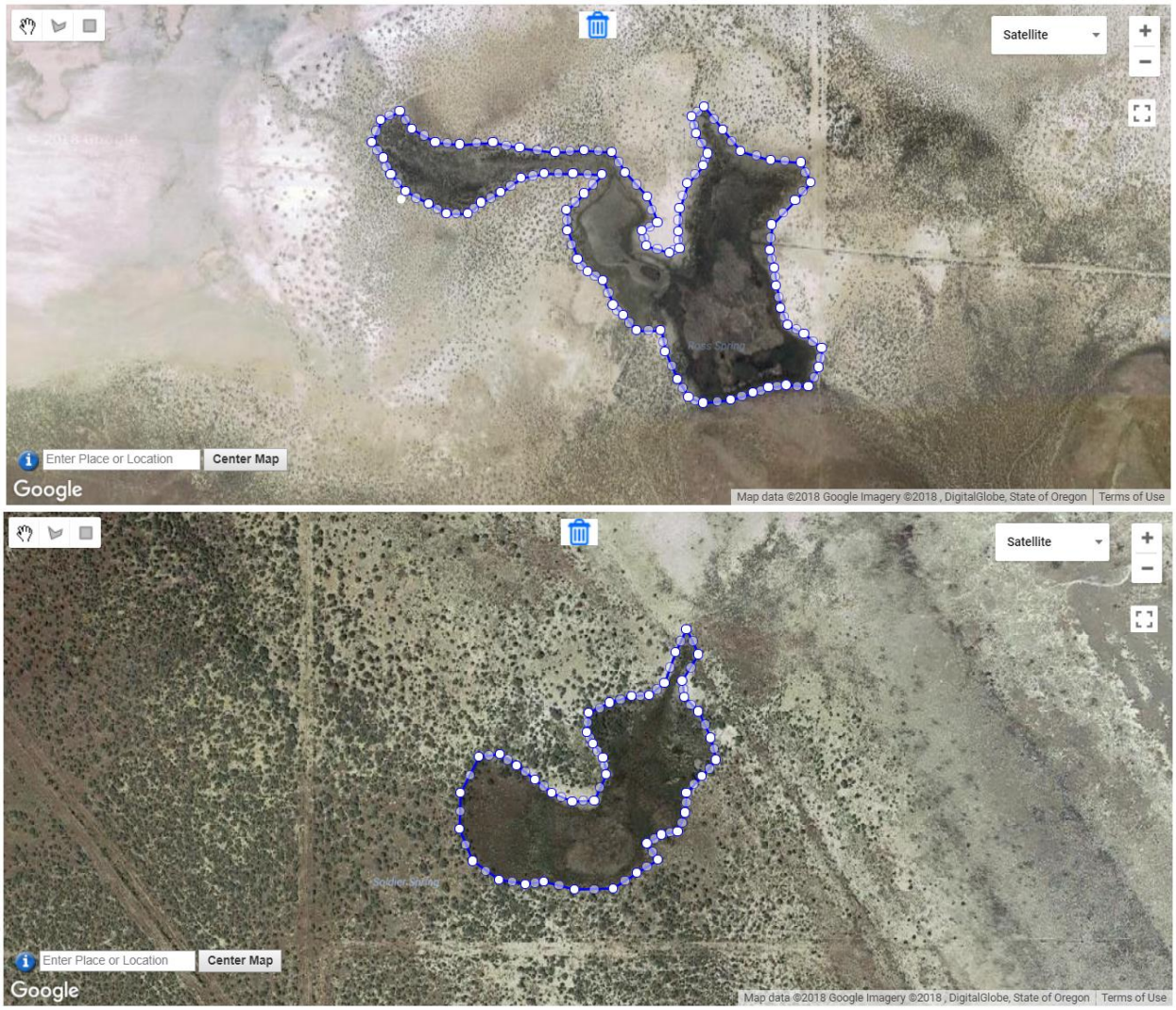

Figure 20: *Ross and Soldier Springs Polygons for Groundwater ET Calculations.* Polygons used for evapotranspiration calculations at Ross Spring (top) and Soldier Spring (bottom) in Google Earth Engine. Polygon vertices can be found in Appendix B.

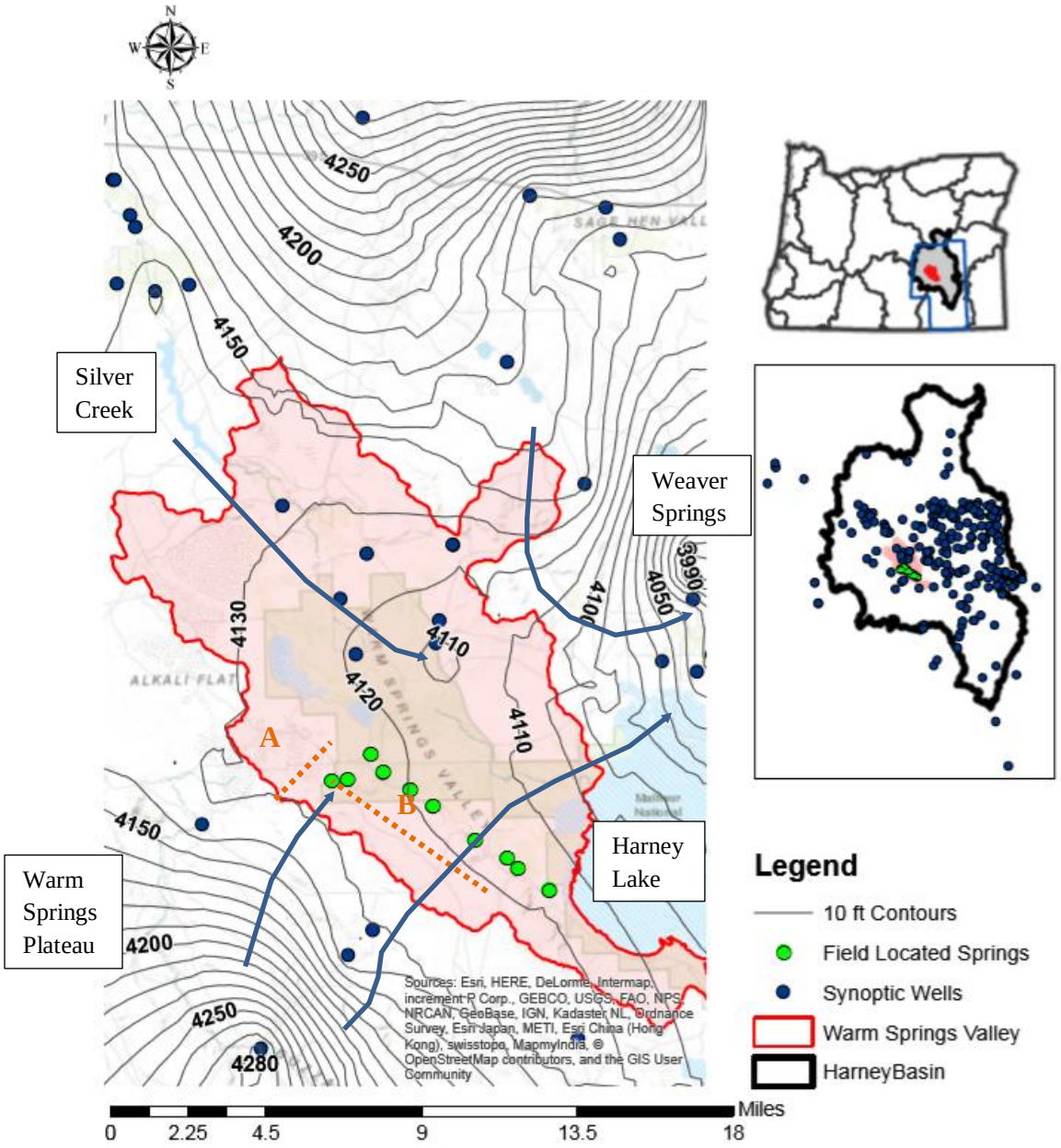

Figure 21: *Contours Interpolated for Static Water Levels in Fall 2017 Synoptic Wells.* Water level contour map generated using the Kriging tool in ESRI's ArcMap with static water level measurements taken during late October - early November spring elevations which, due to elevation uncertainties, were averaged to simplify calculations. All surface elevations were extracted from the USGS topographic map and uses the NGVD1929 datum. Springs are grouped in to A and B based location between contour lines. Arrows show groundwater flow direction. The contour interval is 10 feet. Overall, the contouring suggests groundwater flow toward the springs is coming from two directions: from the southwest plateau and down the Silver Creek watershed drainage to the northwest. Groundwater then flows southeast toward Harney Lake and then curves northeast toward the Weaver Springs area.

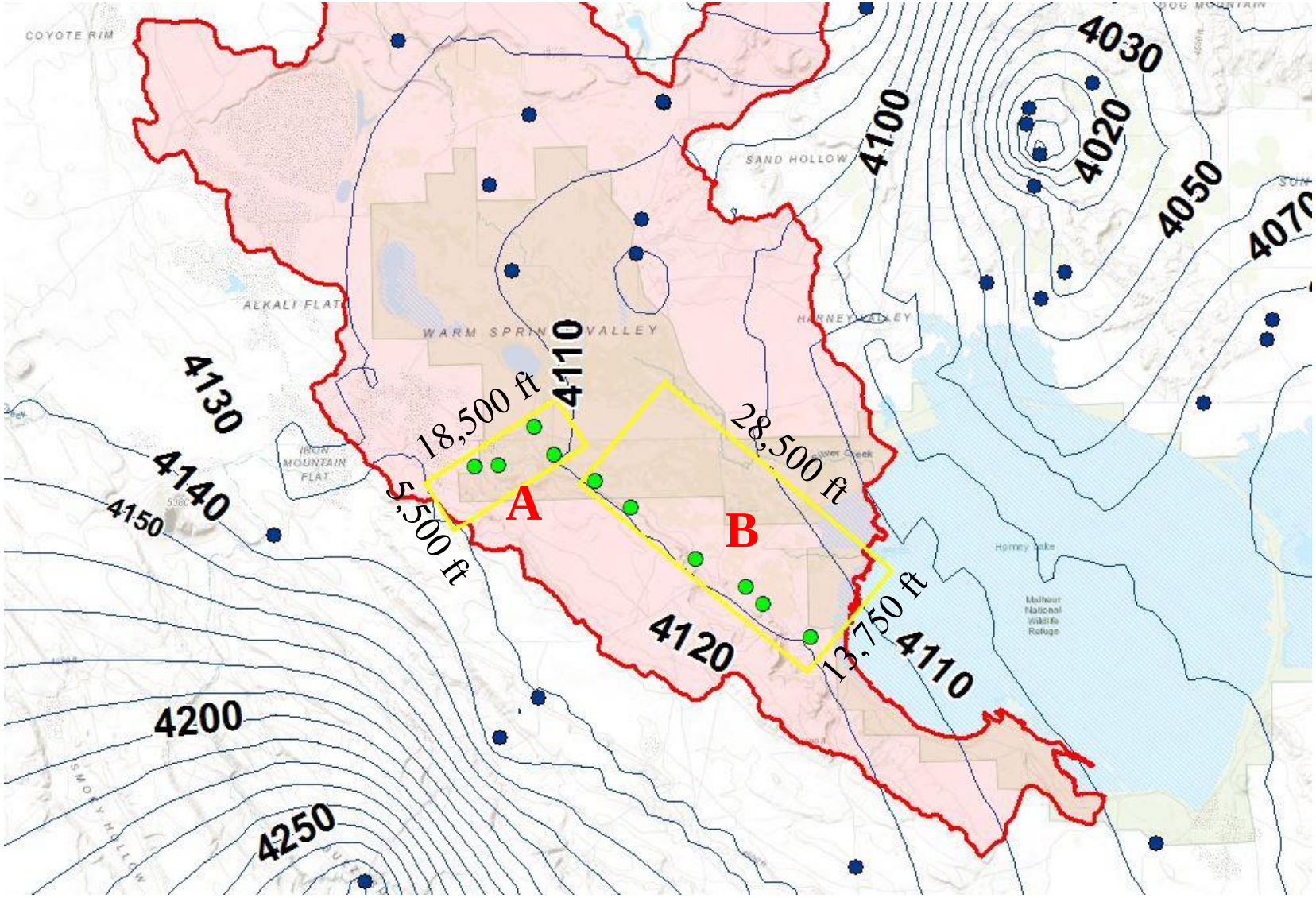

Figure 22: *Horizontal Hydraulic Gradient Calculations.* Based on relative locations between contour lines, boxes were drawn around Groups A and B with sides approximately parallel to contour lines to estimate dh (box's length) and w (box's width).

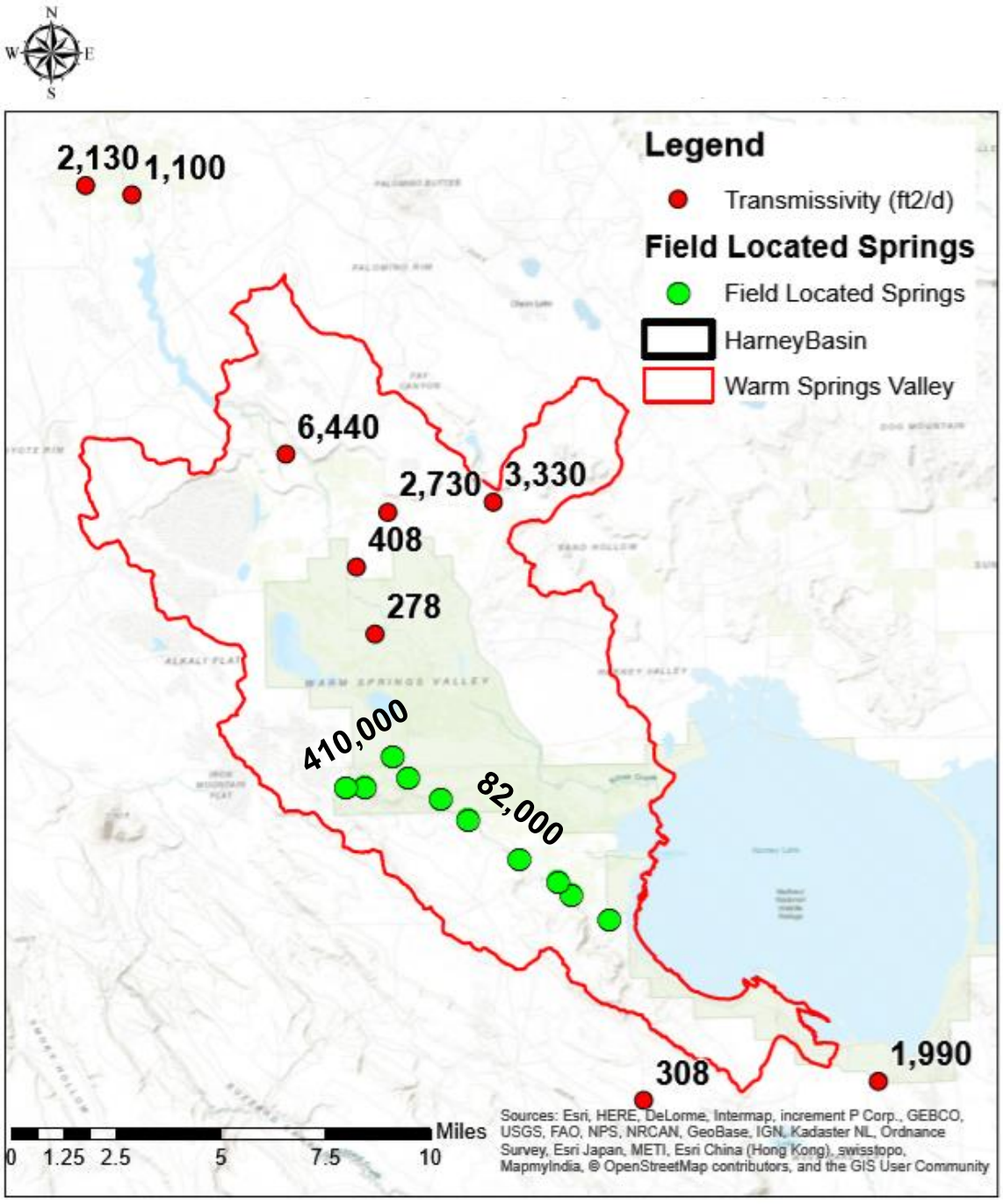

Figure 23: *Transmissivities Calculated at Wells and Springs.* Locations of wells in and around the WSV with pump tests from which a transmissivity value was calculated. Transmissivities are shown in ft^2/day. Transmissivities calculated for each group of springs are also shown here. Transmissivities calculated for springs are one to three orders of magnitude greater than transmissivities calculated at wells.

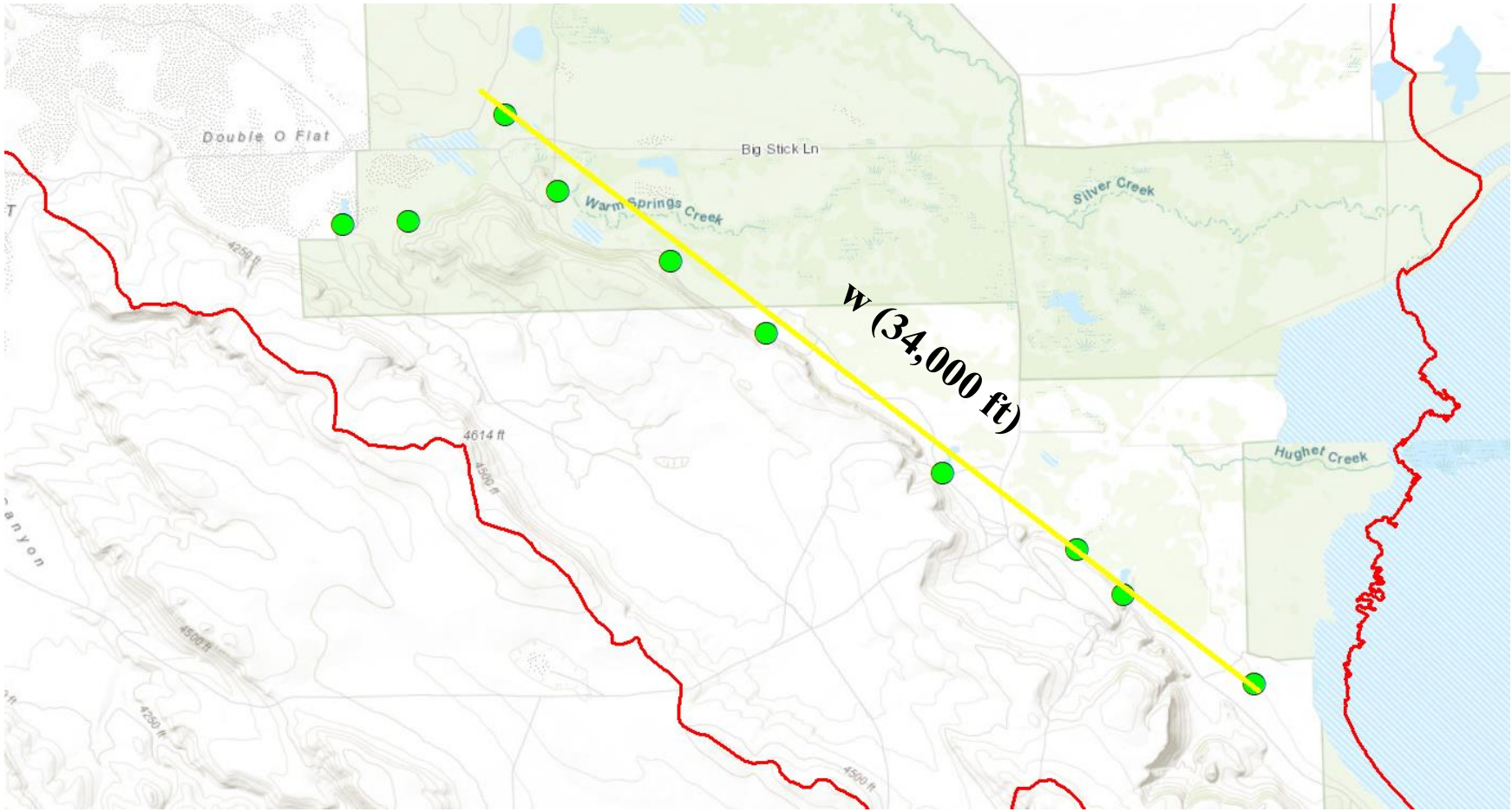

Figure 24: *Vertical Hydraulic Gradient Calculations.* A line was drawn between eight of the ten warm springs with a length of about 34,000 ft (w in Equation 6).

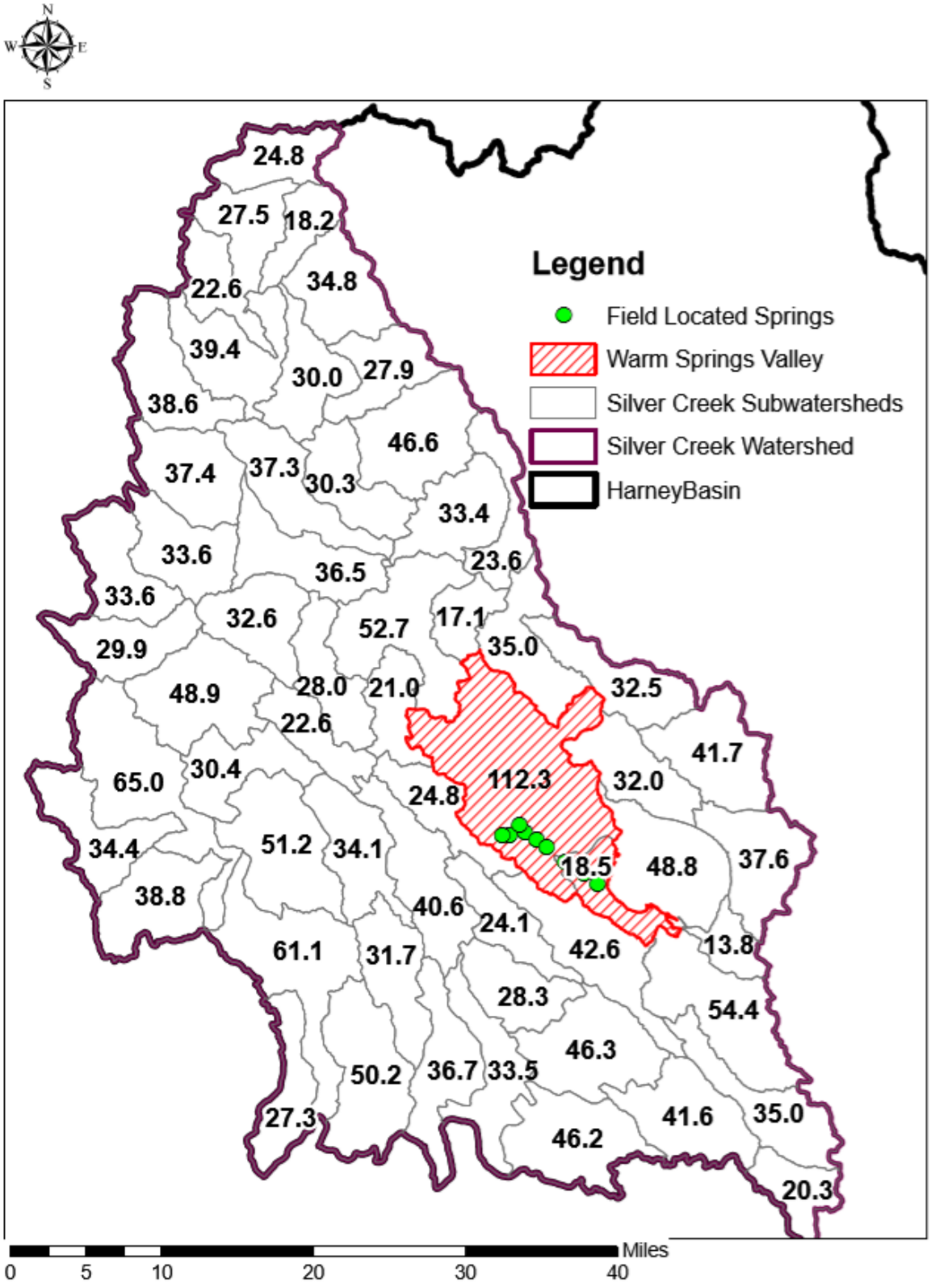

Figure 25: *Areas of Subwatersheds in Silver Creek Watershed.* Areas are in square miles. Subwatersheds are based on HUC-12 delineation (Seaber et al., 1987).

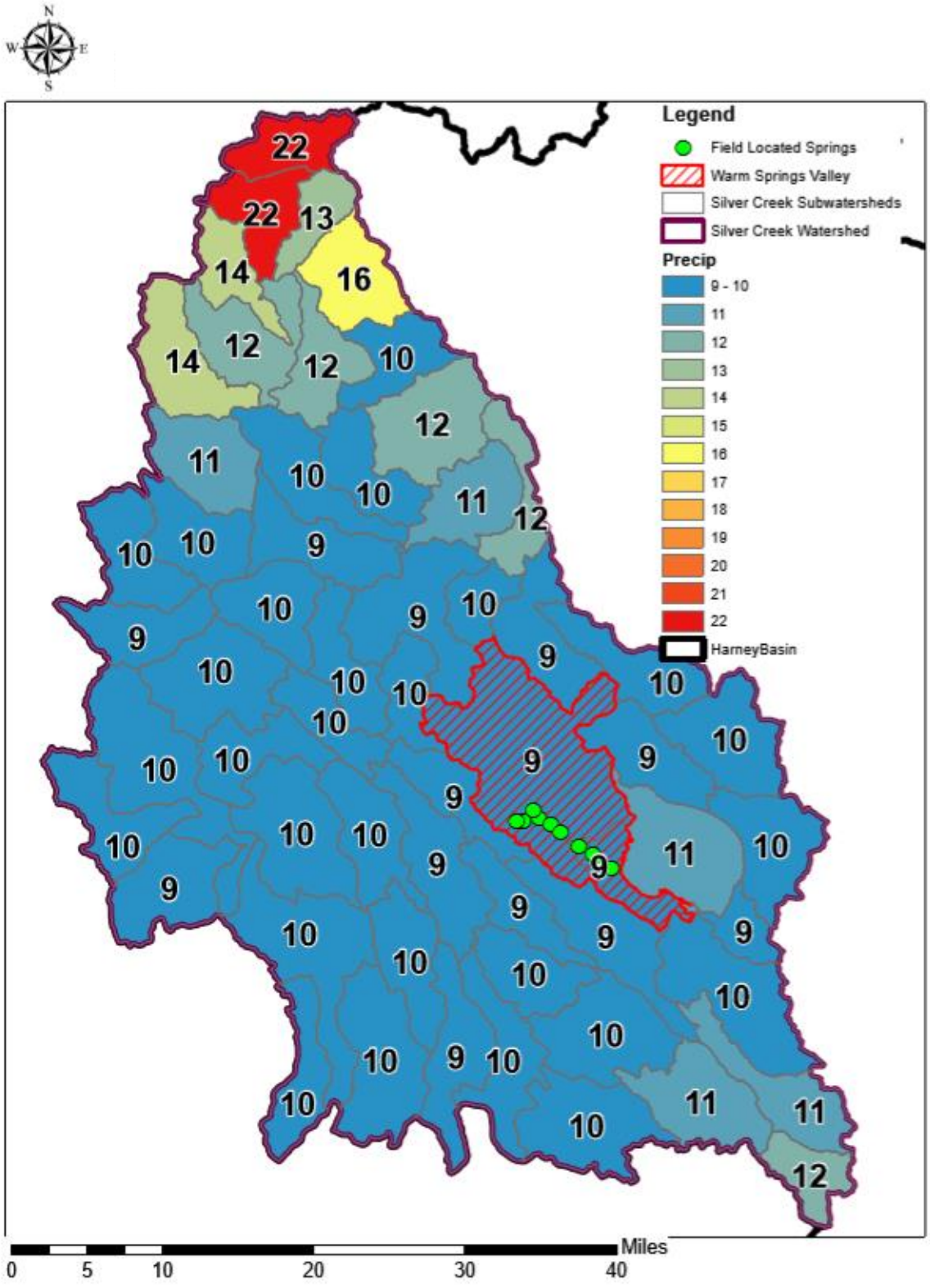

Figure 26: *Average Annual Precipitation for Silver Creek Subwatersheds.* Precipitation for each subwatershed is in inches. Subwatersheds are based on HUC-12 delineation (Seaber et al., 1987).

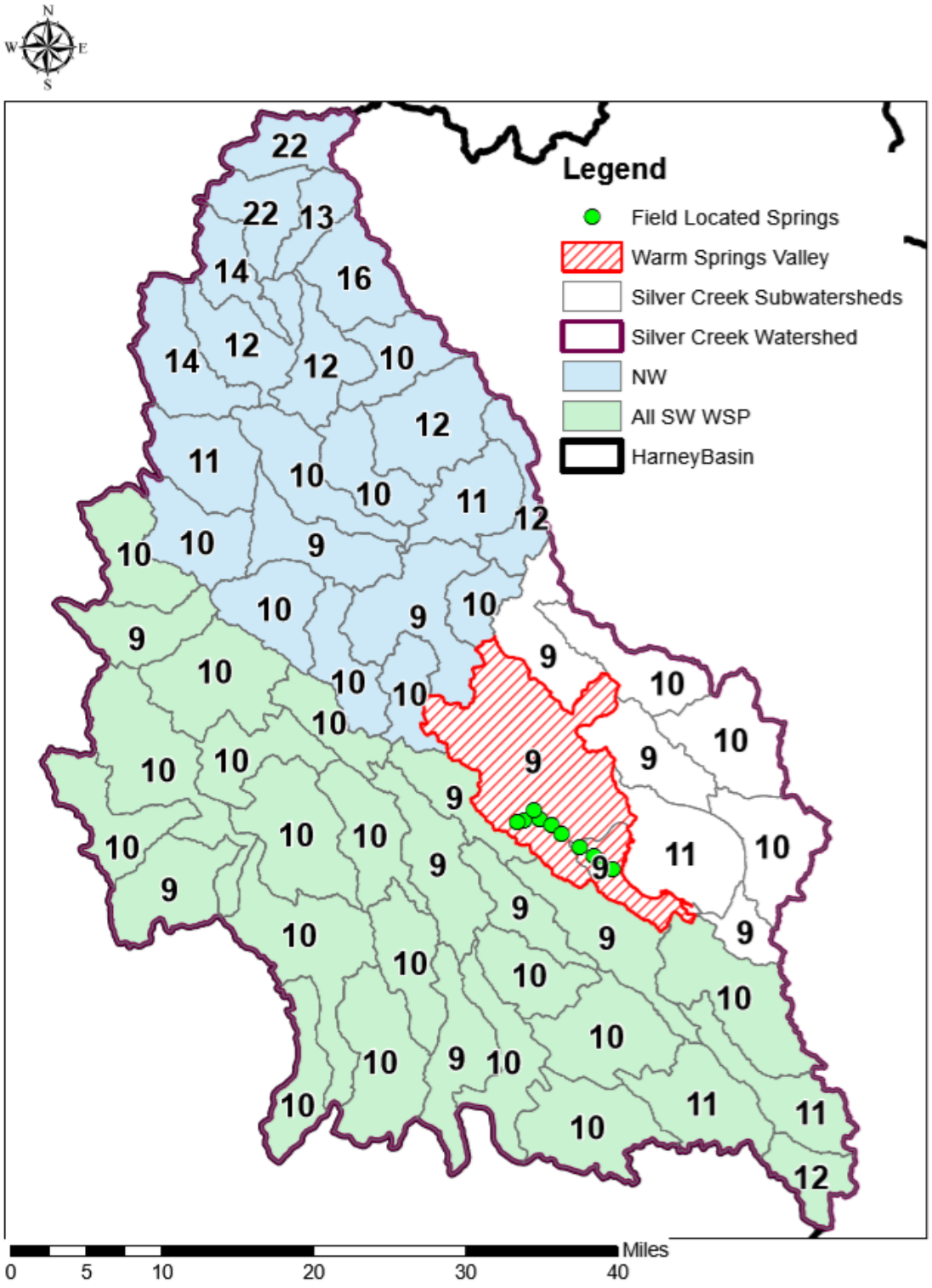

Figure 27: *Potential Catchment Areas in Silver Creek Watershed Used in Calculations.* Potential catchment areas used for calculating percentage of precipitation contributing to spring discharge at WSV warm springs. Subwatersheds are based on HUC-12 delineation (Seaber et al., 1987).

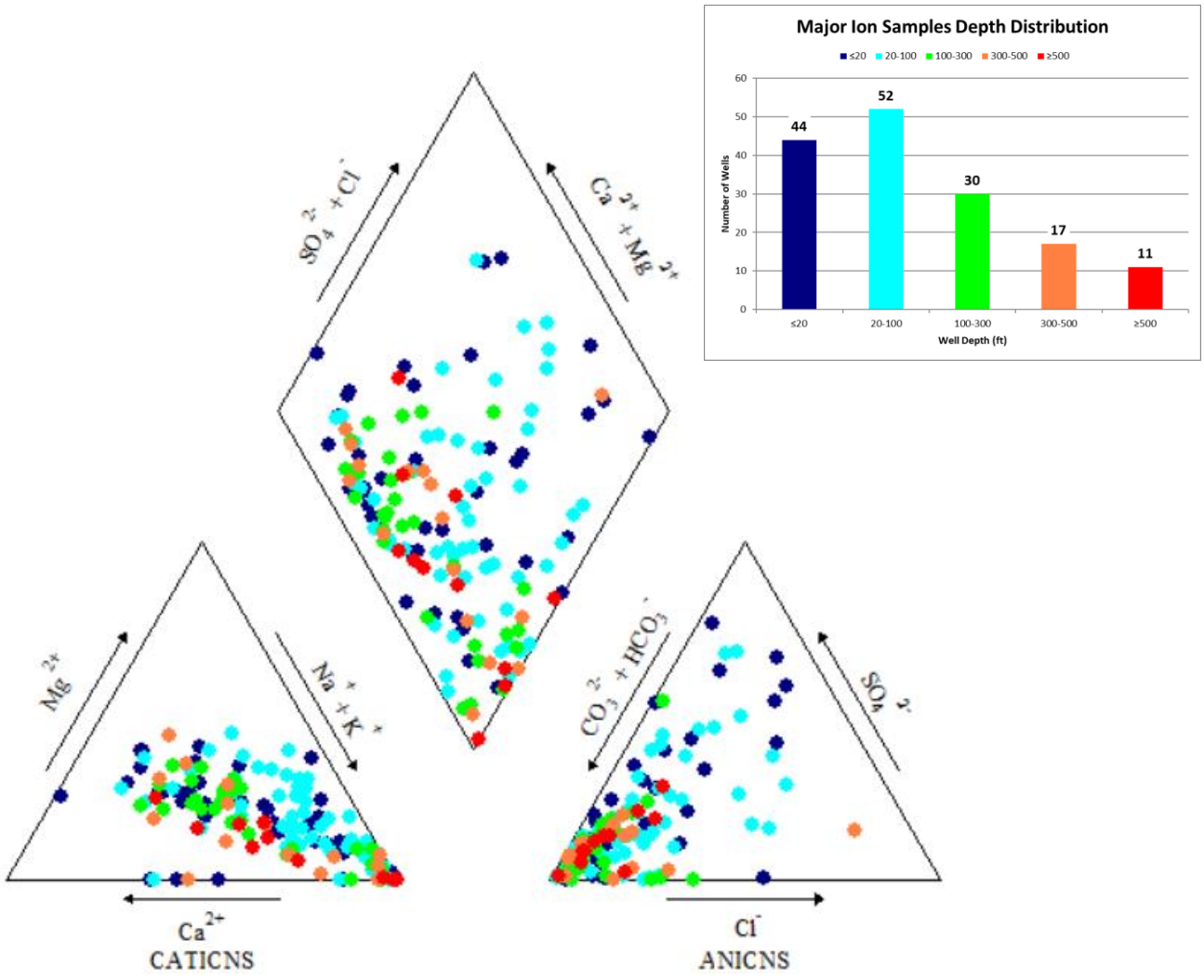

Figure 28: *Major Ions by Well Depth for Harney Basin.* Piper diagram of major ion chemical analyses found in published reports (Appendix G) for wells in Harney Basin organized by well depth.

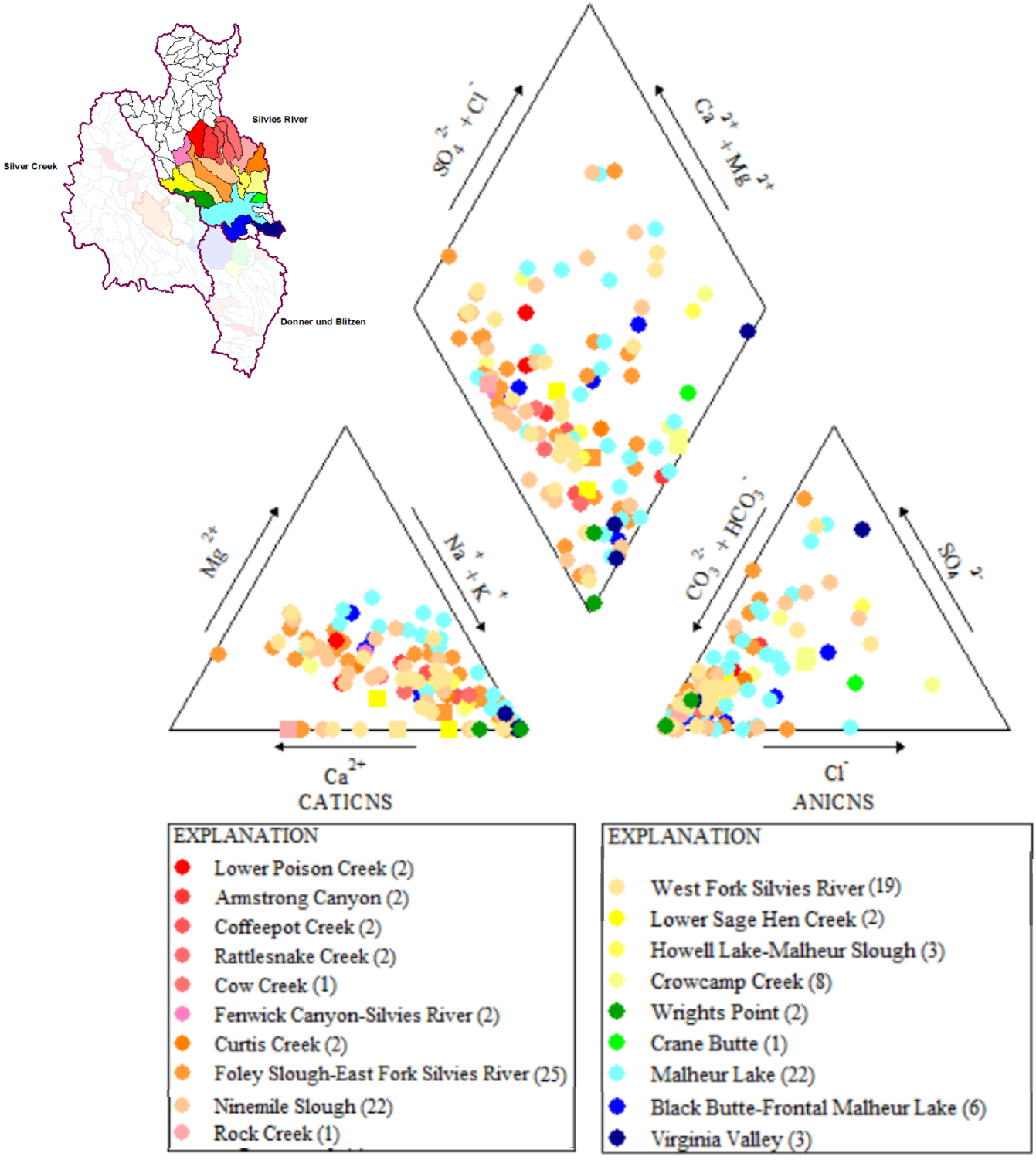

Figure 29: *Silvies River Watershed Major Ions by Subwatershed.* Piper diagram of major ion chemical analyses found in published reports (Appendices G and H) for samples in the Silvies River watershed. Data points are divided by sub-basin. Circles represent well samples and squares represent spring samples. Subwatersheds are based on HUC-12 delineation (Seaber et al., 1987).

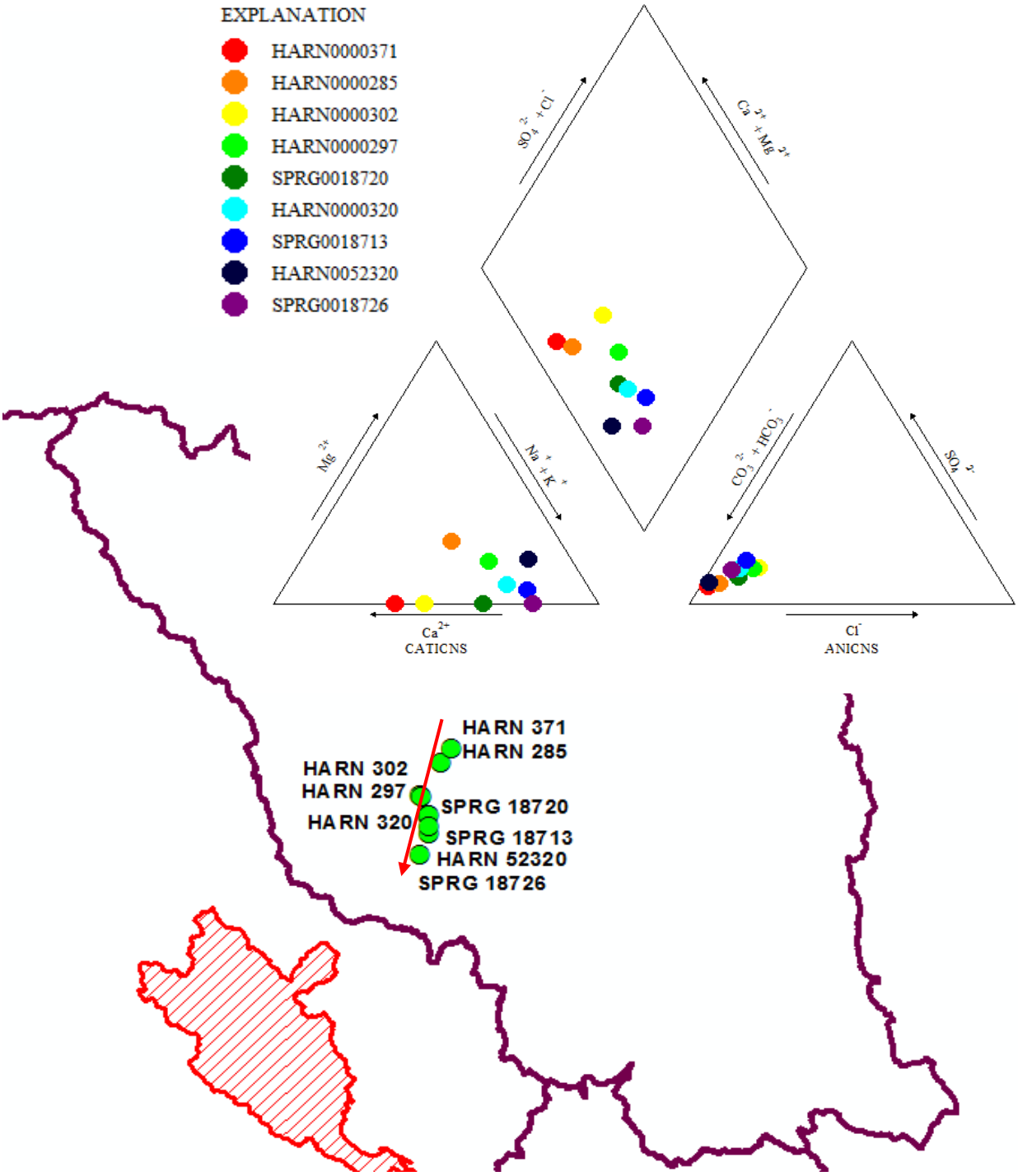

Figure 30: *Silvies River Watershed Major Ions by Flowpath.* Piper diagram of major ion chemical analyses found in published reports (Appendices G and H) for samples along a flowpath in the Silvies River watershed. An arrow (red) shows relative flow direction. The outline of the Warm Springs Valley (red) is based on HUC-12 delineations (Seaber et al., 1987).

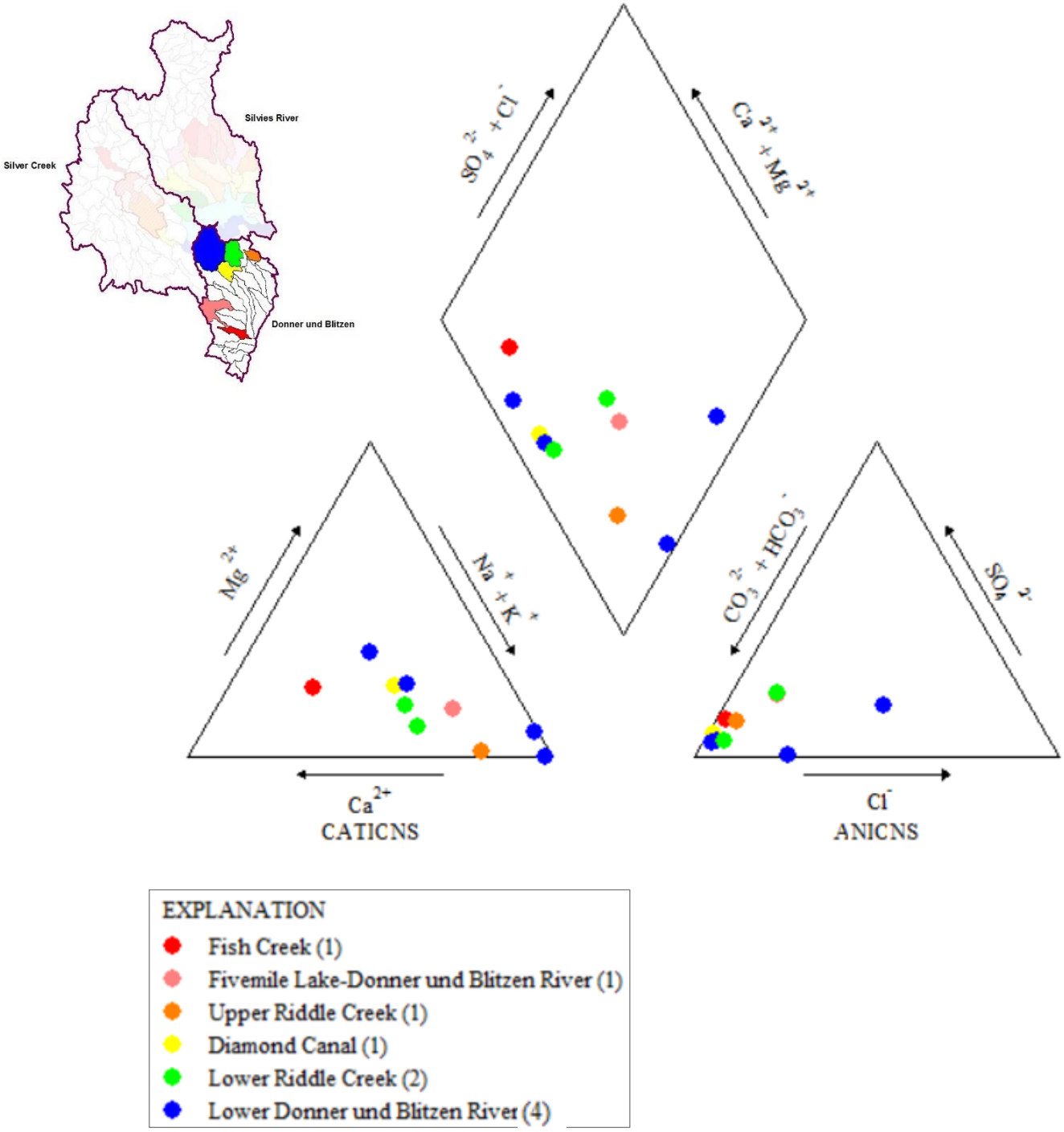

Figure 31: *Donner und Blitzen Watershed Major Ions by Subwatershed.* Piper diagram of major ion chemical analyses found in published reports (Appendices G and H) for samples in the Donner und Blitzen River watershed. Data points are divided by sub-basin. Circles represent well samples and squares represent spring samples. Subwatersheds are based on HUC-12 delineation (Seaber et al., 1987).

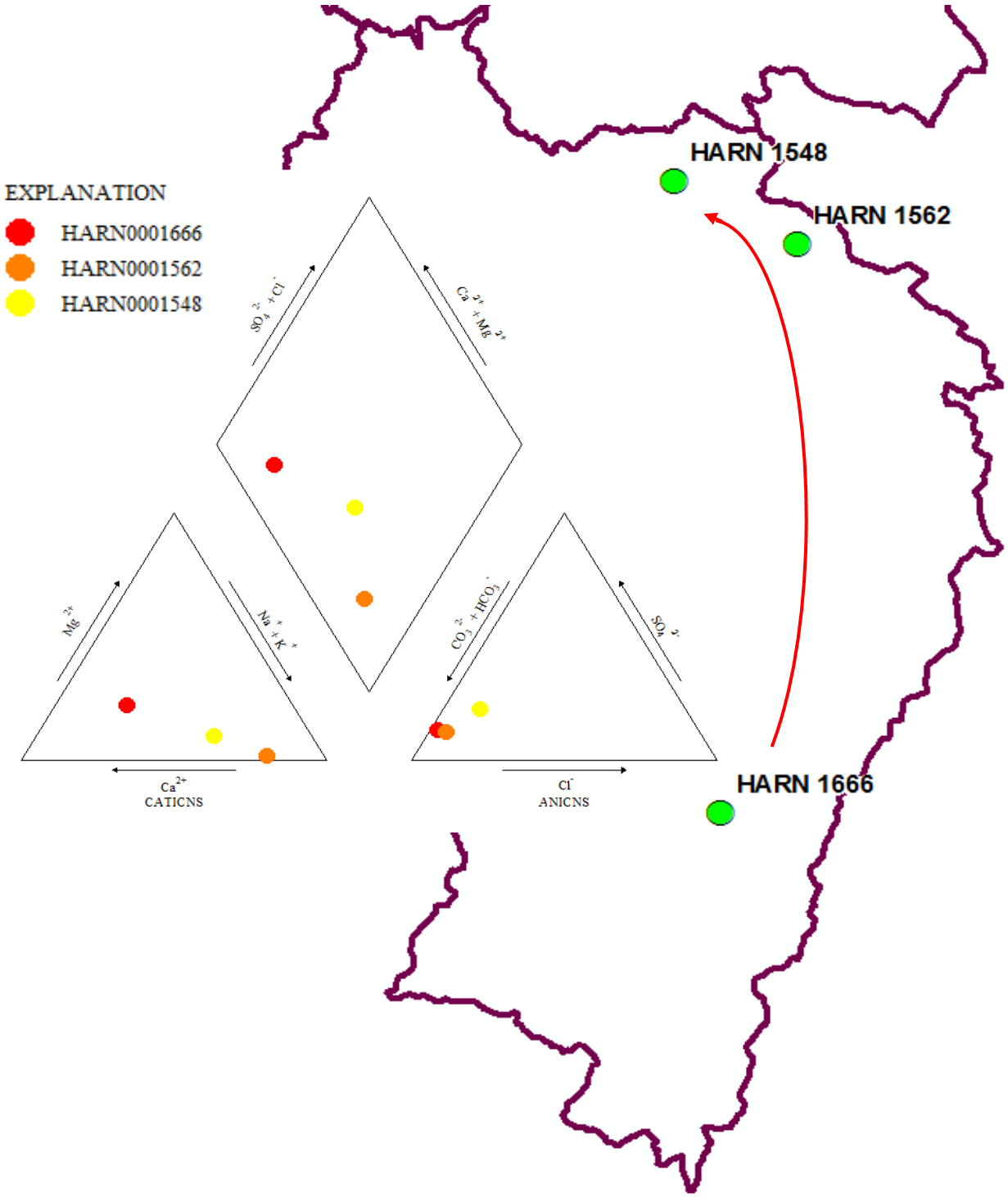

Figure 32: *Donner und Blitzen Watershed Major Ions by Flowpath.* Piper diagram of major ion chemical analyses found in published reports (Appendices G and H) for samples along a flowpath in the Donner und Blitzen watershed. An arrow (red) shows relative flow direction.

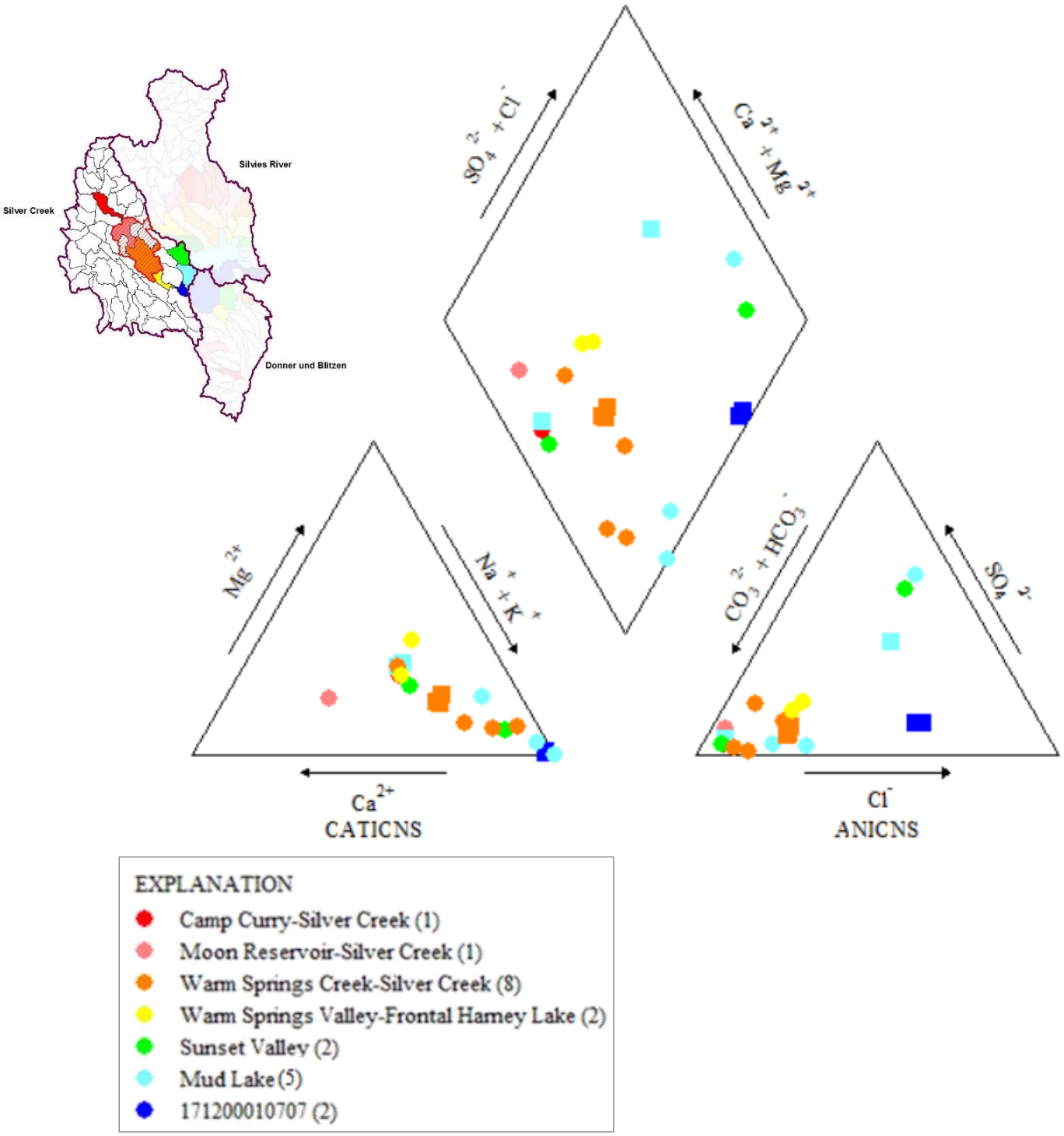

Figure 33: *Silver Creek Watershed Major Ions by Subwatershed.* Piper diagram of major ion chemical analyses found in published reports (Appendices G and H) for samples in the Silver Creek watershed. Data points are divided by sub-basin. Circles represent well samples and squares represent spring samples. Subwatersheds are based on HUC-12 delineation (Seaber et al., 1987).

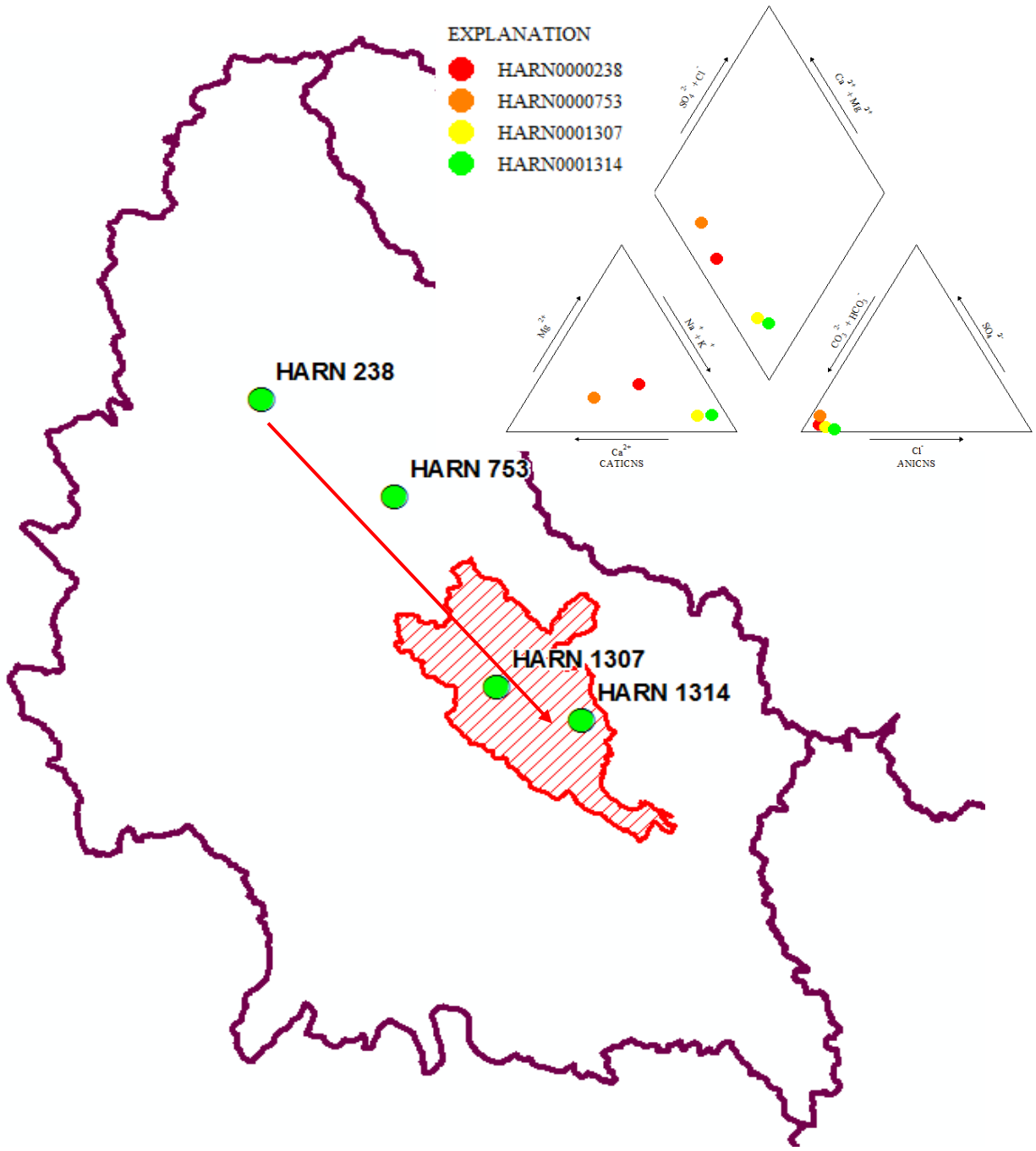

Figure 34: *Silver Creek Watershed Major Ions by Flowpath.* Piper diagram of major ion chemical analyses found in published reports (Appendices G and H) for samples along a flowpath in the Silver Creek watershed. An arrow (red) shows relative flow direction. The outline of the Warm Springs Valley (red) is based on HUC-12 delineations (Seaber et al., 1987).

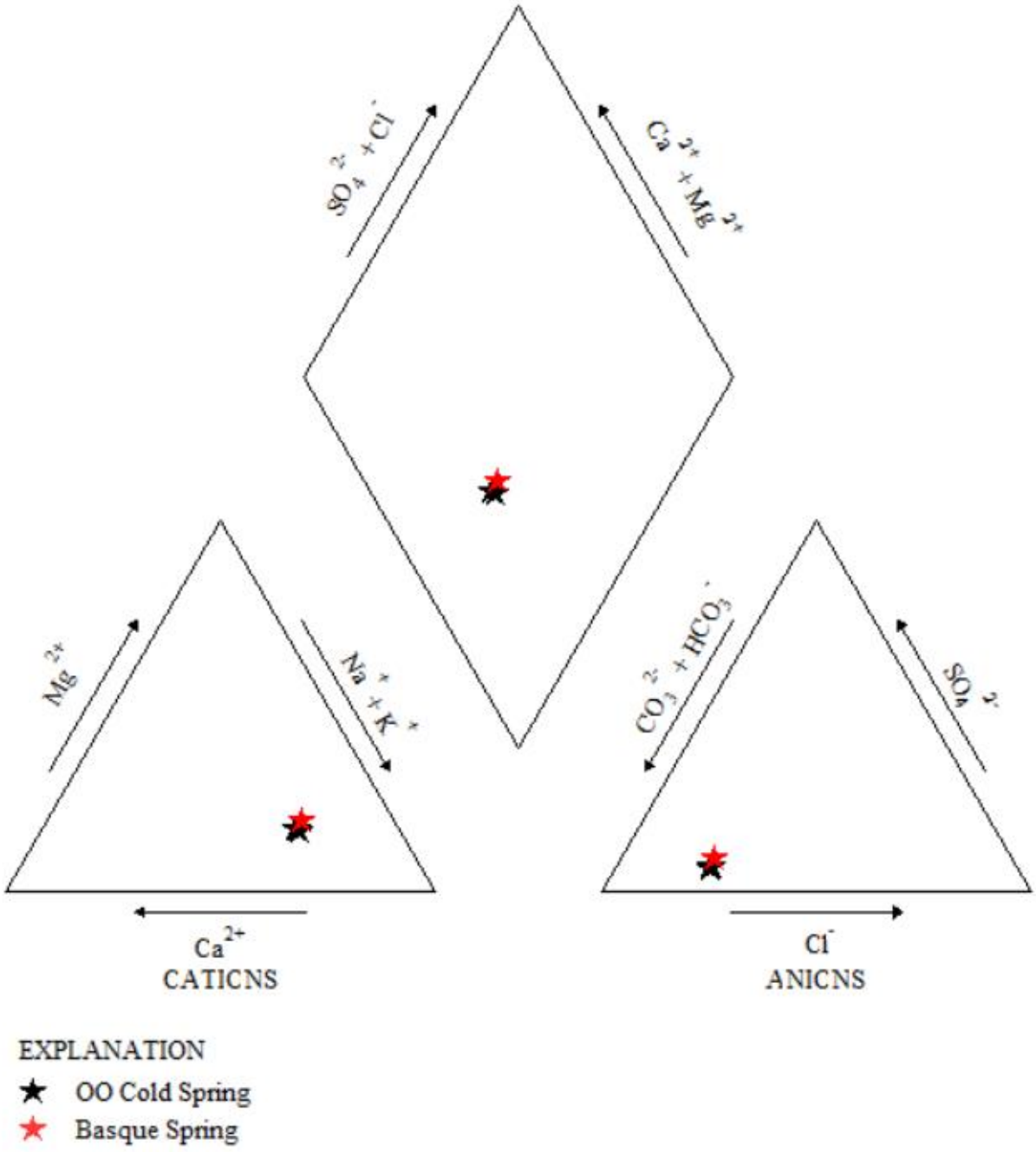

Figure 35: *Major Ions for WSV Warm Springs.* Piper diagram of major ion chemical analyses from published reports for springs in the Warm Springs Valley (Appendix H).

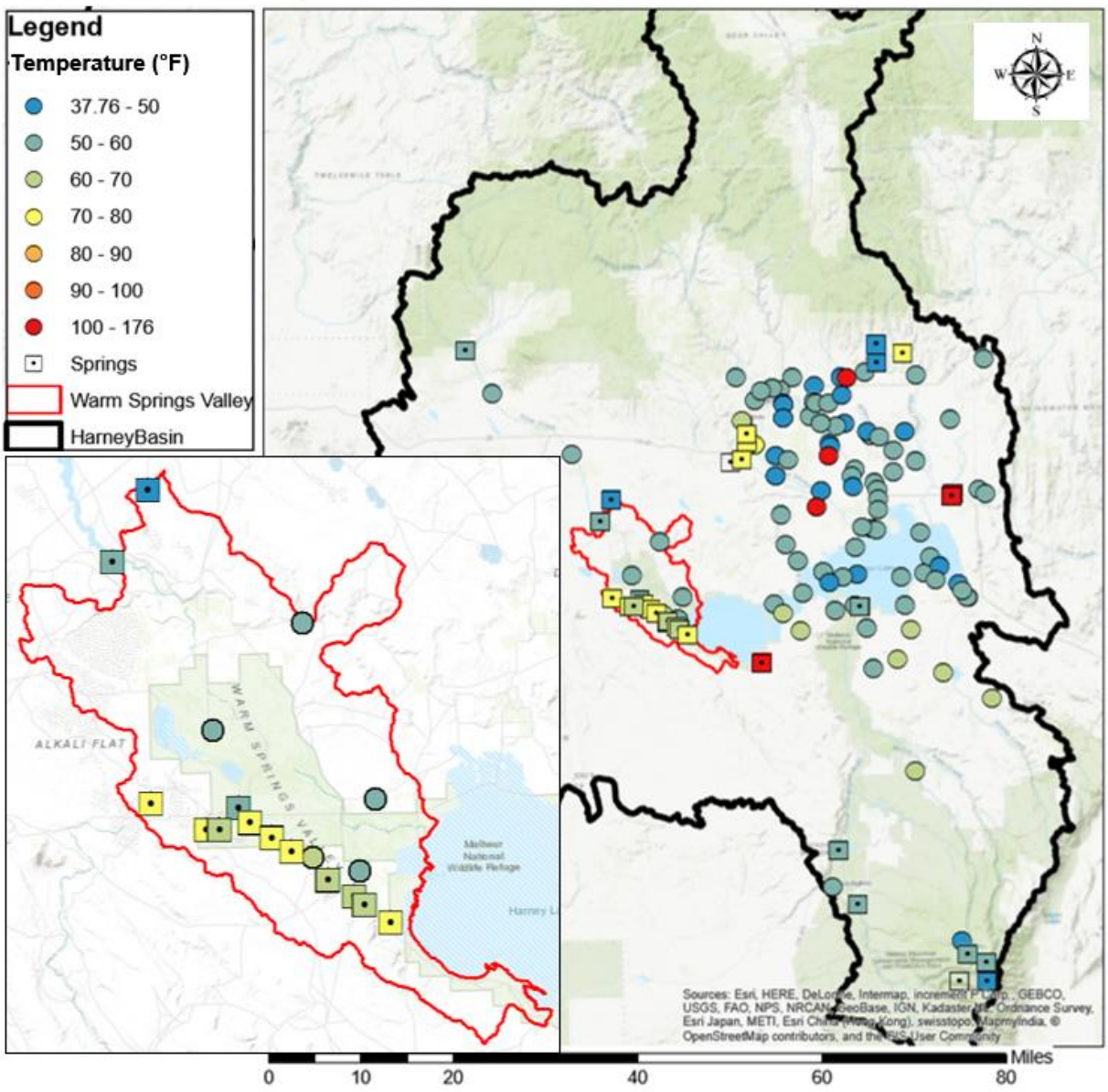

Figure 36: *Geographic Distribution of Temperature Measurements.* Temperatures (°F) measured for wells (circles) and springs (squares).

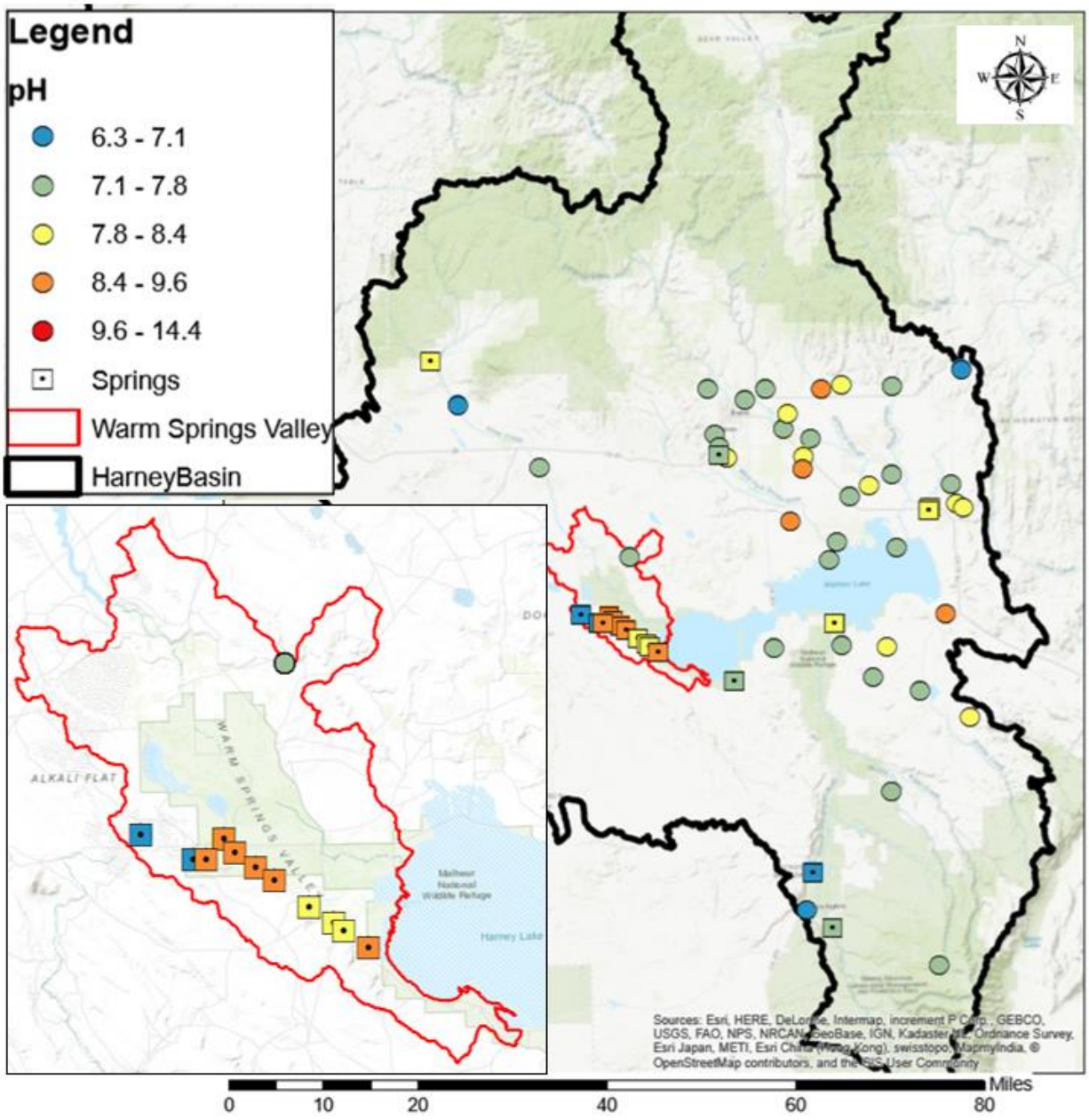

Figure 37: *Geographic Distribution of pH Measurements*. pH measurements for wells (circles) and springs (squares).

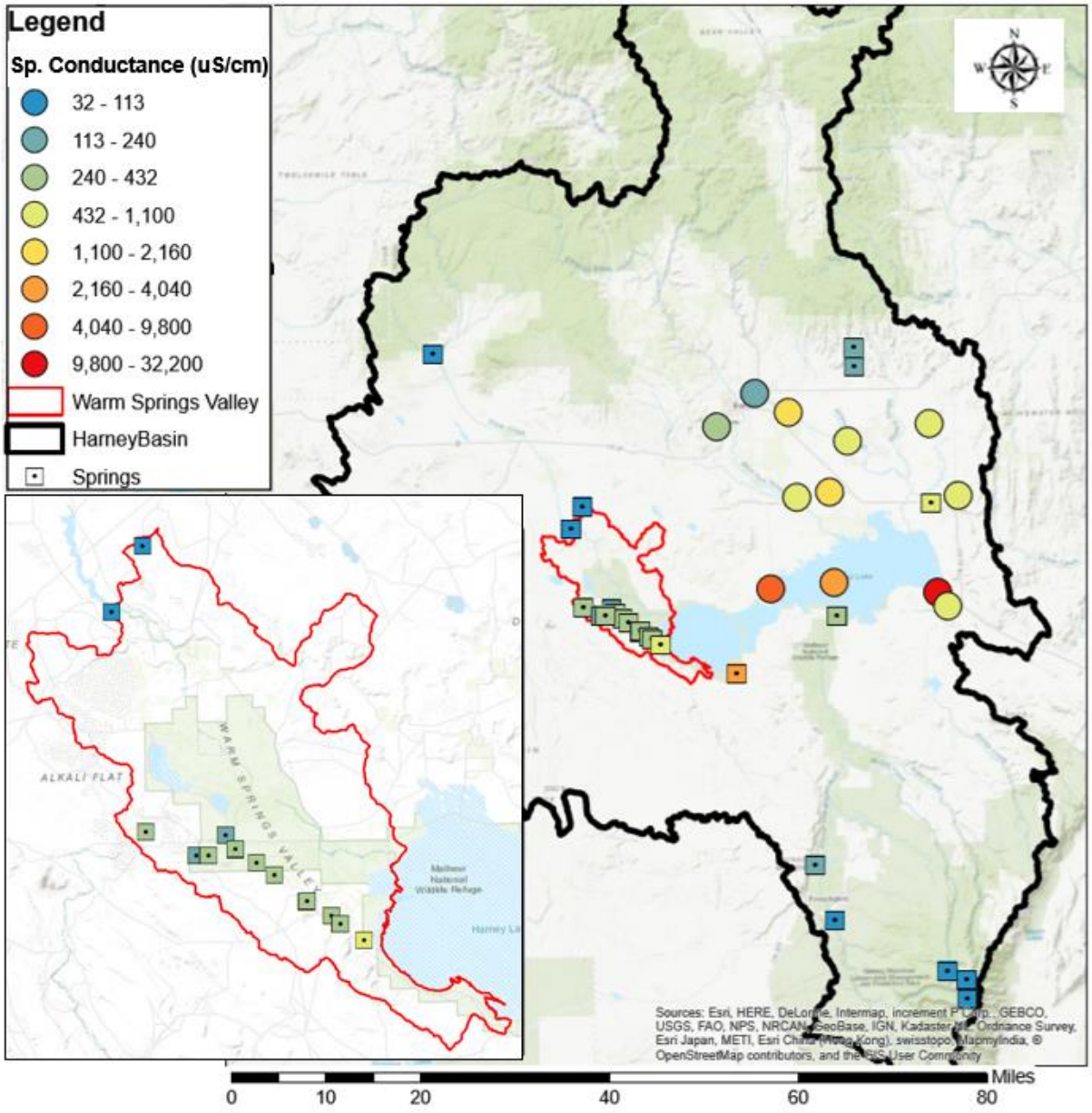

Figure 38*: Geographic Distribution of Specific Conductance Measurements.* Specific conductance measurements (in µS/cm) taken at wells (circles) and springs (squares).

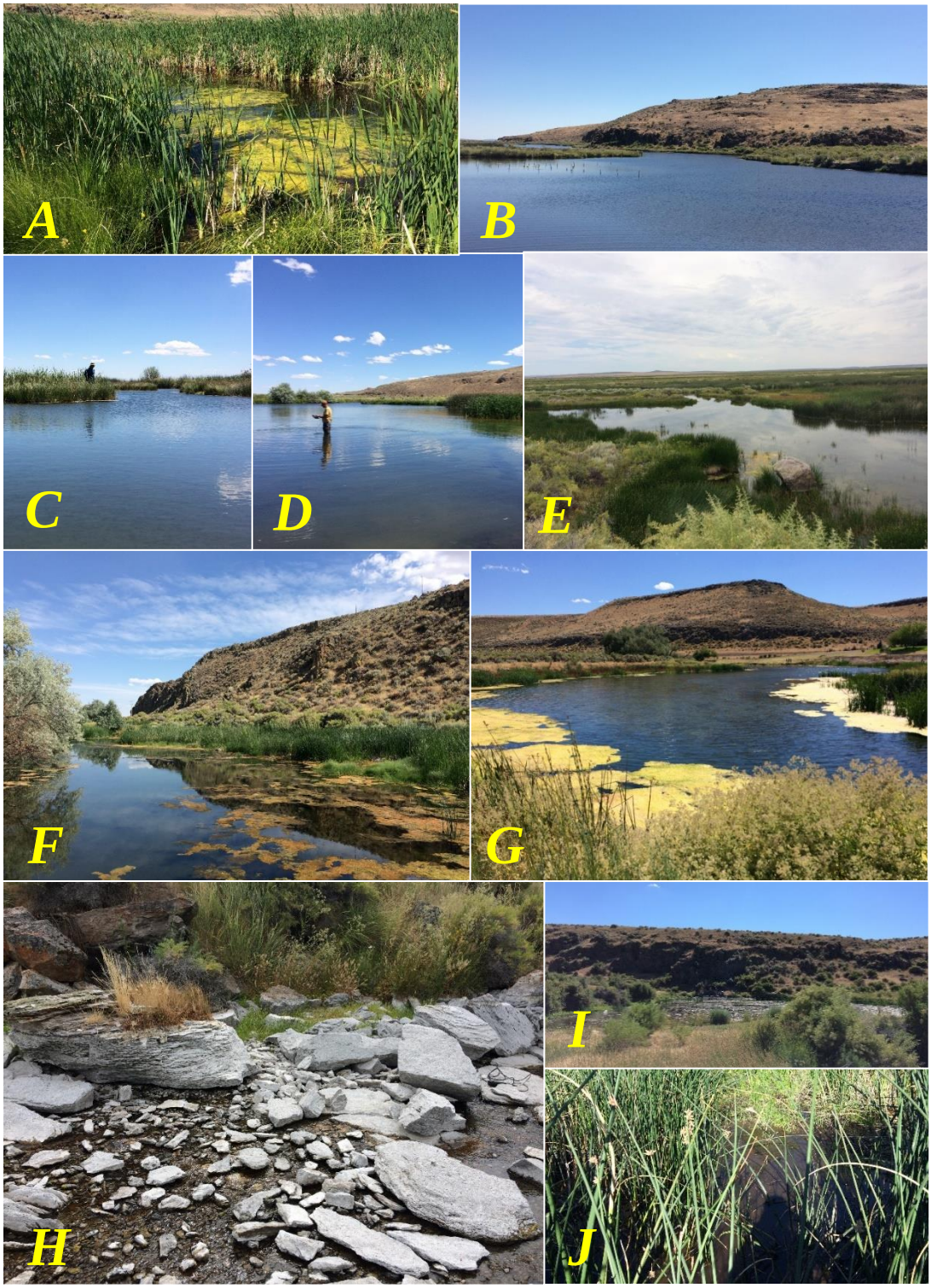

Figure 39: *Photographs of WSV Warm Springs.* A) Ross Spring, B) Hibbard Spring, C) OO Cold Spring, D) Barnyard Spring, E) Basque Spring, F) Johnson Spring, G) Hughet Spring, H) Upper Sizemore Spring, I) Lower Sizemore Spring, and J) Soldier Spring.

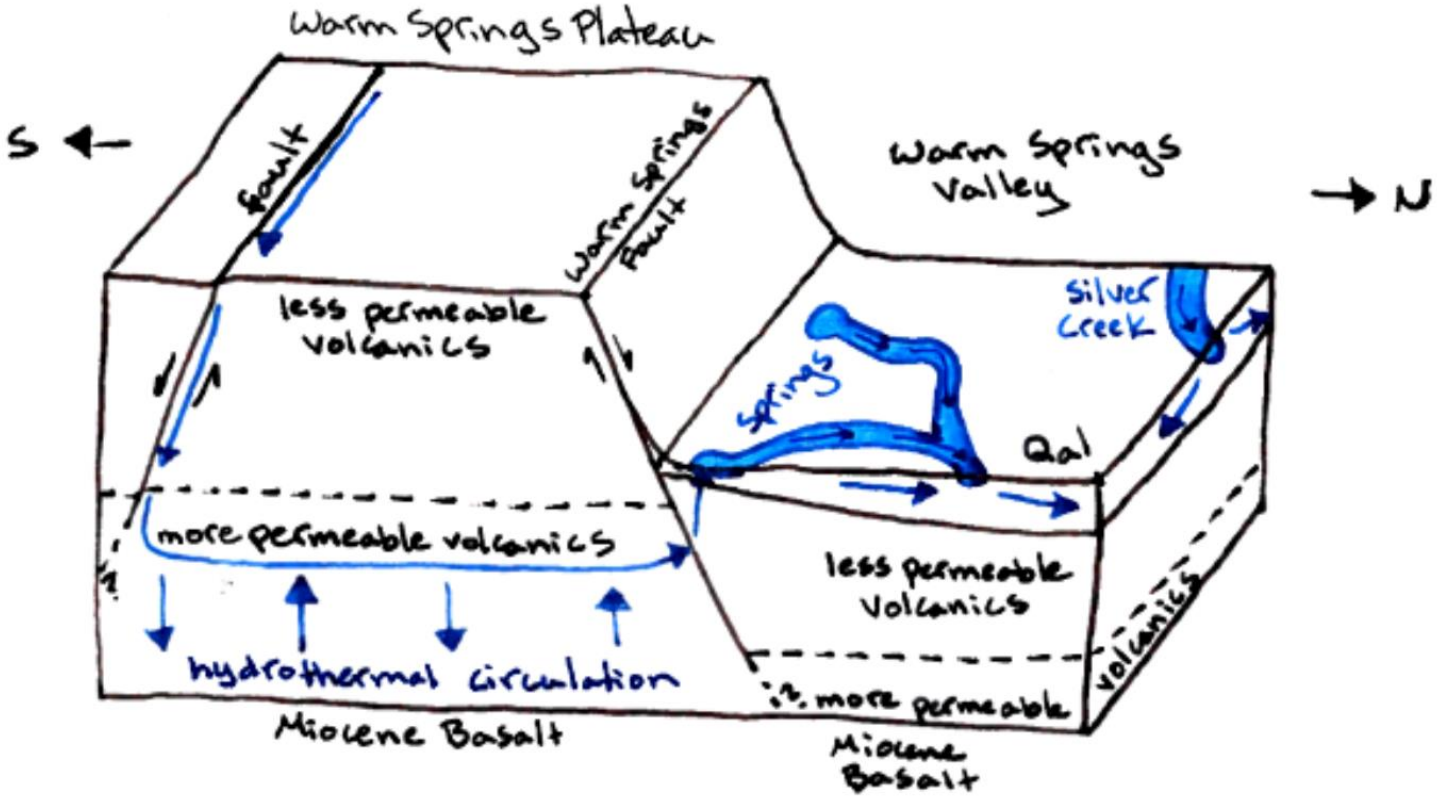

Figure 40*: Conceptual Block Diagram of WSV Warm Springs*. Conceptual model of water flowing from faults on the Warm Springs Plateau then flowing toward the Warm Springs Valley to the north. Geology is generalized and does not reflect the nomenclature set forth by Walker (1979). Less permeable volcanics include ash-flow tuff and more permeable volcanics include, but are not limited to, broken rock, pumice, and sedimentary volcanic material. Qal includes basin fill and alluvium. This diagram is not to scale. Groundwater flows down through faults in the Brothers Fault Zone until it reaches more permeable material, where it begins to flow to the north and undergoes some hydrothermal circulation due to underlying heat. It then rises when it reaches the Warm Springs Fault, where it comes in contact with less permeable volcanic tuff, and emerges from small orifices at the bottom of each spring pond. Surface water and shallow groundwater then flows east toward Harney Lake and may come in contact with water from Silver Creek as it is re-routed to the northeast toward Weaver Springs.

Tables

Table 1: *Data sources and collection methods.*

Data	Source	Method
Spring Locations	• GPS iPhone	Avenza Maps® iPhone application and GPS.
Well Locations	• OWRD GSIS (OWRD, 2017)	Various sources, including GPS locations, water rights maps, topographic maps, and Google Earth imagery.
Well and Spring Elevations	• USGS Topographic Maps	Extracted from USGS topographic maps, based on locations, datum is NGVD1929.
Water Levels in Wells	• OWRD • Well Logs	Fall 2017 Synoptic, which is a series of static water level measurements in wells in and around Harney Basin. There are also some static water levels in well logs which are sometimes associated with a particular depth interval and lithologic unit.
Lithology	• Well Logs	Lithologic descriptions and intervals from drillers' logs.
Specific Capacity and Transmissivity	• Calculated from Well Logs	Pump tests reported on well logs with pumping rate, drawdown, and time were used to calculate specific capacity and transmissivity using saturated thickness and well diameter.
Spring Discharge	• Waring, 1909 • Piper et al., 1939 • Field Measurements • Google Climate Engine	Taken from publications, measured in the field in August 2017, and calculated in Google Climate Engine.
Precipitation	• PRISM annual precipitation (National Center for Atmospheric Research Staff, 2017)	Annual precipitation averaged for subwatersheds in ESRI's ArcGIS.
Major Ions	• Piper et al., 1939 • Leonard, 1970 • Gonthier et al., 1977 • Townley et al., 1980	Compiled from reports and associated with sites in the OWRD groundwater database.
Temperature, pH, and Specific Conductance	• Piper et al., 1939 • Leonard, 1970 • Hubbard, 1975 • Gonthier, 1977 • Townley et al., 1980 • Brown et al., 1980a and b • Well Logs • USGS NWIS Database • Kiri Hargie, written communication, 2017	Compiled from reports, well logs, and the USGS NWIS database. Some measurements were taken in the field during July 2017 during field work with Kiri Hargie.

Table 2: *Geologic units and their associated permeabilities and lithologies modified from Yinger (2012).*

Geologic Unit	Map Symbols1	Permeability	Lithology
Basin Fill	Qs, Qal, Qp, Qf	Variable permeability low (clay) to moderate/high (sand/gravel)	Gravel, sand, silt, clay, sandy clay, clayey sand, gravel, and clayey gravel
Diamond and Voltage Basalts	Qb, Qlb, Qmv	Very permeable	Lava flows, cinders, and vent complexes
Sedimentary Rocks	QTs	Permeable	Conglomerate and sandstone
Intra-basin basalts and cinders	QTb, QTp, QTps	Moderate to high permeability	Lava flows, pyroclastics, palagonite, cinders
Mafic vent complexes	QTmv	High permeability	Near vent related plugs, dikes, ejecta, lava flows
Harney Formation	Tst (?)	Moderate permeability	Sandstone, claystone, and conglomerate
Drinkwater Basalt	Tdw	High permeability	Lava flows
Basalt lavas and cinders	Tb	Moderate to high permeability	Lava flows and cinders
Rhyolite-Rhyodacite	Trr	Medium to high permeability	Domes and Lavas
Tuffaceous and volcaniclastic sediments	Tst	Low to moderate permeability	Clay, claystone, minor sand, sandstone, pumiceous
Rattlesnake Ash-Flow Tuff	Tdo	Aquitard/confining layer	Ash-flow tuff
Prater Creek Ash-Flow Tuff	Twtp	Low permeability aquitard/confining layer	Ash-flow tuff
Devine Canyon Ash-Flow Tuff	Tdv	Low permeability confining layer	Ash-flow tuff
Volcaniclastic sedimentary rocks	Tts, Tsts	Low permeability	Rhyolitic siltstone, claystone, sandstone, conglomerate
Steens Basalt	Tba	Moderately permeable	Lava Flows

[1]*Map symbols are from Greene et al., 1972 and Milliard, 2010.*

Table 3: *Hydrogeologic units defined by Yinger (2012) and their associated lithologies and calculated hydraulic properties. This table was taken directly from Yinger (2012) and is numbered Table 3-1.*

Hydrogeologic Units	**Specific Capacity (gal/ft)**	**Estimated Hydraulic Conductivity (gal/day/ft^2)**	**Lithology**
Basin Fill	0.4 to 41	243 to 728	Gravel, Sand, silt, clay, sandy clay, clayey-sand, gravel, and clayey-gravel
Diamond/Voltage Basalt, includes Mafic vent complexes	81 to 200	2,727 to 7,843	Lavas flows, cinders, and vent complexes
Intra-Basin basalts and cinders, includes: flows within Basin-fill, Harney Formation and Tuffaceous and volcaniclastic sediments	33.3	995	Lavas flows, pyroclastics, palagonite, cinders
Harney Formation	0.1 to 3.3	28.6 to 76.9	Sandstone, claystone, conglomerate, sand and gravel
Tuffaceous and volcaniclastic sediments	0.1 to 50	1.7 to 610	Clay, claystone, minor sand, sandstone, pumiceous
Volcaniclastic sedimentary rocks	1.5 to 7.5	20 and 600	Rhyolitic siltstone, claystone, sandstone, conglomerate
Steens Basalt	1.7 to 510	333 to 46,364	Lava flows

Table 4: *Springs in the Warm Springs Valley and their associated aquifers described by Piper et al., 1939. Also included are correlations to numbered sites in Piper et al. (1939) and "Logid" of each spring from the OWRD GSIS database (OWRD, 2017).*

Spring	Logid[1]	Site Number[2]	Geologic Unit Discharging Groundwater to Each WSV Spring as Identified by Piper et al. (1939)[3]
Ross Spring	SPRG0018732	280	Jointed rhyolite (Danforth formation)
Hibbard Spring	SPRG0023236	280	Jointed rhyolite (Danforth formation)
OO Cold Spring	SPRG0018731	279	Valley fill
Barnyard Spring	SPRG0018733	281	Jointed rhyolite (Danforth formation)
Basque Spring	SPRG0018734	285	Jointed rhyolite (Danforth formation)
Johnson Spring	SPRG0018737	347	Jointed rhyolite and tuff (Danforth formation)
Hughet Spring	SPRG0018738	349	Jointed rhyolite and tuff (Danforth formation)
Upper Sizemore Spring	SPRG0018739	351	Jointed rhyolite and tuff (Danforth formation)
Lower Sizemore Spring	SPRG0018740	354	Danforth formation
Soldier Spring	SPRG0018814	355	Valley fill

[1]Site number in Piper et al. (1939). [2]OWRD Logid in GSIS database (OWRD, 2017). [3] See Figure 6 for an approximate equivalent using the updated nomenclature of Walker (1979).

Table 5: *Warm Springs Valley Springs and associated mapped geologic unit from Greene et al. (1972) and Parker (1974) adjacent to spring locations and valley fill.*

Spring	Exposed Unit Adjacent to Spring Locations		
	Greene et al., 1972	***Parker, 1974***	***Brown et al., 1980a and b***
Ross Spring	Rhyolite and Rhyodacite	Rhyolite of Double O Ranch	Rhyolite of Double O Ranch
Hibbard Spring	Rhyolite and Rhyodacite	Rhyolite of Double O Ranch	Rhyolite of Double O Ranch
OO Cold Spring	Tertiary and Quaternary Basalt	Tertiary and Quaternary Basalt	Upper Pliocene Basalt
Barnyard Spring	Rhyolite and Rhyodacite	Rhyolite of Double O Ranch	Rhyolite of Double O Ranch
Basque Spring	Rhyolite and Rhyodacite	Rhyolite of Double O Ranch	Rhyolite of Double O Ranch
Johnson Spring	Rhyolite and Rhyodacite	Rhyolite of Double O Ranch	Rhyolite of Double O Ranch
Hughet Spring	Tuffaceous Sedimentary Rocks	Tertiary Sedimentary Rocks	Prater Creek Ash-Flow Tuff
Upper Sizemore Spring	Tuffaceous Sedimentary Rocks	Ash-Flow Tuff of Prater Creek	Prater Creek Ash-Flow Tuff
Lower Sizemore Spring	Tuffaceous Sedimentary Rocks	Ash-Flow Tuff of Prater Creek	Prater Creek Ash-Flow Tuff
Soldier Spring	Tuffaceous Sedimentary Rocks	Tertiary Sedimentary Rocks	Tuffaceous Sedimentary Rocks

Table 6: *Summary of available data.*

Data Type - Located Sites	**Number**
Lithcoded Wells	2,296
Wells with Specific Capacity Data	1,462
Synoptic Wells with Static Water Levels for Fall 2017	223
Samples with Published Chemical Analysis Data	209
Samples with Major Ion Data	159

Table 7: *Summary table of historical and recent spring discharge measurements. Historical measurements were taken from Piper et al., 1939 (USGS). Recent measurements were taken by Jonathan LaMarche (OWRD) and are highlighted in yellow.*

Spring	Date	Rate (cfs)	Measured by
Barnyard Spring	04/12/1916	6.6	USGS
	05/15/1916	5.8	USGS
	10/28/1916	7.9	USGS
	04/19/1917	6	USGS
	05/22/1917	5.7	USGS
	10/01/1917	5.1	USGS
	04/26/1918	6	USGS
	06/10/1918	3	USGS
	03/23/1919	6	USGS
	09/05/1919	9.2	USGS
	07/21/1931	3.9	USGS
	08/15/2017	3.7	OWRD
Basque Spring	07/29/1907	4	USGS
	04/12/1916	2.1	USGS
	05/15/1916	2.7	USGS
	10/28/1916	1.8	USGS
	04/19/1917	2.3	USGS
	10/02/1917	2.2	USGS
	07/22/1931	2.7	USGS
	05/30/1932	2.0	USGS
	08/14/2017	1.8	OWRD
Johnson Spring	07/29/1907	2	USGS
	04/12/1916	1.5	USGS
	10/28/1916	1.3	USGS
	05/22/1917	1.7	USGS
	10/02/1917	2	USGS
	07/24/1931	1.9	USGS
	08/14/2017	1.6	OWRD
Hughet Spring	04/12/1916	13.6	USGS
	04/24/1916	9.2	USGS
	10/28/1916	14.5	USGS
	04/19/1917	13.3	USGS
	05/22/1917	12	USGS
	10/02/1917	12.8	USGS
	07/24/1931	13	USGS
	05/30/1932	11.9	USGS
	08/14/2017	13.0	OWRD
Upper Sizemore Spring	04/12/1916	1.5	USGS
	05/14/1916	2.1	USGS
	10/28/1916	1.2	USGS
	05/22/1917	2.8	USGS
	10/02/1917	3.5	USGS
	07/28/1931	2.6	USGS
	08/14/2017	1.4	OWRD
Lower Sizemore Spring	04/12/1916	1.4	USGS
	05/14/1916	1.6	USGS
	10/28/1916	1.3	USGS
	05/22/1917	1.6	USGS
	10/02/1917	3.5	USGS
	07/28/1931	0.9	USGS
	07/20/2017	1.4	OWRD
	08/14/2017	1.7	OWRD
Hibbard Spring	07/30/1907	12.5	USGS
	08/23/1913	20.9	USGS
	04/13/1916	15.8	USGS
	05/14/1916	15.7	USGS
	10/28/1916	16.4	USGS
	04/18/1917	14.1	USGS
	05/22/1917	16	USGS
	10/01/1917	14.1	USGS
	04/26/1918	13.9	USGS
	06/10/1918	8.4	USGS
	03/23/1919	15.2	USGS
	09/05/1919	15	USGS
	04/24/1921	15.2	USGS
	05/30/1932	11.9	USGS
	8/15/2017	9.2	OWRD
OO Cold Spring	07/29/1907	0.7	USGS
	07/22/1931	1	USGS
	Not measured in 2017 due to road flooding		
Ross Spring	No outflow stream in 2017		
Soldier Spring	1931	0.06	USGS
	No outflow stream in 2017		

Table 8: *Spring discharge calculated as groundwater evapotranspiration for Ross and Soldier Springs for years 1983 through 2016 using Landsat coverage.*

Year	Ross Spring Calculated Discharge (cfs)	Soldier Spring Calculated Discharge (cfs)
1983		0.0016
1984	0.044	-0.0013
1985	0.057	-0.0018
1986	0.060	-0.0024
1987	0.054	-0.0003
1988	0.074	0.0011
1989	0.061	0.0020
1990	0.042	0.0016
1991	0.046	0.0025
1992	0.038	0.0014
1993	0.041	0.0021
1994	0.046	0.0016
1995	0.046	0.0024
1996	0.045	0.0020
1997	0.054	0.0016
1998	0.054	0.0017
1999	0.059	0.0014
2000	0.063	0.0020
2001	0.058	0.0016
2002	0.072	0.0022
2003	0.056	0.0019
2004	0.067	0.0020
2005	0.050	0.0020
2006	0.048	0.0017
2007	0.068	0.0023
2008	0.047	0.0018
2009	0.058	0.0020
2010	0.051	0.0018
2011	0.056	0.0017
2012	0.065	0.0020
2013	0.052	0.0018
2014	0.064	0.0019
2015	0.050	0.0018
2016	0.040	0.0017

Table 9: *Wells with pump or bailer tests in and around the WSV, with calculated transmissivity and water-bearing lithology. Aquifer tests were reported on well logs.*

Log ID	Q (gpm)	Draw-down (ft)	Time (hrs)	Diameter (in)	Transmis-sivity (ft^2/d)	Well Depth (ft)	Water-Bearing Material Depth Interval (ft)	Water-Bearing Material Reported by Well Driller
HARN0001085	1,278	97	12	12	3,330	350	30-40 and 338-350	coarse sand and gravel
HARN0001981	15	3	1	6	1,100	100	89-100	conglomerate, talc, and gravel
HARN0050251	1,100	119	6	14	2,130	540	80-217, 281-354, and 400-520	rock, clay, coarse sand, claystone, sandstone, cinders, and pumice
HARN0001841	15	10	1	5	308	450	400-450	claystone, obsidian, and hard broken rock
HARN0001305	20	15	1	6	278	90	19-34	shale and gravel
HARN0051188	25	3	2	6	1,990	60	42-60	gravel, fine sand, and clay
HARN0052022	400	40	24	8	2,730	720	14-24 and 88-270	fine sand, gravel, clay, and cemented gravel
HARN0001078	1,350	52	8	16	6,440	272	195-272	hard clay, gravel, rock, and sandstone
HARN0001304	180	90	4	12	408	1,005	3-36	sandstone, clay, lava, and conglomerate

Table 10: *Calculations for estimating spring discharge (in cubic feet per second) using aquifer transmissivity determined from pump tests in nearby wells (***Figure 23***).*

					Log Number (HARN):	**1085**	**1981**	**50251**	**1841**	**1305**	**51188**	**52022**	**1078**	**1304**	
					Transmissivity (ft^2/d):	3,330	1,100	2,130	308	1,370	1,990	2,730	6,440	408	
					⇩	⇩	⇩	⇩	⇩	⇩	⇩	⇩	⇩		
Group	**dh (ft)**	**dL (ft)**	**dh/dL**	**w (ft)**		**Q (cfs)**									**Avg.**
Group A (4)	10	18500	0.000541	5500.00		0.115	0.038	0.073	0.011	0.047	0.069	0.094	0.222	0.014	0.076
Group B (6)	10	13750	0.000727	28500.00		0.800	0.263	0.512	0.074	0.327	0.478	0.655	1.546	0.098	0.528
Total Q for all 10 springs:						5.259	1.729	3.366	0.486	2.153	3.141	4.307	10.160	0.644	3.471

Table 11: *Estimated aquifer transmissivity needed to produce measured spring discharge values.*

Group	Name	Measured Q (cfs)	dh/dL	w (ft)	T (ft2/day)	Average T (ft2/day)
A	Ross	0.04*	0.00054	1,400	4,700	410,000
	Hibbard	9.2	0.00054	1,400	1,100,000	
	OO Cold	1**	0.00054	1,400	120,000	
	Barnyard	3.7	0.00054	1,400	430,000	
B	Basque	1.8	0.00073	4,800	45,000	82,000
	Johnson	1.6	0.00073	4,800	40,000	
	Hughet	13	0.00073	4,800	330,000	
	Upper Sizemore	1.4	0.00073	4,800	35,000	
	Lower Sizemore	1.7	0.00073	4,800	43,000	
	Soldier	0.06**	0.00073	4,800	1,500	
	Total:	**33.5**		**Average:**	**210,000**	

*Calculated discharge from 2016

** Last published discharge value

Table 12: *Vertical hydraulic gradient calculations for wells with hydraulic head differing with depth. Both h and L values are in feet below land surface.*

Log ID	h_1	h_2	L_1	L_2	dh/dL	T (ft^2/d)
HARN0001085	35	6	30	338	0.094	3,330
HARN0052022	14	11	14	88	0.041	2,730

Table 13: *Summary of hydraulic conductivity calculations using transmissivity estimated in Table 9 and average vertical gradient found in Table 12. K was calculated using Equation 5 and L_1 was calculated using Equation 6 and discharge for the springs along the line drawn in Figure 24, which add up to 24.3 cfs.*

Log ID	T (ft^2/d)	b (ft)	K (ft/d)	Ave. dh/dL	w (ft)	L_1 (ft)
HARN0001085	3,330	12	280	0.067	34,000	5.8
HARN0001981	1,100	11	100	0.067	34,000	16
HARN0050251	2,130	330	6.5	0.067	34,000	250
HARN0001841	308	50	6.2	0.067	34,000	260
HARN0001305	278	15	19	0.067	34,000	86
HARN0051188	1,990	18	110	0.067	34,000	15
HARN0052022	2,730	21	130	0.067	34,000	12
HARN0001078	6,440	77	84	0.067	34,000	19
HARN0001304	408	33	12	0.067	34,000	130
Average:			83	0.067	34,000	19

Table 14: *Percentage of precipitation needed to supply the 33.5 cfs measured total discharge for ten springs in the Warm Springs Valley for various potential catchment areas delineated in Figure 27. Subwatersheds are based on HUC-12 delineations.*

Subwatershed Name	Ave. Annual Precip. (in.)	Subwatershed Surface Area (mi^2)	Percent Needed to Supply 33.5 cfs
171200010707	9	14	370
Angie Canyon	9	24	190
Basque Spring Reservoir	9	43	110
Big Tank Creek	10	65	70
Brown Canyon	9	32	160
Camp Curry-Silver Creek	10	37	140
Capehart Lake	10	28	160
Chain Lake	10	33	140
Chickahominy Reservoir	9	37	140
Dairy Creek-Silver Creek	12	39	89
Deep Canyon	10	34	120
Delintment Creek-Silver Creek	19	28	87
Devils Canyon	10	37	110
Dodson Creek	22	18	120
Dusenberry Lake	9	21	240
Egypt Creek	13	28	120
Fay Canyon	10	35	130
Foster Lake	10	46	89
Harney Lake	9	49	100
Hay Lake	10	30	150
Headwaters Buzzard Creek	11	46	89
Lake On The Trail	9	23	220
Little Tank Creek	10	39	120
Lower Big Stick Creek	10	34	130
Lower Buzzard Creek	9	25	200
Lower Dick Miller Canyon	10	30	150
Lower Jackass Creek	10	54	84
Lower Wickiup Creek	12	30	120
Lower Wilson Creek	10	51	89
Middle Big Stick Creek	10	30	150
Middle Buzzard Creek	9	41	120
Middle Jackass Creek	11	35	110
Moon Reservoir-Silver Creek	9	53	96
Mud Lake	10	38	130
Mule Springs Valley	10	50	91
Nicoll Creek	14	39	84
North Fork Chickahominy Creek	11	37	110
Pine Spring Canyon	12	24	160

Subwatershed Name		Ave. Annual Precip. (in.)	Subwatershed Surface Area (mi^2)	Percent Needed to Supply 33.5 cfs
Rawhide Creek		10	27	170
Rimrock Lake		10	34	120
Rock Lake		10	17	260
Rock Quarry Canyon Reservoir		11	33	120
Sawmill Creek		14	23	130
Smoky Hollow		10	32	140
South Creek		10	34	120
South Fork Chickahominy Creek		10	34	140
South Fork Jackass Creek		12	20	170
Squaw Lake		10	33	140
Still Spring Creek-Silver Creek		22	25	80
Sunset Valley		10	42	120
Upper Big Stick Creek		10	49	93
Upper Buzzard Creek		10	28	160
Upper Dick Miller Canyon		12	47	81
Upper Jackass Creek		11	42	91
Upper Wickiup Creek		16	35	82
Upper Wilson Creek		10	61	74
Warm Springs Creek-Silver Cr		9	112	45
Warm Springs Valley-Frontal Harney Lake		9	19	270
Group	All SW WSP[1]	10	**1,035**	**4.3**
	NW[2]	13	**695**	**5.3**
Total Silver Creek Watershed		11	**2,103**	**2.0**

[1]All Southwest Warm Springs Plateau subwatersheds, [2]Northwest subwatersheds.

Table 15: *Regression model coefficients for estimating ET* (Huntington et al., 2014).*

Equation	β_0	β_1	β_2	Root (x-int.)
Polynomial curve (model)	-0.196	2.904	-1.592	0.068
Upper 90% CI band	-0.177	2.891	-1.528	0.063
Lower 90% CI band	-0.214	2.918	-1.655	0.077
Upper 90% PI band	-0.104	2.889	-1.557	0.037
Lower 90% PI band	-0.287	2.919	-1.626	0.104

Appendices

Appendix A: *List of Abbreviations*

Abbreviation	Definition
cfs	Cubic feet per second
ET	Evapotranspiration
ET*	Normalized evapotranspiration
ET_0	Standardized grass reference evapotranspiration
ET_g	Groundwater evapotranspiration
EVI	Enhanced Vegetation Index
GSIS	Groundwater Site Information System
HUC-12	Hydrologic Unit Code (12-digit)
LSCW	Lower Silver Creek Watershed
NWIS	National Water Information System
OO	"Double O," alternate spelling
OPB	Oregon Public Broadcasting
OSWRB	Oregon State Water Resources Board
OWRD	Oregon Water Resources Department
PPT	Precipitation
PRISM	Parameter elevation Regression on Independent Slopes Model
Refuge	Malhuer National Wildlife Refuge
USFWS	United States Fish and Wildlife Service
USGS	United States Geological Survey
WSF	Warm Springs Fault
WSP	Warm Springs Plateau
WSV	Warm Springs Valley

Appendix B: *Vertices for polygons used in spring evapotranspiration calculations.*

Ross Spring:

-119.339912,43.272389,-119.339375,43.272436,-119.338946,43.27253,-119.338646,43.272608,-119.338303,43.272639,-119.337873,43.272624,-119.33768,43.272889,-119.337616,43.273155,-119.337959,43.273358,-119.338281,43.273483,-119.33841,43.273717,-119.338496,43.27403,-119.338539,43.27428,-119.338624,43.27453,-119.338582,43.274889,-119.338131,43.275233,-119.337831,43.275483,-119.338024,43.275764,-119.338603,43.275795,-119.339182,43.27592,-119.339526,43.276217,-119.33989,43.276545,-119.340127,43.276404,-119.340041,43.27617,-119.339826,43.275889,-119.339912,43.275717,-119.340212,43.275467,-119.340363,43.275123,-119.340384,43.274795,-119.340363,43.274561,-119.340556,43.274498,-119.341006,43.274592,-119.341092,43.274811,-119.340792,43.27492,-119.340985,43.27528,-119.341414,43.275623,-119.341671,43.275905,-119.342208,43.275936,-119.342766,43.275905,-119.343452,43.275967,-119.343967,43.276045,-119.344611,43.276014,-119.345083,43.276045,-119.345534,43.276233,-119.34577,43.276483,-119.346135,43.276358,-119.346306,43.276045,-119.346092,43.275826,-119.345942,43.275592,-119.345663,43.275358,-119.345212,43.275186,-119.344869,43.275045,-119.344461,43.275045,-119.344203,43.275201,-119.343817,43.275342,-119.343431,43.275545,-119.34298,43.275608,-119.342422,43.275608,-119.341865,43.275592,-119.342208,43.275326,-119.342551,43.275092,-119.34253,43.274811,-119.342337,43.274405,-119.342144,43.274233,-119.341843,43.274108,-119.34165,43.273764,-119.341457,43.273624,-119.341199,43.273405,-119.340727,43.273405,-119.340641,43.273108,-119.340405,43.272717,-119.340191,43.272467

Soldier Spring:

-119.216804,43.226154,-119.216895,43.226025,-119.2169,43.225896,-119.216836,43.225783,-119.216707,43.225716,-119.216579,43.225701,-119.216487,43.225709,-119.216337,43.225681,-119.216149,43.225685,-119.216031,43.22574,-119.21593,43.225787,-119.215983,43.225845,-119.215913,43.225877,-119.215833,43.225888,-119.215795,43.225955,-119.21579,43.226025,-119.215715,43.226084,-119.215645,43.226142,-119.215672,43.226221,-119.215731,43.226314,-119.215801,43.226365,-119.215811,43.226424,-119.215731,43.226518,-119.21579,43.226608,-119.215844,43.226525,-119.215897,43.226416,-119.215972,43.226373,-119.216058,43.226369,-119.216166,43.226346,-119.216267,43.22631,-119.216278,43.22624,-119.216246,43.226201,-119.216198,43.22615,-119.216182,43.226092,-119.216241,43.225998,-119.216348,43.225994,-119.21645,43.226025,-119.21653,43.226072,-119.216622,43.226123,-119.216702,43.226162

Appendix C: *Spring discharge field measurements.*

Description	Latitude	Longitude	Q (cfs)	Mmt Rated	qualitative field uncertainty estimate	statistical uncertainty output from ADVM	Description	SC (uS)	Temp ©	Comments	Date
Upper Sizemore Spring near Harney Lake, Total Q	**43.239538**	**-119.240094**	**1.4**	**Poor**	**17%**	**9.7%**	**Added outflow from northern most and southern channels.**			**minimal ET/Evap losses from spring pool**	**8/14/2017**
Upper Sizemore Spring Pond Outflow, south ditch; near Harney Lake	43.23927	-119.23957	1.2	Poor	15%	7.0%	ouflow from south ditch towards Lower Sizemore Spring flow. Measured about 200 feet south of Spring Vent.	289	20.9	cleared periphyton growth, still difficult site to measure	8/14/2017
Upper Sizemore Spring Pond Outflow, east side (northern most outflow); near Harney Lake	43.23964	-119.24001	0.2	Poor	30%	26.0%	outflow from east ditch of spring pond.	320	19.5	small channel	8/14/2017
Lower Sizemore Spring near Harney Lake, Total Q	**43.23517**	**-119.233752**	**1.7**	**Poor**	**24%**	**15%**	**subtract spring pond inflow from Upper Sizemore from spring pond outflow at Lower Sizemore Spring**			**minimal ET/Evap losses from spring pool**	**8/14/2017**
Lower Sizemore Spring Pond Dam Outflow near Harney Lake	43.235349	-119.23387	0.0	excellent	0.0%	0.0%	Outlet at Dam.				8/14/2017
Lower Sizemore Spring Pond Outflow ditch near Harney Lake	43.2359	-119.2324	2.3	Poor	10%	3.5%	Outflow from southernmost ditch. Other outlet (at dam) is dry.	318	21.8	fair measurement section.	8/14/2017
Lower Sizemore Spring Pond Inflow near Harney Lake	43.23555	-119.23397	0.6	Poor	33%	32.0%	Inflow from Upper Sizemore Spring.			measured at culvert into pond.	8/14/2017
Lower Sizemore Spring near Harney	**43.23517**	**-119.23375**	**1.4**	**Fair**	**8%**	**n/a**	**subtract spring pond inflow from**			**minimal ET/Evap**	**7/20/2017**

Description	Latitude	Longitude	Q (cfs)	Mmt Rated	qualitative field uncertainty estimate	statistical uncertainty output from ADVM	Description	SC (uS)	Temp ©	Comments	Date
Lake, Total Q. Previous mmt on 07/20/2017							**Upper Sizemore from spring pond outflow at Lower Sizemore Spring**			**losses from spring pool**	
Lower Sizemore Spring Pond Dam Outflow near Harney Lake	43.235349	-119.23387	1.4	Fair	8%	n/a	0.45' head over 1.5 ft wide rectangular contracted weir. Ideal conditions			$Q = 3.33(L-0.2H)H^{1.5}$	7/20/2017
Lower Sizemore Spring Pond Outflow ditch near Harney Lake	43.2359	-119.2324	0.0	excellent	0%	n/a	Outflow from southernmost ditch. Dry.				7/20/2017
Lower Sizemore Spring Pond Inflow near Harney Lake	43.23555	-119.23397	0.0	excellent	0%	n/a	Dry				7/20/2017
Basque Spring near Harney Lake	**43.26927**	**-119.29462**	**1.8**	**Poor**	**10%**	**3.2%**	**about 15 ft abv confluence with ditch**	**300**	**22.8**	**minimal ET/Evap losses from spring pool. 2-3 foot deep thick dense layer of detritus and algal material. Similar density to muck. No apparent water movement through mat. Measured water column above mat. Clear delineation between**	**8/14/2017**

Description	Latitude	Longitude	Q (cfs)	Mmt Rated	qualitative field uncertainty estimate	statistical uncertainty output from ADVM	Description	SC (uS)	Temp ©	Comments	Date
										open water and mat	
Hughet Spring near Harney Lake, OR	**43.24901**	**-119.25729**	**13.0**	**Poor**	**10%**	**4.4%**	**about 600 feet downstream of spring vent**	**306**	**21.5**	**minimal ET/Evap losses from spring pool. Raked clear channel among periphyton mat. Still had some abnormal velocity profiles. Sample velocity at 0.2/0.6/0.8 depths for these.**	**8/14/2017**
Johnson Spring near Harney Lake, OR	**43.26287**	**-119.27692**	**1.6**	**Poor**	**17%**	**14%**				**significant ET/Evap Losses fro m spring pool**	**8/14/2017**
Johnson Spring near Harney Lake, OR; mmt #1	43.26287	-119.27692	1.5	Poor	15%	7.4%	measured at culvert outlet from pond next to house. No flow at other culvert to the south.	301	22.9	subtancial ET/Evap Losses. No flow out of other pond outlet. Better than 2nd mmt	8/14/2017
Johnson Spring near Harney Lake, OR; mmt #2	"	"	1.9	Poor	33%	33.0%	"	"	"	"	"
Johnson Spring near Harney Lake; South Outlet	43.262631	-119.276931	0.0	excellent	0%		dry				"

Description	Latitude	Longitude	Q (cfs)	Mmt Rated	qualitative field uncertainty estimate	statistical uncertainty output from ADVM	Description	SC (uS)	Temp ©	Comments	Date
Barnyard SpringPond nr Harney Lake. Total Q	**43.27589**	**-119.309584**	**3.7**	**Poor**	**20%**	**15%**	**measured at culvert outlet. 3ft culvert fully submerged.**	**251**	**19.6**	**minimal ET/Evap Losses from spring pool**	**8/15/2017**
Barnyard SpringPond northern most Outlet (east side of Pond) nr Harney Lake. Mmt#1	43.27623	-119.30914	3.5	Poor	33%	32.0%	measured at culvert outlet. 3ft culvert fully submerged.	251	19.6	minimal ET/Evap Losses fro spring pool	8/15/2017
Barnyard SpringPond northern most Outlet (east side of Pond) nr Harney Lake. Mmt#2	"	"	3.3	Poor	15%	5.0%	measured channel downstream of culvert. Thick muck/algal mat with no apparent flow through mat. Measured open water column above mat.	251	19.6	minimal ET/Evap Losses spring pool	8/15/2017
Barnyard SpringPond southern Outlet nr Harney Lake.	43.27541	-119.30916	0.4	Poor	50%	30.0%	thick muck/detritus/algal mat on bottom 3/4 of depth. Extremely low velocities. Measured open water portion of channel. No apparent flow through mat.	251	19.6	minimal ET/Evap Losses from spring pool	8/15/2017
Hibbard Spring near Harney Lake, Total Outflow			**9.2**	**Poor**	**17%**	**14%**	**Other outlet is dry**			**significant ET/evap losses from spring pool**	**8/15/2017**
Hibbard Spring near Harney Lake, north outflow @ culvert near house. Mmt #1	43.28036	-119.31987	9.6	Poor	33%	33.0%	measured at culvert. Culvert is running partially full	275	22.1	large ET/evap losses from spring pool	8/15/2017
Hibbard Spring near Harney Lake, north outflow @ culvert near house. Mmt #2	"	"	9.1	Poor	15%	6.0%	measured x-section in front of culvert.			large ET/evap losses spring pool	8/15/2017

Description	Latitude	Longitude	Q (cfs)	Mmt Rated	qualitative field uncertainty estimate	statistical uncertainty output from ADVM	Description	SC (uS)	Temp ©	Comments	Date
Total measured Q for Springs in August >>>			**32.4**		**4.7**	**3.1**					
					15%	**9%**					

Appendix D1: *Calculations for estimating spring discharge for Ross Spring.*

Year	EVI	ET 0 (mm)	PPT (mm)	B 0	B 1	B 2	ET*	ET g (mm/yr)	ET g (ft/s)	Area (ft2)	Q (cfs)
1984	0.26	1069.26	348.61	-0.196	2.904	-1.592	0.454117	327.2601365	3.40421E-08	1296708	0.044143
1985	0.28	1090.03	225.31	-0.196	2.904	-1.592	0.490696	424.3160423	4.4138E-08	1296708	0.057234
1986	0.29	1123.05	254.62	-0.196	2.904	-1.592	0.509298	442.2927892	4.6008E-08	1296708	0.059659
1987	0.25	1164.57	227.76	-0.196	2.904	-1.592	0.42522	398.349417	4.14369E-08	1296708	0.053732
1988	0.31	1192.82	206.95	-0.196	2.904	-1.592	0.553164	545.3458563	5.67277E-08	1296708	0.073559
1989	0.31	1133.11	299.01	-0.196	2.904	-1.592	0.543169	453.0539197	4.71274E-08	1296708	0.06111
1990	0.19	1153.37	134.04	-0.196	2.904	-1.592	0.30311	308.9676323	3.21393E-08	1296708	0.041675
1991	0.22	1159.47	233.13	-0.196	2.904	-1.592	0.368909	341.7381583	3.55481E-08	1296708	0.046096
1992	0.18	1227.17	177.80	-0.196	2.904	-1.592	0.26743	280.6318797	2.91918E-08	1296708	0.037853
1993	0.25	1047.37	351.83	-0.196	2.904	-1.592	0.43618	303.3821599	3.15583E-08	1296708	0.040922
1994	0.21	1191.62	182.27	-0.196	2.904	-1.592	0.339604	342.7802422	3.56565E-08	1296708	0.046236
1995	0.24	1125.17	303.44	-0.196	2.904	-1.592	0.411185	337.8850782	3.51473E-08	1296708	0.045576
1996	0.23	1152.86	308.58	-0.196	2.904	-1.592	0.396364	334.6411096	3.48099E-08	1296708	0.045138
1997	0.26	1155.36	277.99	-0.196	2.904	-1.592	0.45391	398.2439327	4.1426E-08	1296708	0.053717
1998	0.31	1075.59	339.25	-0.196	2.904	-1.592	0.547601	403.2203396	4.19436E-08	1296708	0.054389
1999	0.27	1127.29	218.86	-0.196	2.904	-1.592	0.478345	434.5420664	4.52017E-08	1296708	0.058613
2000	0.26	1227.25	206.03	-0.196	2.904	-1.592	0.457222	466.9246771	4.85702E-08	1296708	0.062981
2001	0.26	1150.00	174.62	-0.196	2.904	-1.592	0.444343	433.4014505	4.50831E-08	1296708	0.05846
2002	0.28	1223.29	141.88	-0.196	2.904	-1.592	0.492508	532.6027063	5.54022E-08	1296708	0.07184
2003	0.24	1227.00	209.67	-0.196	2.904	-1.592	0.410116	417.2267938	4.34006E-08	1296708	0.056278
2004	0.29	1189.81	209.71	-0.196	2.904	-1.592	0.507908	497.8005777	5.1782E-08	1296708	0.067146
2005	0.27	1099.08	330.21	-0.196	2.904	-1.592	0.477531	367.1575485	3.81923E-08	1296708	0.049524
2006	0.25	1145.89	314.54	-0.196	2.904	-1.592	0.427123	355.0869729	3.69367E-08	1296708	0.047896
2007	0.28	1197.59	170.28	-0.196	2.904	-1.592	0.489487	502.8541443	5.23077E-08	1296708	0.067828
2008	0.22	1116.99	187.00	-0.196	2.904	-1.592	0.375273	349.0000067	3.63035E-08	1296708	0.047075
2009	0.28	1153.32	265.72	-0.196	2.904	-1.592	0.488276	433.3935663	4.50823E-08	1296708	0.058459
2010	0.27	1074.71	268.27	-0.196	2.904	-1.592	0.472636	381.1536165	3.96482E-08	1296708	0.051412
2011	0.32	1074.56	357.23	-0.196	2.904	-1.592	0.574962	412.4405171	4.29027E-08	1296708	0.055632

Year	EVI	ET 0 (mm)	PPT (mm)	B 0	B 1	B 2	ET*	ET g (mm/yr)	ET g (ft/s)	Area (ft2)	Q (cfs)
2012	0.28	1200.70	200.60	-0.196	2.904	-1.592	0.484434	484.481546	5.03965E-08	1296708	0.06535
2013	0.25	1147.01	270.11	-0.196	2.904	-1.592	0.438487	384.5100935	3.99973E-08	1296708	0.051865
2014	0.28	1181.44	227.29	-0.196	2.904	-1.592	0.497529	474.7202216	4.93811E-08	1296708	0.064033
2015	0.24	1175.79	285.97	-0.196	2.904	-1.592	0.412894	367.3987143	3.82174E-08	1296708	0.049557
2016	0.20	1167.77	266.58	-0.196	2.904	-1.592	0.32723	294.8970397	3.06757E-08	1296708	0.039777

Appendix D2: *Calculations for estimating spring discharge for Soldier Spring.*

Year	EVI	ET 0 (mm)	PPT (mm)	B 0	B 1	B 2	ET*	ET g (mm/yr)	ET g (ft/s)	Area (ft2)	Q (cfs)
1983	0.26	1053.78	375.26	-0.196	2.904	-1.592	0.443717	301.0698944	3.13178E-08	52494	0.001644
1984	-0.04	1069.62	342.41	-0.196	2.904	-1.592	-0.31713	-230.622354	-2.399E-08	52494	-0.00126
1985	-0.06	1087.45	217.99	-0.196	2.904	-1.592	-0.38962	-338.761436	-3.5238E-08	52494	-0.00185
1986	-0.10	1126.42	256.24	-0.196	2.904	-1.592	-0.50813	-442.161696	-4.5994E-08	52494	-0.00241
1987	0.05	1162.58	224.38	-0.196	2.904	-1.592	-0.06606	-61.9775693	-6.447E-09	52494	-0.00034
1988	0.15	1202.65	195.85	-0.196	2.904	-1.592	0.195999	197.3309738	2.05267E-08	52494	0.001078
1989	0.25	1135.78	282.93	-0.196	2.904	-1.592	0.427757	364.8105982	3.79482E-08	52494	0.001992
1990	0.19	1158.52	142.49	-0.196	2.904	-1.592	0.292301	296.9870178	3.08931E-08	52494	0.001622
1991	0.28	1162.37	231.35	-0.196	2.904	-1.592	0.497128	462.837635	4.81451E-08	52494	0.002527
1992	0.17	1236.86	183.68	-0.196	2.904	-1.592	0.251435	264.8070504	2.75456E-08	52494	0.001446
1993	0.30	1055.67	350.41	-0.196	2.904	-1.592	0.533283	376.1035432	3.91229E-08	52494	0.002054
1994	0.18	1199.64	180.56	-0.196	2.904	-1.592	0.282582	287.9715645	2.99553E-08	52494	0.001572
1995	0.30	1118.52	299.40	-0.196	2.904	-1.592	0.536588	439.5337851	4.5721E-08	52494	0.0024
1996	0.25	1154.57	298.68	-0.196	2.904	-1.592	0.43702	374.0397466	3.89082E-08	52494	0.002042
1997	0.21	1142.23	288.50	-0.196	2.904	-1.592	0.352993	301.3597799	3.13479E-08	52494	0.001646
1998	0.25	1076.66	342.37	-0.196	2.904	-1.592	0.429235	315.1846687	3.2786E-08	52494	0.001721
1999	0.19	1123.21	219.93	-0.196	2.904	-1.592	0.293223	264.8621597	2.75514E-08	52494	0.001446
2000	0.22	1225.11	201.66	-0.196	2.904	-1.592	0.358981	367.3990572	3.82174E-08	52494	0.002006
2001	0.19	1147.02	184.05	-0.196	2.904	-1.592	0.300586	289.4559901	3.01097E-08	52494	0.001581
2002	0.23	1216.78	146.98	-0.196	2.904	-1.592	0.384224	411.0408815	4.27571E-08	52494	0.002244

Year	EVI	ET 0 (mm)	PPT (mm)	B 0	B 1	B 2	ET*	ET g (mm/yr)	ET g (ft/s)	Area (ft2)	Q (cfs)
2003	0.22	1212.93	213.96	-0.196	2.904	-1.592	0.35477	354.4041742	3.68657E-08	52494	0.001935
2004	0.23	1184.29	208.29	-0.196	2.904	-1.592	0.382046	372.8778813	3.87873E-08	52494	0.002036
2005	0.27	1102.19	316.09	-0.196	2.904	-1.592	0.471614	370.7364511	3.85646E-08	52494	0.002024
2006	0.23	1150.28	316.09	-0.196	2.904	-1.592	0.382264	318.8825298	3.31707E-08	52494	0.001741
2007	0.24	1205.14	167.06	-0.196	2.904	-1.592	0.410758	426.3992815	4.43547E-08	52494	0.002328
2008	0.22	1127.81	185.70	-0.196	2.904	-1.592	0.358981	338.2008359	3.51802E-08	52494	0.001847
2009	0.24	1154.09	252.14	-0.196	2.904	-1.592	0.404975	365.2661676	3.79956E-08	52494	0.001995
2010	0.24	1079.57	266.45	-0.196	2.904	-1.592	0.416092	338.332882	3.51939E-08	52494	0.001847
2011	0.26	1072.77	364.36	-0.196	2.904	-1.592	0.451836	320.0829947	3.32955E-08	52494	0.001748
2012	0.22	1204.57	199.06	-0.196	2.904	-1.592	0.366048	368.0628108	3.82865E-08	52494	0.00201
2013	0.22	1151.33	257.56	-0.196	2.904	-1.592	0.367809	328.7342558	3.41955E-08	52494	0.001795
2014	0.22	1182.77	225.07	-0.196	2.904	-1.592	0.361414	346.126097	3.60046E-08	52494	0.00189
2015	0.22	1181.38	287.65	-0.196	2.904	-1.592	0.361193	322.8069877	3.35789E-08	52494	0.001763
2016	0.2137	1167.316	265.6511	-0.196	2.904	-1.592	0.351882	317.2793611	3.30039E-08	52494	0.001733

Appendix E: *Static water level measurements from the Fall 2017 OWRD synoptic. Locations from OWRD (2017).*

Log ID	Latitude	Longitude	Measured Date	Elevation from USGS Quads (NGVD1929)	Water Level Below Land Surface Datum	Water Level Elevation
CROO0002936	43.7829	-120.07802	10/25/2017	4162.39	28.12	4134.27
CROO0053256	43.85795	-120.299065	10/25/2017	4754.14	49.88	4704.26
CROO0053258	43.84654	-120.29701	10/25/2017	4775.73	67.59	4708.14
CROO0053444	43.87305	-120.29876	10/25/2017	4806.49	105.22	4701.27
DESC0053516	43.75926922	-120.3577621	10/25/2017	4442.49	166.02	4276.47
GRAN0000800	44.030417	-118.937861	10/31/2017	4573.22	11.80	4561.42
HARN0000008	43.87566	-119.27279	11/7/2017	4816.86	19.21	4797.65
HARN0000009	43.92535749	-118.9627877	10/31/2017	4694.65	12.80	4681.85
HARN0000198	43.63892744	-118.7346712	10/31/2017	4163.95	39.70	4124.25
HARN0000219	43.62818	-118.63258	11/3/2017	4178.80	20.52	4158.28
HARN0000243	43.589	-119.58798	11/2/2017	4305.15	157.95	4147.20
HARN0000255	43.52419	-119.59368	10/31/2017	4322.86	172.61	4150.25
HARN0000274	43.5397	-119.53631	11/7/2017	4234.30	86.75	4147.55
HARN0000296	43.57235	-119.08923	11/3/2017	4245.38	109.44	4135.94
HARN0000323	43.53402	-119.07876	11/8/2017	4139.50	4.30	4135.20
HARN0000440	43.58570085	-118.9701503	11/3/2017	4147.63	11.88	4135.75
HARN0000441	43.58572006	-118.9701498	11/3/2017	4147.63	32.00	4115.63
HARN0000463	43.57696748	-119.0081605	10/31/2017	4147.12	17.00	4130.12
HARN0000503	43.5675	-118.9448	10/31/2017	4143.98	36.20	4107.78
HARN0000547	43.590173	-118.935909	10/31/2017	4138.74	35.60	4103.14
HARN0000607	43.55134	-118.90589	11/8/2017	4136.81	54.68	4082.13
HARN0000637	43.60491	-118.82015	11/8/2017	4134.08	39.40	4094.68
HARN0000657	43.5662	-118.7158	10/31/2017	4128.88	57.40	4071.48
HARN0000696	43.55372	-118.58967	11/7/2017	4143.93	16.90	4127.03
HARN0000722	43.58357	-118.58431	11/3/2017	4151.90	11.27	4140.63
HARN0000751	43.52576	-119.45932	11/2/2017	4210.90	64.76	4146.14

Log ID	Latitude	Longitude	Measured Date	Elevation from USGS Quads (NGVD1929)	Water Level Below Land Surface Datum	Water Level Elevation
HARN0000754	43.50599	-119.44796	11/2/2017	4197.51	49.53	4147.98
HARN0000755	43.51099	-119.45086	11/2/2017	4189.38	44.69	4144.69
HARN0000782	42.72757	-119.09897	11/2/2017	4564.89	102.60	4462.29
HARN0000812	43.51130305	-119.1773233	11/8/2017	4178.88	33.30	4145.58
HARN0000813	43.49793	-119.16927	11/8/2017	4161.78	26.30	4135.48
HARN0000991	43.50459	-118.65405	11/6/2017	4121.67	12.04	4109.63
HARN0000994	43.50408	-118.62437	11/6/2017	4121.71	38.83	4082.88
HARN0001078	43.38852	-119.36562	11/7/2017	4142.08	11.17	4130.91
HARN0001085	43.37090607	-119.2677749	11/7/2017	4131.67	11.02	4120.65
HARN0001094	43.36334	-119.13353	11/1/2017	4133.34	133.82	3999.52
HARN0001245	43.43530005	-118.5892198	11/7/2017	4139.09	65.14	4073.95
HARN0001303	43.30922	-119.54724	10/30/2017	4212.20	77.73	4134.47
HARN0001304	43.34916	-119.3328	11/8/2017	4134.60	9.77	4124.83
HARN0001305	43.32595	-119.32454	11/8/2017	4123.91	6.57	4117.34
HARN0001309	43.33955791	-119.2765751	11/7/2017	4142.05	24.83	4117.22
HARN0001335	43.31626	-119.12918	11/1/2017	4113.80	72.30	4041.50
HARN0001363	43.26208	-118.85809	11/8/2017	4105.84	8.30	4097.54
HARN0001387	43.31181	-118.58266	11/8/2017	4137.39	50.00	4087.39
HARN0001393	43.29136	-118.68628	11/2/2017	4113.82	17.55	4096.27
HARN0001405	43.26908658	-118.650055	11/2/2017	4134.09	35.32	4098.77
HARN0001408	43.264	-118.63708	11/8/2017	4123.88	25.70	4098.18
HARN0001441	43.19998	-119.33153	10/31/2017	4362.37	233.23	4129.14
HARN0001458	43.23112	-118.97324	11/8/2017	4227.19	182.75	4044.44
HARN0001459	43.18749	-118.98785	11/8/2017	4262.91	183.27	4079.64
HARN0001464	43.2473	-118.89654	11/7/2017	4165.34	75.92	4089.42
HARN0001467	43.246	-118.89289	11/7/2017	4113.44	14.43	4099.01
HARN0001472	43.21905	-118.73727	11/1/2017	4389.97	286.95	4103.02
HARN0001473	43.22837	-118.73656	11/1/2017	4514.82	420.58	4094.24

Log ID	Latitude	Longitude	Measured Date	Elevation from USGS Quads (NGVD1929)	Water Level Below Land Surface Datum	Water Level Elevation
HARN0001474	43.18278	-118.76705	11/1/2017	4480.05	377.95	4102.10
HARN0001477	43.2612	-118.61953	11/2/2017	4125.87	29.93	4095.94
HARN0001482	43.21142	-118.66802	11/2/2017	4212.15	110.17	4101.98
HARN0001485	43.21359	-118.60878	11/2/2017	4526.09	429.27	4096.82
HARN0001488	43.24578	-118.53899	11/2/2017	4109.70	23.96	4085.74
HARN0001495	43.24397	-118.52906	11/2/2017	4114.29	30.99	4083.30
HARN0001509	43.191574	-118.5776877	11/1/2017	4377.52	272.53	4104.99
HARN0001510	43.17599	-118.55821	11/1/2017	4257.26	154.69	4102.57
HARN0001517	43.20012	-118.40779	11/2/2017	4114.48	77.24	4037.24
HARN0001537	43.12619	-118.93866	11/6/2017	4148.18	69.90	4078.28
HARN0001540	43.16913	-118.81858	11/1/2017	4230.27	127.31	4102.96
HARN0001541	43.1025	-118.82377	11/6/2017	4139.97	24.48	4115.49
HARN0001547	43.17047	-118.60273	11/6/2017	4254.02	155.72	4098.30
HARN0001548	43.16088	-118.6688	11/6/2017	4501.84	403.11	4098.73
HARN0001556	43.16212	-118.48551	11/2/2017	4219.73	104.69	4115.04
HARN0001557	43.17229	-118.46707	11/2/2017	4185.80	79.93	4105.87
HARN0001562	43.11704	-118.56575	11/1/2017	4370.63	126.65	4243.98
HARN0001566	43.1529	-118.30267	11/2/2017	4200.01	227.97	3972.04
HARN0001588	43.00572	-118.7339	11/1/2017	4436.64	269.59	4167.05
HARN0001603	42.9751	-118.87266	11/6/2017	4159.23	12.78	4146.45
HARN0001611	42.97716	-118.7904	11/1/2017	4448.76	236.52	4212.24
HARN0001640	42.75819	-119.0703	10/30/2017	4593.80	129.09	4464.71
HARN0001643	42.82634	-118.91521	11/6/2017	4203.42	13.76	4189.66
HARN0001656	42.71922	-118.62425	10/30/2017	7658.51	10.12	7648.39
HARN0001690	42.66577253	-118.471314	11/1/2017	4243.97	30.80	4213.17
HARN0001753	42.40934	-118.63452	11/1/2017	4080.76	24.10	4056.66
HARN0001806	42.15849501	-118.551011	11/1/2017	4132.73	20.65	4112.08
HARN0001841	43.16337	-119.20083	10/31/2017	4409.33	283.29	4126.04

Log ID	Latitude	Longitude	Measured Date	Elevation from USGS Quads (NGVD1929)	Water Level Below Land Surface Datum	Water Level Elevation
HARN0001894	43.55032	-119.31627	10/31/2017	4548.02	264.21	4283.81
HARN0001950	43.21033	-119.31726	10/31/2017	4487.92	356.83	4131.09
HARN0001979	43.60685	-119.05383	11/6/2017	4163.92	27.50	4136.42
HARN0001981	43.47887	-119.43683	11/2/2017	4174.50	48.05	4126.45
HARN0001990	43.37440601	-119.1086955	11/2/2017	4133.66	108.50	4025.16
HARN0050151	43.2475	-118.59249	11/2/2017	4135.34	33.80	4101.54
HARN0050174	43.63818	-119.65871	11/2/2017	4363.48	84.80	4278.68
HARN0050178	43.4431	-118.70437	11/7/2017	4108.85	16.29	4092.56
HARN0050179	43.44279	-118.70519	11/7/2017	4109.18	54.15	4055.03
HARN0050184	43.54917754	-119.6117472	10/31/2017	4294.86	149.76	4145.10
HARN0050233	43.29351	-118.98243	11/4/2017	4119.02	25.16	4093.86
HARN0050237	43.58298	-118.57262	11/3/2017	4172.06	21.16	4150.90
HARN0050251	43.48226	-119.45895	11/2/2017	4178.09	31.01	4147.08
HARN0050301	43.6419	-118.84984	11/8/2017	4226.54	55.40	4171.14
HARN0050309	43.53164122	-119.7797212	10/30/2017	4471.34	331.02	4140.32
HARN0050381	43.58313	-119.63669	10/31/2017	4318.10	157.54	4160.56
HARN0050399	43.3042	-119.04592	11/8/2017	4175.32	88.05	4087.27
HARN0050407	43.47089	-118.64482	11/7/2017	4118.36	67.56	4050.80
HARN0050460	43.61269	-118.79501	11/8/2017	4133.79	17.20	4116.59
HARN0050462	43.63018	-119.104	11/6/2017	4222.38	75.97	4146.41
HARN0050474	43.0455	-118.84118	11/6/2017	4143.57	5.05	4138.52
HARN0050514	43.58369	-118.72892	11/3/2017	4128.88	23.80	4105.08
HARN0050598	42.90784	-118.89141	11/6/2017	4163.59	8.86	4154.73
HARN0050612	42.88708	-118.89906	11/6/2017	4176.48	2.19	4174.29
HARN0050707	43.26419	-118.84334	11/7/2017	4187.04	90.03	4097.01
HARN0050719	43.39548	-118.80487	11/2/2017	4103.94	11.04	4092.90
HARN0050734	43.30945	-119.04392	11/8/2017	4122.02	35.68	4086.34
HARN0050751	43.45789005	-118.5899898	11/7/2017	4139.09	91.41	4047.68

Log ID	Latitude	Longitude	Measured Date	Elevation from USGS Quads (NGVD1929)	Water Level Below Land Surface Datum	Water Level Elevation
HARN0050765	43.61919	-119.61903	11/2/2017	4353.11	199.49	4153.62
HARN0050766	43.62743	-118.79282	11/8/2017	4129.67	111.86	4017.81
HARN0050795	43.25475	-118.95803	11/7/2017	4133.70	35.21	4098.49
HARN0050891	43.59552	-119.04976	11/3/2017	4156.72	7.60	4149.12
HARN0050904	43.62466	-119.06893	11/6/2017	4197.13	40.61	4156.52
HARN0050936	43.57406	-119.56632	10/31/2017	4267.65	122.37	4145.28
HARN0050947	43.50764	-118.70864	11/6/2017	4120.68	44.57	4076.11
HARN0050950	43.28745	-119.06983	11/8/2017	4123.94	39.70	4084.24
HARN0050958	43.59605	-119.59594	10/31/2017	4316.31	170.54	4145.77
HARN0050962	43.50982	-118.88306	11/9/2017	4128.90	43.29	4085.61
HARN0050979	43.50266	-119.02093	11/3/2017	4130.85	9.25	4121.60
HARN0051004	43.42009005	-118.5887398	11/7/2017	4131.50	63.07	4068.43
HARN0051008	43.79951	-118.9876	11/6/2017	5354.38	152.85	5201.53
HARN0051010	43.24796	-118.994	11/8/2017	4124.04	29.96	4094.08
HARN0051013	43.5923	-118.60188	10/30/2017	4222.07	102.03	4120.04
HARN0051014	43.59446	-118.60029	10/31/2017	4210.14	87.94	4122.20
HARN0051015	43.5871	-118.60603	10/30/2017	4149.62	7.03	4142.59
HARN0051017	42.94831961	-118.8786398	11/6/2017	4161.99	5.78	4156.21
HARN0051020	43.64078	-119.00159	11/3/2017	4195.17	56.47	4138.70
HARN0051040	42.97479	-118.78423	11/1/2017	4448.12	232.14	4215.98
HARN0051076	43.41542	-118.57781	11/7/2017	4135.15	61.00	4074.15
HARN0051188	43.16868	-119.08994	11/1/2017	4124.38	27.41	4096.97
HARN0051205	43.59442	-118.59939	10/30/2017	4207.62	109.97	4097.65
HARN0051237	43.44715005	-118.5890698	11/7/2017	4137.45	83.41	4054.04
HARN0051238	43.44714005	-118.5891898	11/7/2017	4137.45	89.53	4047.92
HARN0051266	43.42339	-119.04229	11/1/2017	4176.00	81.57	4094.43
HARN0051276	43.44099084	-118.786665	11/2/2017	4111.72	19.31	4092.41
HARN0051292	43.61096	-119.08356	11/6/2017	4272.08	132.30	4139.78

Log ID	Latitude	Longitude	Measured Date	Elevation from USGS Quads (NGVD1929)	Water Level Below Land Surface Datum	Water Level Elevation
HARN0051298	43.91799	-119.5897	11/7/2017	5435.24	84.62	5350.62
HARN0051302	43.48004	-119.71449	10/31/2017	4639.94	501.55	4138.39
HARN0051327	43.37626	-118.86065	11/2/2017	4103.93	10.47	4093.46
HARN0051343	43.52364	-119.0921	11/3/2017	4164.34	28.18	4136.16
HARN0051368	43.45028	-119.00544	11/9/2017	4133.83	18.52	4115.31
HARN0051382	43.06607	-118.86845	11/6/2017	4142.58	16.00	4126.58
HARN0051448	43.355034	-119.128932	11/4/2017	4155.69	175.23	3980.46
HARN0051466	43.57028	-118.93799	11/8/2017	4141.34	37.92	4103.42
HARN0051467	43.1614	-119.38206	10/31/2017	4518.02	233.27	4284.75
HARN0051510	43.61851	-118.66378	11/8/2017	4304.28	188.83	4115.45
HARN0051524	43.49737	-118.77047	11/3/2017	4124.46	45.50	4078.96
HARN0051542	43.57461	-118.74849	11/3/2017	4128.88	58.22	4070.66
HARN0051546	43.51296	-119.05216	11/3/2017	4135.94	9.40	4126.54
HARN0051547	43.52682	-118.81968	11/3/2017	4123.94	30.47	4093.47
HARN0051573	43.41051	-118.99498	11/1/2017	4108.87	38.39	4070.48
HARN0051574	42.65577002	-118.72824	10/30/2017	5333.92	109.97	5223.95
HARN0051584	43.42835	-118.68848	11/2/2017	4107.88	15.54	4092.34
HARN0051586	43.42733	-118.68462	11/2/2017	4108.53	51.66	4056.87
HARN0051589	43.50492	-118.59094	11/9/2017	4133.87	31.47	4102.40
HARN0051610	43.36341	-118.57693	10/19/2017	4131.84	54.92	4076.92
HARN0051610	43.36341	-118.57693	11/7/2017	4131.84	54.07	4077.77
HARN0051611	43.27343	-118.63438	11/2/2017	4128.40	33.10	4095.30
HARN0051613	43.60997	-119.17904	11/7/2017	4768.44	307.89	4460.55
HARN0051651	43.60763	-119.0523	11/6/2017	4164.29	10.38	4153.91
HARN0051697	43.38868	-118.70835	10/19/2017	4100.98	9.44	4091.54
HARN0051697	43.38868	-118.70835	11/7/2017	4100.98	9.64	4091.34
HARN0051718	43.84034	-118.95216	11/6/2017	5131.81	46.40	5085.41
HARN0051722	43.4725	-118.63483	11/7/2017	4119.03	73.18	4045.85

Log ID	Latitude	Longitude	Measured Date	Elevation from USGS Quads (NGVD1929)	Water Level Below Land Surface Datum	Water Level Elevation
HARN0051724	43.64911	-119.07088	11/6/2017	4222.57	64.87	4157.70
HARN0051733	43.46975	-118.94328	11/8/2017	4118.38	7.80	4110.58
HARN0051734	43.44733	-118.89663	11/8/2017	4108.87	9.75	4099.12
HARN0051736	43.3835	-118.9031	11/2/2017	4103.95	14.24	4089.71
HARN0051737	43.4337	-118.95212	11/8/2017	4124.57	29.54	4095.03
HARN0051738	43.6217	-118.743	10/31/2017	4139.65	67.70	4071.95
HARN0051756	43.52583	-119.46056	11/2/2017	4212.69	62.90	4149.79
HARN0051761	43.3467	-119.13082	11/4/2017	4181.59	134.76	4046.83
HARN0051767	43.32095	-119.14908	11/1/2017	4123.23	53.46	4069.77
HARN0051784	43.36581	-119.00914	11/4/2017	4116.16	72.93	4043.23
HARN0051830	43.60558	-118.97607	11/8/2017	4147.95	16.28	4131.67
HARN0051864	43.35309	-118.97982	11/4/2017	4109.75	18.18	4091.57
HARN0051885	43.57756	-119.06377	11/3/2017	4150.90	13.99	4136.91
HARN0051890	43.58316	-118.72872	11/3/2017	4128.88	55.98	4072.90
HARN0051896	43.37531	-119.52344	10/30/2017	4262.25	123.76	4138.49
HARN0051921	43.48135	-119.41736	11/2/2017	4176.44	31.50	4144.94
HARN0051922	43.59492	-118.76795	11/3/2017	4128.86	58.60	4070.26
HARN0051963	43.61177	-119.0211	11/3/2017	4160.28	19.36	4140.92
HARN0051973	43.32347	-119.12025	11/4/2017	4134.67	99.68	4034.99
HARN0052001	43.56172	-118.64394	11/6/2017	4131.20	30.31	4100.89
HARN0052008	42.93513	-119.17226	10/30/2017	4873.91	562.47	4311.44
HARN0052021	43.62772	-118.79576	11/8/2017	4133.15	106.36	4026.79
HARN0052022	43.36793	-119.31767	11/7/2017	4133.75	7.98	4125.77
HARN0052048	43.45044	-119.01017	11/9/2017	4130.59	16.71	4113.88
HARN0052068	43.3817	-118.98254	11/4/2017	4108.87	25.39	4083.48
HARN0052096	43.2555	-119.41401	10/31/2017	4155.52	23.79	4131.73
HARN0052102	43.59059	-119.5458	11/2/2017	4295.57	145.53	4150.04
HARN0052111	43.5046	-118.65308	11/6/2017	4121.98	69.93	4052.05

Log ID	Latitude	Longitude	Measured Date	Elevation from USGS Quads (NGVD1929)	Water Level Below Land Surface Datum	Water Level Elevation
HARN0052136	43.51674	-119.22075	11/8/2017	4261.02	104.39	4156.63
HARN0052234	43.44603	-118.79486	11/2/2017	4108.25	12.14	4096.11
HARN0052235	43.44599	-118.79501	11/2/2017	4108.20	65.08	4043.12
HARN0052255	43.55524	-118.93143	11/8/2017	4138.61	42.90	4095.71
HARN0052487	43.33418	-119.59628	10/30/2017	4230.24	92.19	4138.05
HARN0052494	43.61006	-118.63974	11/6/2017	4144.27	18.62	4125.65
HARN0052502	43.55833	-118.62922	11/6/2017	4133.80	23.32	4110.48
HARN0052524	43.60045	-118.8628	11/3/2017	4134.44	48.30	4086.14
HARN0052530	43.59167	-118.604	10/30/2017	4157.33	21.18	4136.15
HARN0052531	42.94837	-118.62746	11/7/2017	4783.64	207.40	4576.24
HARN0052534	43.37114	-119.268	11/7/2017	4133.75	8.29	4125.46
HARN0052546	42.95688	-119.16788	10/30/2017	4902.14	589.76	4312.38
HARN0052599	43.39576	-119.19184	11/1/2017	4389.99	246.33	4143.66
HARN0052602	43.60471	-119.03697	11/3/2017	4159.59	22.62	4136.97
HARN0052606	43.43585	-119.00109	11/1/2017	4124.30	30.75	4093.55
HARN0052607	43.22673	-118.48157	11/2/2017	4121.67	35.45	4086.22
HARN0052608	43.22684	-118.48171	11/2/2017	4121.07	35.36	4085.71
HARN0052617	43.06464	-118.88678	10/30/2017	4162.40	30.27	4132.13
HARN0052619	43.59539	-118.86637	11/3/2017	4133.79	48.12	4085.67
HARN0052629	43.43579	-119.00106	11/1/2017	4124.30	49.29	4075.01
HARN0052630	43.36779	-119.13224	11/1/2017	4151.10	137.98	4013.12
HARN0052631	43.36791	-119.13226	11/1/2017	4151.54	143.81	4007.73
HARN0052657	43.44736	-119.23534	11/1/2017	4426.55	263.72	4162.83
LAKE0001223	43.20053	-119.99709	10/18/2017	4353.73	67.52	4286.21
LAKE0001223	43.20053	-119.99709	10/30/2017	4353.73	67.47	4286.26
LAKE0001468	43.08569	-119.97315	10/16/2017	4314.05	24.13	4289.92
LAKE0001468	43.08569	-119.97315	10/30/2017	4314.05	24.13	4289.92
MALH0002322	43.33008	-119.27848	11/7/2017	4139.02	32.63	4106.39

Appendix F: *Spring elevations used in water level contour map with elevations extracted from USGS topo map in NGVD1929. Locations were GPS located in the field.*

Name	Latitude	Longitude	Elevation	Average
Ross Spring	43.27312447	-119.3396242	4128.83	
Hibbard Spring	43.27335145	-119.3306864	4130.72	
OO Cold Spring	43.28384834	-119.3172354	4128.14	
Barnyard Spring	43.27610413	-119.3102036	4124.84	
Basque Spring	43.26895609	-119.2949161	4122.93	4122.47
Johnson Spring	43.26164846	-119.2819464	4122.43	
Hughet Spring	43.24737241	-119.258195	4115.97	
Upper Sizemore Spring	43.23961222	-119.2399628	4124.46	
Lower Sizemore	43.23506177	-119.2338628	4125.57	
Soldier Spring	43.22594664	-119.2161322	4100.78	

Appendix G: *Major ion data for wells from published reports (Piper et al., 1939; Leonard, 1970; Gonthier et al., 1977; and Townley et al., 1980). Well logs and locations are from the OWRD database.*

Major Ions (mg/L)															
Logid		**Sample Date**	**Ca**	**Mg**	**Na**	**K**	**CO_3**	**HCO_3**	**Cl**	**SO_4**	**TDS Rptd**	**Latitude**	**Longitude**	**Horiz. Error**	**Well Depth**
HARN0000544	[1]	05/31/1931	66	26	125	125	0	950	24	2	836	43.61392013	-118.9342848	500	19.5
HARN0000302	[1]	08/16/1931	12	0	7.5	7.5	0	86	10	13	112	43.56057453	-119.0925559	200	340
HARN0001442	[1]	08/21/1931	16	17	23.5	23.5	0	143	25	24	193	43.25162248	-119.2365255	300	48
HARN0001443	[1]	08/21/1931	13	4.1	33.5	33.5	16	134	26	20	212	43.2584365	-119.2677478	9999	47
HARN0001454	[1]	08/21/1931	1	0	149	149	89	428	90	20	680	43.25713638	-119.0099243	2500	315
HARN0001379	[1]	08/22/1931	18	12	21	21	0	163	13	8	168	43.26764919	-118.7478678	9999	215
HARN0000411	[1]	08/26/1931	35	0	15	15	0	180	6	20	191	43.58531496	-119.0012176	450	12
HARN0000410	[1]	08/26/1931	24	0	10.5	10.5	0	145	1.8	12	140	43.58752324	-119.0025366	9999	43
HARN0000792	[1]	08/26/1931	9.6	1.7	30	2.4	0	95	5.2	13	159	43.52365346	-119.0647572	50	478
HARN0000285	[1]	08/27/1931	14	6	18	4.9	0	108	3.8	7.5	167	43.59285938	-119.062865	50	253
HARN0052322	[1]	08/31/1931	154	43	117	117	0	498	109	387	1303	43.55587126	-118.9219318	500	15.5
HARN0000547	[1]	09/01/1931	64	22	117	4	0	151	138	175	652	43.590173	-118.935909	150	93
HARN0000549	[1]	09/01/1931	11	2.7	38	2.9	0	141	3.6	4.7	188	43.58619646	-118.9310297	350	218
HARN0000694	[1]	09/02/1931	32	14	109.5	109.5	0	453	64	88	715	43.55787227	-118.6416885	350	18.5
HARN0001194	[1]	09/02/1931	85	72	196	196	0	903	68	499	1568	43.43539433	-118.8007217	300	22
HARN0000870	[1]	09/04/1931	73	33	158.5	158.5	0	307	334	274	1182	43.47284342	-119.0210346	350	53
HARN0000939	[1]	09/04/1931	7	0	97.5	97.5	0	524	14	4	465	43.44851169	-118.9238931	9999	400
HARN0000941	[1]	09/04/1931	25	0	115	115	45	596	49	8	663	43.44850496	-118.923874	9999	12
HARN0000970	[1]	09/04/1931	12	0	246	246	0	1034	212	3	1205	43.44919172	-118.8018506	1000	180
HARN0001119	[1]	09/04/1931	14	0	79	79	0	410	14	35	413	43.41358336	-119.0114333	300	105
HARN0000157	[1]	09/05/1931	14	0	8	8	0	102	2.5	4	97	43.63366773	-118.8248219	350	11
HARN0000660	[1]	09/05/1931	2	0	99	99	0	438	17	60	481	43.53371493	-118.8151024	9999	52
HARN0000661	[1]	09/05/1931	29	9.2	21	8.1	0	176	4.2	11	219	43.54028507	-118.8216733	200	18
HARN0000865	[1]	09/08/1931	45	0	38.5	38.5	0	358	12	24	348	43.498817	-118.9931428	9999	11
HARN0001183	[1]	09/08/1931	45	98	245	245	0	1292	104	358	1731	43.3595853	-118.8528067	9999	21
HARN0001364	[1]	09/08/1931	14	58	815	815	0	1804	1148	570	4138	43.26740488	-118.8554843	9999	25
HARN0001365	[1]	09/08/1931	3	0	103.5	103.5	73	353	101	3	485	43.267405	-118.855484	9999	53
HARN0001371	[1]	09/08/1931	76	133	372	372	0	1624	311	560	2626	43.316609	-118.848784	9999	60
HARN0001376	[1]	09/08/1931	87	67	61	61	0	864	12	32	746	43.304845	-118.909582	9999	18
HARN0001380	[1]	09/08/1931	24	86	431.5	431.5	63	1761	318	280	2502	43.34218061	-118.6913099	9999	70

Major Ions (mg/L)															
Logid		**Sample Date**	**Ca**	**Mg**	**Na**	**K**	**CO_3**	**HCO_3**	**Cl**	**SO_4**	**TDS Rptd**	**Latitude**	**Longitude**	**Horiz. Error**	**Well Depth**
HARN0001381	1	09/08/1931	17	48	439	439	124	1396	417	202	2374	43.32752373	-118.6718184	9999	20
HARN0000583	1	09/09/1931	12	0	51	51	0	321	2.8	2	281	43.55716201	-118.9216509	300	44
HARN0000332	1	05/09/1932	109	36	46	46	0	650	59	5	621	43.60433841	-118.9777935	1000	13
HARN0000560	1	05/09/1932	19	10	84	84	0	470	47	3	478	43.59353559	-118.8295808	9999	18.5
HARN0000627	1	05/09/1932	8.5	7	58	58	0	312	19	18	322	43.61220777	-118.7458609	350	15
HARN0000708	1	05/09/1932	46	22	241.5	241.5	12	299	340	490	1540	43.53469685	-118.6615489	9999	16
HARN0000861	1	05/10/1932	29	18	94	94	0	298	92	175	649	43.50579529	-119.0207727	350	10
HARN0000871	1	05/10/1932	34	15	63	63	0	339	26	49	417	43.47287409	-119.0214656	350	11
HARN0001198	1	05/10/1932	38	71	249	249	31	769	12	740	1769	43.41703116	-118.8017117	300	14
HARN0001463	1	05/10/1932	24	12	30	30	0	268	6	12	246	43.26170502	-118.8982577	400	18
HARN0000928	1	05/11/1932	18	23	191.5	191.5	20	909	93	61	1046	43.48266203	-118.8503249	400	57
HARN0000932	1	05/11/1932	46	56	275	275	0	925	85	633	1826	43.47148827	-118.8570846	350	46
HARN0000973	1	05/11/1932	63	68	204	204	0	1302	172	14	1366	43.45102852	-118.7701849	400	35
HARN0001044	1	05/11/1932	15	5.2	214.5	214.5	16	531	119	347	1193	43.4399177	-118.6411615	100	21
HARN0001199	1	05/11/1932	34	58	1079	1079	368	2560	790	1141	5810	43.42441912	-118.7471294	300	22
HARN0001217	1	05/11/1932	36	20	106	106	0	565	62	79	687	43.4211432	-118.7029363	350	21
HARN0001240	1	05/11/1932	5.5	6.1	132.5	132.5	76	117	211	91	712	43.39173742	-118.6280541	300	28.5
HARN0000554	1	05/13/1932	21	12	38.5	38.5	0	278	17	16	280	43.58682778	-118.9046717	9999	14
HARN0000575	1	05/13/1932	164	62	79.5	79.5	0	330	178	470	1196	43.57923453	-118.9387146	9999	24
HARN0000591	1	05/13/1932	36	13	19	19	0	168	8	73	251	43.55382155	-118.8697766	9999	11
HARN0000664	1	05/13/1932	14	15	25.5	25.5	0	229	5	12	210	43.53184272	-118.7955491	9999	24
HARN0000947	1	05/13/1932	106	129	435.5	435.5	0	1154	375	1166	3230	43.50283756	-118.8149506	9999	41
HARN0000948	1	05/13/1932	19	9.4	65	65	9.8	389	12	16	388	43.50975399	-118.7655744	9999	40
HARN0000452	1	05/14/1932	20	10	4.9	4.9	0	109	3	18	114	43.58253425	-118.9681253	1000	12.5
HARN0000467	1	05/14/1932	24	12	6	6	0	129	2	25	134	43.58504279	-119.0389943	350	12
HARN0000496	1	05/14/1932	26	14	16	16	0	214	3	12	192	43.56461276	-119.0026161	9999	54
HARN0000497	1	05/14/1932	20	7.2	15.5	15.5	0	164	2	9.1	150	43.56461276	-119.0026161	9999	13
HARN0052320	1	05/14/1932	9	7	35	35	0	224	3	16	215	43.52180929	-119.0820912	9999	15
HARN0000860	1	05/14/1932	5	4.4	17.5	17.5	0	107	8	6.6	112	43.50594424	-119.0207752	350	44.5
HARN0000867	1	05/14/1932	51	20	31.5	31.5	0	380	7	24	352	43.49763194	-118.9606515	250	11
HARN0000903	1	05/14/1932	8.5	6.6	156	156	61	538	37	126	816	43.51373129	-118.9291729	9999	105
HARN0001370	1	05/16/1932	44	11	90	90	15	227	139	133	634	43.316358	-118.704868	100	35
HARN0001390	1	05/16/1932	20	7.2	39	39	0	187	49	26	272	43.30551663	-118.6811507	5000	15
HARN0001395	1	05/16/1932	5	6.1	4135	4135	2168	7510	3250	3530	20930	43.29828595	-118.6320079	9999	11

Major Ions (mg/L)															
Logid		**Sample Date**	**Ca**	**Mg**	**Na**	**K**	**CO_3**	**HCO_3**	**Cl**	**SO_4**	**TDS Rptd**	**Latitude**	**Longitude**	**Horiz. Error**	**Well Depth**
HARN0001398	1	05/16/1932	1.5	2.4	55.5	55.5	55	131	15	33	282	43.27838286	-118.6145122	9999	35
HARN0001400	1	05/16/1932	2.9	44	10905	10905	546	4020	8560	30100	63000	43.28924379	-118.6245371	9999	16
HARN0001341	1	05/17/1932	717	341	4255	4255	153	3770	4850	11060	27500	43.33828804	-119.0204201	400	14
HARN0001159	1	05/18/1932	144	65	175.5	175.5	0	1539	55	48	1421	43.36502756	-119.0024329	9999	22
HARN0001355	1	05/18/1932	50	137	226.5	226.5	0	1800	65	102	1694	43.28893003	-118.9668369	9999	24
HARN0001358	1	05/18/1932	327	348	1575	1575	0	1172	2065	5020	11490	43.27291	-119.029672	9999	13
HARN0001375	1	05/18/1932	10	18	482	482	40	1936	380	5	2371	43.32168344	-118.9221505	9999	46
HARN0001374	1	05/18/1932	7	2	1420	1420	449	4370	425	1221	7100	43.321683	-118.922151	9999	21
HARN0001202	1	05/19/1932	111	140	139	139	0	919	87	559	1628	43.3884115	-118.8154937	9999	23.5
HARN0001204	1	05/19/1932	212	322	698	698	0	1081	505	3160	6139	43.386177	-118.806114	50	47
HARN0001368	1	05/19/1932	30	162	325	325	0	1346	158	795	2458	43.33981923	-118.9767192	9999	18
HARN0001373	1	05/19/1932	468	291	307.5	307.5	0	1140	335	2204	4480	43.313734	-118.880657	9999	18
HARN0001377	1	05/20/1932	34	27	27.5	27.5	0	348	12	12	311	43.2712429	-118.7429006	9999	25.5
HARN0001206	1	05/24/1932	65	22	26.5	26.5	0	273	25	104	404	43.39210666	-118.7573894	9999	18
HARN0001207	1	05/24/1932	22	27	51.5	51.5	48	90	45	165	454	43.389364	-118.755619	100	50
HARN0001210	1	05/24/1932	123	107	163.5	163.5	0	1284	43	331	1564	43.38846135	-118.7183562	9999	12
HARN0001187	1	05/25/1932	7	5.5	86	86	21	317	81	5.3	448	43.42483891	-118.7216589	400	86
HARN0001372	1	05/25/1932	16	5.9	37.5	37.5	18	175	25	17	243	43.312274	-118.75512	9999	46
HARN0001346	1	05/26/1932	4.5	25	1320	1320	511	4990	428	299	6370	43.3089267	-118.9819954	300	17
HARN0000616	1	05/28/1932	32	13	8.5	8.5	0	191	2	10	168	43.52826288	-118.9051713	9999	12.5
HARN0000902	1	05/28/1932	10	7.9	80.5	80.5	25	426	7	6.2	427	43.51920292	-118.9026448	400	51
HARN0000489	1	05/29/1932	32	9.2	6.5	6.5	0	154	3	15	148	43.56797961	-119.0326892	300	64
HARN0000490	1	05/29/1932	30	9.6	6.5	6.5	0	149	4	15	145	43.56797292	-119.0335494	300	15
HARN0001307	1	05/30/1932	9.5	3.9	42.5	42.5	0	241	15	4.9	237	43.32189732	-119.3345127	9999	33
HARN0001314	1	05/30/1932	8	7.4	83	83	0	425	41	4.9	437	43.286876	-119.225214	9999	130
HARN0001442	1	05/30/1932	19	10	21	21	0	137	27	29	194	43.25162248	-119.2365255	300	48
HARN0000177	1	05/31/1932	24	14	41.5	41.5	0	291	20	31	315	43.62680043	-118.8765859	300	14
HARN0000346	1	05/31/1932	28	13	7.5	7.5	0	160	7	14	156	43.60956678	-119.0082484	75	98
HARN0000556	1	05/31/1932	12	7.6	31	31	0	185	13	26	212	43.59872295	-118.8751816	350	33
HARN0000667	1	05/31/1932	38	31	171.5	171.5	0	910	83	102	1045	43.53891935	-118.7407922	9999	20
HARN0000936	1	05/31/1932	19	22	248	248	19	841	120	314	1404	43.45579249	-118.8548623	9999	16
HARN0001164	1	05/31/1932	31	44	117	117	79	418	43	222	859	43.43617539	-118.8461357	400	43
HARN0001165	1	05/31/1932	225	108	156.5	156.5	0	425	41	1230	2126	43.43541437	-118.8463278	300	13
HARN0000411	1	06/01/1932	107	22	1.8	1.8	0	363	20	38	369	43.58531496	-119.0012176	450	12

Major Ions (mg/L)															
Logid		**Sample Date**	**Ca**	**Mg**	**Na**	**K**	**CO_3**	**HCO_3**	**Cl**	**SO_4**	**TDS Rptd**	**Latitude**	**Longitude**	**Horiz. Error**	**Well Depth**
HARN0000410	1	06/01/1932	28	7.4	9.5	9.5	0	147	2	18	147	43.58752324	-119.0025366	9999	43
HARN0000477	1	06/01/1932	18	6.6	7	7	0	100	5	14	107	43.5783015	-119.0499636	9999	110
HARN0000371	1	09/07/1932	30	0	13	13	0	180	3.1	10	174	43.60703587	-119.0497525	9999	14
HARN0000075	2	07/23/1968	10	4.8	13	4.5	0	82	2.5	5.2	138	43.62985148	-119.1032024	50	127
HARN0000134	2	07/23/1968	23	4.8	22	5	0	124	8.5	16	204	43.62864564	-118.9810836	50	725
HARN0000356	2	07/23/1968	25	10	13	4.1	0	143	3	14	199	43.61270348	-119.0252529	100	400
HARN0000602	2	07/23/1968	5.4	3.9	172	5.6	0	472	16	0.4	491	43.54929686	-118.8881473	50	250
HARN0000619	2	07/23/1968	5.9	4.2	160	5.8	0	450	7	3.2	456	43.52377113	-118.9041714	450	270
HARN0000297	2	07/24/1968	15	5.7	35	6.9	0	128	13	18	221	43.55873756	-119.0898069	9999	345
HARN0000320	2	07/24/1968	11	2	33	4	0	105	7	14	180	43.53997452	-119.081234	100	200
HARN0000500	2	07/24/1968	21	6.2	32	4.3	0	164	5	15	205	43.56687873	-118.9452572	1000	114
HARN0000953	2	07/24/1968	5.4	4.6	255	14	0	504	117	2.6	729	43.49351013	-118.7183549	25	275
HARN0000210	2	07/25/1968	24	8.1	40	8	0	190	7.5	23	268	43.62735323	-118.713706	50	182
HARN0001030	2	07/25/1968	97	32	706	28	0	348	975	269	2350	43.47520606	-118.594554	25	340
HARN0000202	2	07/26/1968	16	4.4	39	3.7	0	154	5.5	12	220	43.63143698	-118.8206573	100	647
HARN0000792	2	09/11/1968	8.8	1.4	31	2.9	0	93	5	12	155	43.52365346	-119.0647572	50	564
HARN0052265	2	09/12/1968	0.8	0.2	135	1.6	84	94	11	29	396	43.50371981	-118.906048	50	2812
HARN0052266	2	09/13/1968	1	0.2	157	1.8	92	49	38	89	499	43.62615697	-118.8633685	700	1000
HARN0052268	2	06/11/1969	65	44	113	18	0	552	35	105	711	43.47554435	-118.7666466	100	50
HARN0000965	2	06/11/1969	12	40	724	33	0	1430	478	0	2120	43.46153037	-118.8083115	150	185
HARN0000547	2	06/12/1969	21	4.5	22	3.6	0	137	3.5	3.6	179	43.590173	-118.935909	150	93
HARN0001068	2	06/12/1969	65	19	37	4.5	0	249	41	55	403	43.44645791	-118.5843702	50	503
HARN0001072	2	06/12/1969	32	8.1	20	3.5	0	170	4.5	11	219	43.43891519	-118.569811	50	128
HARN0052269	2	06/12/1969	0.5	0.2	386	4.4	144	674	9	8	957	43.42294997	-118.9337117	350	1345
HARN0052273	2	06/12/1969	95	177	662	31	0	635	195	1550	3090	43.39145722	-118.8365139	100	60
HARN0052275	2	06/12/1969	6.4	36	835	28	0	2000	236	0	2260	43.363527	-118.853838	300	400
HARN0052277	2	06/12/1969	11	22	681	19	0	888	630	5.2	1880	43.38020426	-118.7115946	700	12
HARN0000232	3	06/14/1977	20	6.9	25	3.8	0	120	8.9	18	186	43.6519532	-118.5662803	250	134
HARN0001548	3	06/17/1977	25	4.5	47	9.6	0	150	16	36	272	43.16088	-118.6688	25	578
HARN0001562	3	06/17/1977	7.2	0.4	34	3.1	0	92	3.7	10	136	43.11704	-118.56575	25	338
HARN0001474	3	06/19/1977	20	6.1	32	8.6	0	160	5.6	6.9	212	43.18278	-118.76705	25	572
HARN0001397	3	06/20/1977	1.1	0.1	140	1.2	35	250	17	27	390	43.27722008	-118.6113247	100	115
HARN0001473	3	06/20/1977	3.5	0.5	130	3.6	0	270	36	5.6	360	43.22837	-118.73656	25	576
HARN0001540	3	06/20/1977	28	17	30	3.9	0	230	3.6	8.9	246	43.16913	-118.81858	10	278

Major Ions (mg/L)															
Logid		**Sample Date**	**Ca**	**Mg**	**Na**	**K**	**CO_3**	**HCO_3**	**Cl**	**SO_4**	**TDS Rptd**	**Latitude**	**Longitude**	**Horiz. Error**	**Well Depth**
HARN0052259	[3]	06/21/1977	25	13	37	4.6	0	210	8.1	11	243	43.23300452	-118.8313101	200	152
HARN0000238	[4]	06/28/1979	8.2	4.2	13	2.1	0	67	2.6	2.1	64*	43.61024	-119.630992	250	141
HARN0000753	[4]	07/05/1979	18	3.7	10	2.3	0	87	2.5	6.6	138	43.512315	-119.46023	150	408
HARN0001084	[4]	07/05/1979	27	16	41	8.6	0	220	14	37	302	43.37447	-119.27297	25	457
HARN0001458	[4]	07/05/1979	3.4	2.9	130	2.4	0	268	67	9.4	385	43.23112	-118.97324	10	341
HARN0001588	[4]	07/18/1979	15	6.3	21	5.5	0	115	1.3	7.2	186	43.00572	-118.7339	25	325
HARN0001643	[4]	07/19/1979	14	6.7	51	4	0	134	15	31	264	42.82634	-118.91521	25	78
HARN0001666	[4]	07/21/1979	4.9	1.2	2.2	0.4	0	20	0.4	2.2	40	42.73895	-118.64197	25	110
HARN0000055	[4]	08/09/1979	21	9.8	18	5.8	0	102	10	23	158	43.643299	-119.008009	250	215

*Calculated, otherwise reported; [1]Piper et al. (1939); [2]Leonard (1970); [3]Gonthier et al. (1977); [4]Townley et al. (1980)

Appendix H: *Major ion data for springs from published reports (Piper et al., 1939; Leonard, 1970; Hubbard, 1975; Brown et al., 1980b; Townley et al., 1980, and USGS, 2017). Logid identifiers and locations are from the OWRD database (OWRD, 2017).*

Major Ions (mg/L)																	
Logid	**Site Name**		**Sample Date**	**Ca**	**Mg**	**Na**	**K**	**CO_3**	**HCO_3**	**Cl**	**SO_4**	**TDS**	**Latitude**	**Longitude**	**Horiz. Error**	**Temp (F)**	**pH**	**Cond. (uS/cm)**
SPRG0018734	Basque Spring	[1]	8/21/1931	14	7.5	41	4.2	0	134	24	14	230	43.26896	-119.295	100	68		
SPRG0018745	UNNAMED HOT SPRING 361	[1]	8/21/1931	13	3	622	12	0	601	562	140	1782	43.1811	-119.057	100	139		
SPRG0018735	Sodhouse Spring	[1]	8/22/1931	20	13	34	3.9	0	195	7.4	8.6	226	43.26638	-118.845	50	55		
SPRG0018720	Mill Pond Spring	[1]	8/26/1931	14	0	18.5	18.5	0	109	8	11	121	43.5403	-119.082	500	78		
SPRG0018726	Roadland Spring	[1]	8/26/1931	7	0	20	20	0	104	5	13	113	43.50001	-119.093	150	72		
SPRG0018729	CRANE HOT SPRING	[1]	8/30/1931	2	0	85.5	85.5	22	173	82	80	427	43.43709	-118.642	9999	120		
SPRG0018717		[1]	9/2/1931	16	0	6	6	0	86	1.9	4	72	43.66345	-118.741	250	72		
SPRG0018727		[1]	5/28/1932	14	2.4	15.5	15.5	0	100	9	17	123	43.49628	-119.117	9999			
SPRG0018729	CRANE HOT SPRING	[2]	9/1/1968	3.8	0.2	170	3.6	0	199	78	81	536	43.43709	-118.642	9999	176	8.3	
SPRG0018714		[3]	9/12/1968	3.8	0.2	170	3.6	0	199	78	81	536	43.44094	-118.639	500	176	8.3	
SPRG0018713	GOODMAN SPRING (HOTCHKISS)	[3]	9/13/1968	8.2	1.4	35	3.2	0	92	7	16	165	43.5285	-119.081	600	72	7.5	
SPRG0018729	CRANE HOT SPRING	[2]	1/1/1972	3.7	0.1	170	3.9	0	202	79	86	542*	43.43709	-118.642	9999	172.4	8.1	
SPRG0018745	UNNAMED HOT SPRING 361	[4]	7/1/1972	12	1.8	630	13	1	566	590	140	1810	43.1811	-119.057	100	154	7.3	
SPRG0018735	Sodhouse Spring	[5]	10/16/1973	22	13	35	4.8	0	10	7.3	10	196*	43.26638	-118.845	50		7.8	
SPRG0018731	OO Cold Spring	[6]	5/10/1988	14	5.9	38	5.2	7	108	22	9	703*	43.28385	-119.317	100		8.8	
SPRG0018731	OO Cold Spring	[6]	5/10/1988	14	5.9	37	5.1	7	108	22	8.8	711*	43.28385	-119.317	100		8.8	814
SPRG0018731	OO Cold Spring	[6]	9/15/1988	14	6.1	37	5.3	12	99	22	8.4	723*	43.28385	-119.317	100		8.8	810

*Calculated, otherwise reported; [1]Piper et al. (1939); [2]Brown et al. (1980b); [3]Leonard (1970); [4]Townley et al. (1980); [5]Hubbard (1975); [6]NWIS

Appendix I: *Measurements taken at wells and springs in Harney Basin of temperature, pH, and specific conductance (uS/cm) (Piper et al., 1939; Leonard, 1970; Gonthier et al., 1977; Brown et al., 1980b; Townley et al., 1980; Hubbard, 1975; USGS, 2017; and Kiri Hargie, 2017). Locations are from the OWRD database.*

Log ID	Source	Sample Date	Latitude	Longitude	Horizontal Error	Temp (F)	pH	Specific Conductance (uS/cm)
HARN0000544	1	5/31/1931	43.61392	-118.934	500	46		
HARN0000302	1	8/16/1931	43.56057	-119.093	200	62		
HARN0001442	1	8/21/1931	43.25162	-119.237	300	53		
HARN0001443	1	8/21/1931	43.25844	-119.268	9999	68		
HARN0001454	1	8/21/1931	43.25714	-119.01	2500	65.5		
HARN0001379	1	8/22/1931	43.26765	-118.748	9999	54		
HARN0000410	1	8/26/1931	43.58752	-119.003	9999	51.5		
HARN0000411	1	8/26/1931	43.58531	-119.001	450	49		
HARN0000792	1	8/26/1931	43.52365	-119.065	50	80		
HARN0000285	1	8/27/1931	43.59286	-119.063	50	58		
HARN0052322	1	8/31/1931	43.55587	-118.922	500	52		
HARN0000547	1	9/1/1931	43.59017	-118.936	150	48		
HARN0000549	1	9/1/1931	43.5862	-118.931	350	56		
HARN0000694	1	9/2/1931	43.55787	-118.642	350	52		1100
HARN0001194	1	9/2/1931	43.43539	-118.801	300	52		
HARN0000870	1	9/4/1931	43.47284	-119.021	350	51		
HARN0000939	1	9/4/1931	43.44851	-118.924	9999	55		
HARN0000941	1	9/4/1931	43.4485	-118.924	9999	48		1020
HARN0000970	1	9/4/1931	43.44919	-118.802	1000	57		
HARN0001119	1	9/4/1931	43.41358	-119.011	300	51		
HARN0000157	1	9/5/1931	43.63367	-118.825	350	53		
HARN0000660	1	9/5/1931	43.53371	-118.815	9999	51		740
HARN0000661	1	9/5/1931	43.54029	-118.822	200	50		
HARN0000865	1	9/8/1931	43.49882	-118.993	9999	51		
HARN0001183	1	9/8/1931	43.35959	-118.853	9999	52		
HARN0001364	1	9/8/1931	43.2674	-118.855	9999	52.5		
HARN0001365	1	9/8/1931	43.26741	-118.855	9999	54		
HARN0001371	1	9/8/1931	43.31661	-118.849	9999	50		4040

Log ID	Source	Sample Date	Latitude	Longitude	Horizontal Error	Temp (F)	pH	Specific Conductance (uS/cm)
HARN0001376	1	9/8/1931	43.30485	-118.91	9999	50		
HARN0001380	1	9/8/1931	43.34218	-118.691	9999	52		
HARN0001381	1	9/8/1931	43.32752	-118.672	9999	50		
HARN0000583	1	9/9/1931	43.55716	-118.922	300	50		
HARN0000332	1	5/9/1932	43.60434	-118.978	1000			
HARN0000560	1	5/9/1932	43.59354	-118.83	9999			
HARN0000627	1	5/9/1932	43.61221	-118.746	350			
HARN0000708	1	5/9/1932	43.5347	-118.662	9999			
HARN0000861	1	5/10/1932	43.5058	-119.021	350	46		
HARN0000871	1	5/10/1932	43.47287	-119.021	350	46		
HARN0001198	1	5/10/1932	43.41703	-118.802	300	52		
HARN0001463	1	5/10/1932	43.26171	-118.898	400	51		
HARN0000928	1	5/11/1932	43.48266	-118.85	400	52		
HARN0000932	1	5/11/1932	43.47149	-118.857	350	52		
HARN0000973	1	5/11/1932	43.45103	-118.77	400			
HARN0001044	1	5/11/1932	43.43992	-118.641	100	54		
HARN0001199	1	5/11/1932	43.42442	-118.747	300			
HARN0001217	1	5/11/1932	43.42114	-118.703	350			
HARN0001240	1	5/11/1932	43.39174	-118.628	300			
HARN0000554	1	5/13/1932	43.58683	-118.905	9999	54		
HARN0000575	1	5/13/1932	43.57923	-118.939	9999			1840
HARN0000591	1	5/13/1932	43.55382	-118.87	9999	50		
HARN0000664	1	5/13/1932	43.53184	-118.796	9999	52		
HARN0000947	1	5/13/1932	43.50284	-118.815	9999			
HARN0000948	1	5/13/1932	43.50975	-118.766	9999	54		
HARN0000452	1	5/14/1932	43.58253	-118.968	1000			
HARN0000467	1	5/14/1932	43.58504	-119.039	350			
HARN0000496	1	5/14/1932	43.56461	-119.003	9999	50		
HARN0000497	1	5/14/1932	43.56461	-119.003	9999	47		
HARN0000860	1	5/14/1932	43.50594	-119.021	350	54		
HARN0000867	1	5/14/1932	43.49763	-118.961	250			
HARN0000903	1	5/14/1932	43.51373	-118.929	9999			

Log ID	Source	Sample Date	Latitude	Longitude	Horizontal Error	Temp (F)	pH	Specific Conductance (uS/cm)
HARN0052320	1	5/14/1932	43.52181	-119.082	9999	54		
HARN0001370	1	5/16/1932	43.31636	-118.705	100	56		
HARN0001390	1	5/16/1932	43.30552	-118.681	5000	52		
HARN0001395	1	5/16/1932	43.29829	-118.632	9999	50		32200
HARN0001398	1	5/16/1932	43.27838	-118.615	9999	54		
HARN0001400	1	5/16/1932	43.28924	-118.625	9999	51		
HARN0001341	1	5/17/1932	43.33829	-119.02	400			
HARN0001159	1	5/18/1932	43.36503	-119.002	9999	56		
HARN0001355	1	5/18/1932	43.28893	-118.967	9999	52		
HARN0001358	1	5/18/1932	43.27291	-119.03	9999	52		
HARN0001374	1	5/18/1932	43.32168	-118.922	9999	52		
HARN0001375	1	5/18/1932	43.32168	-118.922	9999	51		
HARN0001202	1	5/19/1932	43.38841	-118.815	9999	49		
HARN0001204	1	5/19/1932	43.38618	-118.806	50	52		
HARN0001368	1	5/19/1932	43.33982	-118.977	9999	51		
HARN0001373	1	5/19/1932	43.31373	-118.881	9999	51		
HARN0001377	1	5/20/1932	43.27124	-118.743	9999			
HARN0001206	1	5/24/1932	43.39211	-118.757	9999			
HARN0001207	1	5/24/1932	43.38936	-118.756	100			
HARN0001210	1	5/24/1932	43.38846	-118.718	9999			
HARN0001187	1	5/25/1932	43.42484	-118.722	400			
HARN0001372	1	5/25/1932	43.31227	-118.755	9999	51		
HARN0001346	1	5/26/1932	43.30893	-118.982	300			9800
HARN0000616	1	5/28/1932	43.52826	-118.905	9999			
HARN0000902	1	5/28/1932	43.5192	-118.903	400	50		
HARN0000489	1	5/29/1932	43.56798	-119.033	300			
HARN0000490	1	5/29/1932	43.56797	-119.034	300			
HARN0001307	1	5/30/1932	43.3219	-119.335	9999	54		
HARN0001314	1	5/30/1932	43.28688	-119.225	9999	52		
HARN0001442	1	5/30/1932	43.25162	-119.237	300	52		
HARN0000177	1	5/31/1932	43.6268	-118.877	300	46		
HARN0000346	1	5/31/1932	43.60957	-119.008	75	52		240

Log ID	Source	Sample Date	Latitude	Longitude	Horizontal Error	Temp (F)	pH	Specific Conductance (uS/cm)
HARN0000556	1	5/31/1932	43.59872	-118.875	350	50		
HARN0000667	1	5/31/1932	43.53892	-118.741	9999	49		
HARN0000936	1	5/31/1932	43.45579	-118.855	9999	49		2160
HARN0001164	1	5/31/1932	43.43618	-118.846	400			
HARN0001165	1	5/31/1932	43.43541	-118.846	300			
HARN0000410	1	6/1/1932	43.58752	-119.003	9999			
HARN0000411	1	6/1/1932	43.58531	-119.001	450	42		
HARN0000477	1	6/1/1932	43.5783	-119.05	9999			
HARN0000371	1	9/7/1932	43.60704	-119.05	9999	50.5		
HARN0000075	2	7/23/1968	43.62985	-119.103	50	57	7.5	
HARN0000134	2	7/23/1968	43.62865	-118.981	50	58	7.7	
HARN0000356	2	7/23/1968	43.6127	-119.025	100	52	7.4	
HARN0000602	2	7/23/1968	43.5493	-118.888	50	60	7.6	
HARN0000619	2	7/23/1968	43.52377	-118.904	450	55	8	
HARN0000297	2	7/24/1968	43.55874	-119.09	9999	64	7.8	340
HARN0000320	2	7/24/1968	43.53997	-119.081	100	76	7.8	
HARN0000500	2	7/24/1968	43.56688	-118.945	1000	51	7.7	
HARN0000953	2	7/24/1968	43.49351	-118.718	25	58	7.5	
HARN0000210	2	7/25/1968	43.62735	-118.714	50	58	7.5	
HARN0001030	2	7/25/1968	43.47521	-118.595	25		7.8	
HARN0000202	2	7/26/1968	43.63144	-118.821	100		8	
HARN0000792	2	9/11/1968	43.52365	-119.065	50	80	8.1	
HARN0052265	2	9/12/1968	43.50372	-118.906	50	115	9.6	
HARN0052266	2	9/13/1968	43.62616	-118.863	700	172	9.5	
HARN0000965	2	6/11/1969	43.46153	-118.808	150	58	7.8	
HARN0052268	2	6/11/1969	43.47554	-118.767	100	54	7.9	
HARN0000547	2	6/12/1969	43.59017	-118.936	150	51	8.3	
HARN0001068	2	6/12/1969	43.44646	-118.584	50	53	7.9	620
HARN0001072	2	6/12/1969	43.43892	-118.57	50	53	8	
HARN0052269	2	6/12/1969	43.42295	-118.934	350	105	9.3	
HARN0052273	2	6/12/1969	43.39146	-118.837	100	51	7.4	
HARN0052275	2	6/12/1969	43.36353	-118.854	300		7.6	

Log ID	Source	Sample Date	Latitude	Longitude	Horizontal Error	Temp (F)	pH	Specific Conductance (uS/cm)
HARN0052277	2	6/12/1969	43.3802	-118.712	700	53	7.6	
HARN0000232	3	6/14/1977	43.65195	-118.566	250	57	6.7	
HARN0001548	3	6/17/1977	43.16088	-118.669	25	68	7.5	
HARN0001562	3	6/17/1977	43.11704	-118.566	25	69	7.9	
HARN0001474	3	6/19/1977	43.18278	-118.767	25	65	7.6	
HARN0001397	3	6/20/1977	43.27722	-118.611	100	55	8.9	600
HARN0001473	3	6/20/1977	43.22837	-118.737	25	65	8.3	
HARN0001540	3	6/20/1977	43.16913	-118.819	10	60		
HARN0052259	3	6/21/1977	43.233	-118.831	200	57	7.4	
HARN0000238	4	6/28/1979	43.61024	-119.631	250	54	6.3	
HARN0000753	4	7/5/1979	43.51232	-119.46	150	53	7.6	
HARN0001084	4	7/5/1979	43.37447	-119.273	25	53	7.7	
HARN0001458	4	7/5/1979	43.23112	-118.973	10	68	7.6	
HARN0001588	4	7/18/1979	43.00572	-118.734	25	66	7.4	
HARN0001643	4	7/19/1979	42.82634	-118.915	25	55	6.9	
HARN0001666	4	7/21/1979	42.73895	-118.642	25	41	7.4	
SPRG0018734	1	8/21/1931	43.26896	-119.295	100	68		
SPRG0018745	1	8/21/1931	43.1811	-119.057	100	154	7.3	
SPRG0018735	1	8/22/1931	43.26638	-118.845	50		7.8	
SPRG0018720	1	8/26/1931	43.5403	-119.082	500	78		
SPRG0018726	1	8/26/1931	43.50001	-119.093	150	72		
SPRG0018729	1	8/30/1931	43.43709	-118.642		172.4	8.1	810
SPRG0018717	1	9/2/1931	43.66345	-118.741	250	72		
SPRG0018727	1	5/28/1932	43.49628	-119.117	9999			
SPRG0018729	5	9/1/1968	43.43709	-118.642	9999	120		
SPRG0018714	2	9/12/1968	43.44094	-118.639	500	176	8.3	
SPRG0018713	2	9/13/1968	43.5285	-119.081	600	72	7.5	
SPRG0018729	5	1/1/1972	43.43709	-118.642		176	8.3	814
SPRG0018745	5	7/1/1972	43.1811	-119.057	100	139		
SPRG0018735	6	10/16/1973	43.26638	-118.845	50	55		
SPRG0018735	7	10/16/1973	43.26638	-118.845	50		7.8	361
SPRG0018735	7	9/17/1984	43.26638	-118.845	50			

Log ID	Source	Sample Date	Latitude	Longitude	Horizontal Error	Temp (F)	pH	Specific Conductance (uS/cm)
SPRG0018731	7	5/10/1988	43.28385	-119.317	100		8.8	
SPRG0018731	7	5/10/1988	43.28385	-119.317	100		8.8	
SPRG0018735	7	7/21/1988	43.26638	-118.845	50	53.06	7.8	432
SPRG0018731	7	9/15/1988	43.28385	-119.317	100		8.8	
SPRG0018735	7	9/16/1988	43.26638	-118.845	50	53.24	8	421
SPRG0018738	8	8/1/2016	43.24755	-119.258		68.24	7.9	311.77
SPRG0018738	7	10/19/2016	43.24737	-119.258	100	67.82		318
SPRG0000062	7	4/17/2017	43.4058	-119.4	9999	57.56		103
SPRG0000064	7	4/17/2017	43.441	-119.376	9999	42.8		94
SPRG0000061	7	4/18/2017	43.67818	-118.798	9999	47.12		225
SPRG0000065	7	4/18/2017	43.64942	-118.798	9999	49.28		166
SPRG0018731	7	4/19/2017	43.28385	-119.317	100	57.92	14	275
SPRG0018732	7	4/19/2017	43.27312	-119.34	250	71.24		301
SPRG0018733	7	4/19/2017	43.2761	-119.31	150	71.06		251
SPRG0018735	7	4/19/2017	43.26638	-118.845	50	51.08		328
SPRG0023236	7	4/19/2017	43.27335	-119.331	50	70.88		290
SPRG0000046	7	7/17/2017	42.67489	-118.59	9999	37.76		32
SPRG0000047	7	7/17/2017	42.67472	-118.649	9999			
SPRG0000048	7	7/17/2017	42.67472	-118.649	9999			
SPRG0000049	7	7/17/2017	42.70372	-118.59	9999	50.54		33
SPRG0000050	7	7/17/2017	42.70372	-118.59	9999	52.7		43
SPRG0000051	7	7/17/2017	42.71822	-118.63	9999	51.98		76
SPRG0018735	7	7/18/2017	43.26638	-118.845	50	58.1		329
SPRG0018732	7	7/19/2017	43.27312	-119.34	250	73.4	7	577
SPRG0000045	7	7/20/2017	43.28638	-119.376	150	71.6	7	268
SPRG0000054	7	7/20/2017	42.7985	-118.862	9999	51.8	7.3	95
SPRG0000059	7	7/20/2017	42.88537	-118.9	9999	50.8	6.7	155
SPRG0018731	7	7/20/2017	43.28385	-119.317	100	57.02	14	269
SPRG0018733	7	7/20/2017	43.2761	-119.31	150	71.6		253
SPRG0018738	7	7/20/2017	43.24737	-119.258	100	66.92		296
SPRG0018740	7	7/20/2017	43.23506	-119.234	150	66.92		296
SPRG0018814	7	7/20/2017	43.22595	-119.216	11	71.6	9	556

Log ID	Source	Sample Date	Latitude	Longitude	Horizontal Error	Temp (F)	pH	Specific Conductance (uS/cm)
SPRG0023236	7	7/20/2017	43.27335	-119.331	50	71.06		292
SPRG0000062	7	7/21/2017	43.4058	-119.4	9999	58.64		91
SPRG0000063	7	7/21/2017	43.67707	-119.687	9999	57.2	8	113
SPRG0018733	8	7/24/2017	43.27637	-119.31		72.05	8.4	251.9
SPRG0018734	8	7/24/2017	43.26882	-119.295		72.68	8.8	299.6
SPRG0018739	8	7/24/2017	43.23952	-119.24		66.02	8.2	323.5
SPRG0018740	8	7/24/2017	43.235	-119.234		65.84	8	324.7
SPRG0018731	8	7/25/2017	43.28388	-119.317		57.92	8.6	165
SPRG0018732	8	7/25/2017	43.27329	-119.34		77.72	7.1	184.1
SPRG0018737	8	7/25/2017	43.26197	-119.282		73.85	8.8	290.8
SPRG0018738	8	7/25/2017	43.24755	-119.258		68.18	8.3	313
SPRG0023236	8	7/25/2017	43.27316	-119.331		69.44	8.4	289.6
SPRG0018745	8	7/27/2017	43.1811	-119.057	100	143.38	7.4	3065.5
SPRG0018739	8	7/28/2017	43.23952	-119.24		65.84	8	323.8
SPRG0018740	8	7/28/2017	43.235	-119.234		66.02	8.1	324

[1]Piper et al. (1939); [2]Leonard (1970); [3]Gonthier et al. (1977); [4]Brown et al. (1980b); [5]Townley et al. (1980); [6]Hubbard (1975); [7]NWIS; [8]Kiri Hargie